Development of Repair and Strengthening System Using Conductive Strengthening Layer with Steel Corrosion Monitorability

January 2007

Phanuphan Piboonsak

Development of Repair and Strengthening System Using Conductive Strengthening Layer with Steel Corrosion Monitorability

January 2007

Phanuphan Piboonsak

Acknowledgements

The author would like to express deepest gratitude and sincere appreciation to his academic advisor, Professor Toyoaki Miyagawa of Kyoto University, for his invaluable guidance, continuous and indisputable support during 5.5 years of study in Japan. The author is also truly grateful to his advisor and Kyoto University for offering the financial support.

Sincerely appreciation is also extended to the member of Dissertation Committee, Professor Hirotaka Kawano, for all his valuable suggestions of this thesis.

The author would like to acknowledge to Associate Professor Atsushi Hattori, who has been troubled most frequently by the author. The author's problems were perfectly solved after discussion. His study would not be nearly as successful with out any of his contribution. The author's acknowledgement is also extended to Research Associate Takashi Yamamoto for all his support and help in every matter.

The author also wishes to thanks Dr.Yuzuru Tamai, a former graduate student, for his useful and generous advice. Thanks are also extended every former and present members of Structural Material Engineering laboratory for their friendship, humor and everything that constitute the author's study life in Japan.

Sincerely gratitude is also expressed to my supervisor and instructors in Thailand, Professor Somnuk Tangtermsirikul for his kind recommendations for studying in Japan. Profound thanks are also extended to Ministry of Education, Culture, Sports, Science and Technology of Japan for the financial support to come this far and study at Kyoto University, Japan.

It is also appropriated to my friends, both in Thailand, Kyoto and abroad for their care, assistance and cheer up whenever I needed.

Last but not Least, the author wishes to express his gratitude to his parents, sister, brother, who have been great support and encouragement for his study and life.

Abstract

After the columns and/or members are repaired and strengthened by wrapping or bonding with the strengthening materials, it is unable to identify the corrosion activity under the strengthening materials. The new repair and strengthening system is developed by employing the material called "conductive epoxy resin", which is the epoxy resin added with carbon black (CB) power, to make the strengthening layer to be conductive. The materials used in the research are 2 types of epoxy resin (5%CB and 8%CB epoxy resin) and 3 types of strengthening material (carbon fiber (CF) sheet, aramid fiber (AF) sheet and steel plate). The main objective of this research is to study the effect of conductive strengthening layer to the steel corrosion monitoring method, half-cell potential (HCP) and polarization resistance (PR), by directly measurement on the surface of strengthening materials both in experimental and analytical respects. The materials properties, its volume resistivity and its electrical interaction to the embedded steel, are also investigated.

In the material properties testing, the former, the resistivity test both in longitudinal and vertical direction are measured. The results from both directions with 3 different applied voltages give the consistency results in comparison between different types of layer, but different in magnitude. The results show that the layer applied with CF sheet has much lower resistivity than both the layer without fiber sheet and the layer with AF sheet. And number of layer does not show any obvious different in resistivity.

The latter, the electrical interaction test between steel and conductive strengthening layer is conducted by simulating the galvanic anode system, which is directly electrical connection between these two materials, and observes the direction and magnitude of the current flow. The results indicate that the conductive strengthening layer can be applied on concrete surface, and not leading the steel to be corroded.

In the experimental part, two experiments to investigate the effect of conductive strengthening layer to the electrochemical steel corrosion monitoring technique are conducted. The former one is studied on specimen with uniform Cl^- content in concrete. Beside that, the blister/gap under CFRP/steel plate on concrete surface is also considered. The 8%CB epoxy resin is used to bond strengthening material on concrete specimen's surface. Three types of strengthening materials, CF sheet, AF sheet, and steel plate, are used in the experiment. Moreover, the hole is drilled on the conductive layer in order to compare the reading with one without hole. The corrosion monitoring techniques, which

are HCP and PR, are employed in this experiment. PR is measured by 2 methods that are double rectangular pulse method and AC impedance method. In the case of double rectangular pulse method, the counter electrode is introduced. The conductive layers themselves were used as counter electrode while the copper plate was used in case of specimen without attachment. The results show that values of half-cell potential obtained on all types of conductive layer, with hole and without hole, are in the same tendency with one obtained from concrete surface. In case of PR, The values obtained by double rectangular pulse method give more reliable results than one obtained by AC impedance method that negative and/or enormous values always come out. PR obtained on conductive layer with hole is closer to one of concrete surface than one of conductive layer without hole. It can say in this section that HCP give more satisfactory results than PR.

Due to the good results of HCP in the former experiment, only HCP measurement is investigated in the latter. HCP measurement on conductive strengthening layer on long concrete specimens with longitudinal distribution of chloride content in concrete is studied by varying types of layer, patter of distribution of chloride content, and concrete cover thickness. The results demonstrate HCP measured on conductive layer has the same tendency with HCP measured from concrete surface. The conductive strengthening layer without any applied sheet gives more satisfactory results than the layer with sheet. The patterns of longitudinal distribution of chloride content in concrete also affect to the HCP reading both on concrete surface and conductive strengthening layer.

In the analytical part, the simple analysis of the individual effect of three parameters, which the resistivity of conductive strengthening layer both isotropic and anisotropic properties and the resistivity of concrete, to the potential distribution on the conductive strengthening layer is investigated at the first place. The results indicate that the resistivity of the layer with isotropic property and the resistivity of concrete are found to have an effect on the potential distribution on the layer while the resistivity of the layer with anisotropic property is not. After the basic behaviors are understood from the simple analysis, the precise analysis was proposed by using the experimental results as the case studies. The adjust coefficient and the layer's resistivity variation factor were introduced in the precise analysis to shift the analytical value of potential distribution on the layer to meet with experimental results.

Table of Contents

List of Tables

List of Figures

Chapter 1

Introductions

1.1 General

Steel corrosion is the important problem causes the deterioration of the reinforced concrete (RC) structures and bridges. The reinforcing steel in concrete is normally protected from corrosion by a passive film of the iron oxides on the steel surface that resulted from the alkalinity of the surrounding concrete. The corrosion of steel causes reducing in the cross-sectional area of reinforcing steel, reducing of bond strength, and leading to cracking and/or even spalling of concrete cover. Structures undergo corrosion do not only give the poor performance in terms of appearance, but in extreme cases, it can be lose the structural integrity. Such kind of corrosion may be affected by many factors such as concrete composition, casting process, and exposure to aggressive agents such as chlorides, carbon dioxide, sulphates, acids, etc. in the surrounding environment.

Therefore, one important field that should be emphasized is the reinforcement corrosion inspection in order to accurately investigate the condition of the steel in RC structures and be able to predict its serviceability and remaining service life both for economical efficiency and human safety. As corrosion is an electrochemical process, therefore, the electrochemical techniques are especially well suited to assess the corrosion state of the reinforcement, to mark the corrosion area and to measure the corrosion rate. Two important and well used in the corrosion inspection are half-cell potential and polarization resistance.

In case of RC structures undergo severe deterioration stage, they need to be repaired or to be strengthened. Nowadays, various repair and strengthening options are available for the rehabilitation of the structured damaged by corrosion of steel reinforcement. Some recommendation and standards have been proposed by many organizations, such as RILEM 124-SRC and CEN TC 104 or EN 1504, to help the designers for the choice of repair and strengthening strategy.

Although concrete and steel generally are the primary materials in structural members. But the new materials are introduced more and more these days. One of

them is fiber-reinforced polymer which are used as cost-efficient alternatives for rehabilitation and strengthening of concrete member and/or column because their high stiffness- to-weight and strength to weight ratios, durability, corrosion resistance, and combined with the declination of FRP manufacturing cost, and workability (ease for using, applying and handling), therefore, their uses are increasing and expanding.

There are several type and shape of FRP using nowadays. Among these, FRP sheet has been used to wrap concrete column, to bond under concrete slap or concrete girder. In case of wrapping column, it increases the concrete confinement, increases the column strength and ductility, and also reduces or slows down the corrosion of reinforcing steel due to the reducing the diffusion rate of oxygen and moisture into the concrete, then, increasing in the concrete resistivity, and the ingression of the aggressive substance also reduces as written in some research works (Debaiky et al. (2001), Wootton et al (2003), Maaddawy et al (2006)). Hearn and Aiello (1998) said that the FRP wrapping affected the corrosion of the reinforcement because the consolidation and densification of the corrosion products around the reinforcement hindered the corrosion mechanism by compacting the layer of corrosion residual around the reinforcement and also limiting the access of water and oxygen into uncorroded steel. Moreover some said the repairing corrosion-damage reinforced concrete column with FRP wraps greatly improved their strength and also retarded the rate of post-repair corrosion (Lee et al. 2000).

Most of the previous research done on the effect of fiber-reinforced polymer wraps or bonds are only point to the corrosion resistance ability, but only few concerned the corrosion monitoring techniques. For example, Maaddawy et al.(2006), electrically accelerated the corrosion of the wrapped cylindrical concrete specimens, and directly converted the applied current into the corrosion current density, Debaiky et al. (2001) obtained half-cell potential and polarization resistance by submerging the wrapped cylinder in the water. These methods are only applicable in the laboratory test, not in the in-situ work.

Therefore, the reinforcement corrosion monitoring need to be developed, even in the view of material or the view of methodology, to investigate the reinforcement corrosion state under the strengthening material. One option is to develop a new repair and strengthening system by improving the conductivity of the strengthening layer or coating material, and investigate its effect to the corrosion monitorability. Here, The material, called "conductive epoxy resin" (hereafter, CER), was introduced in order to make the strengthening layer conductive (hereafter, conductive strengthening layer).

1.2Objective of Study

The main objective of the research is to study the effect of a new material, CER,

which uses to bond the strengthening material on the concrete surface, or a new repair and strengthening system, to the electrochemical corrosion monitoring by direct measuring on the surface of the strengthening material as same as simply done in the in situ cases both in the experimental and analytical respects.

1.3 Scope of study

The main interest of the research is to study the effect of these conductive strengthening layers to electrochemical corrosion monitoring both experimental and analytical respects. This research consists of the experiment to investigate the material properties in Chapter 3 and the experiment to study the effect of conductive strengthening layer to electrochemical corrosion monitoring technique in Chapter 4 and 5.

Chapter 2, the theoretical backgrounds of the corrosion of reinforcement, corrosion monitoring and developments, repair and strengthening, and the literatures of the previous researches are summarized.

Chapter 3, the material properties were investigated. The experiment for measurement the resistivity and durability of each conductive strengthening layer were conducted. And the interaction between this material and steel embedded inside the concrete was also carried out.

Chapter 4, the 2 electrochemical corrosion monitoring techniques, which are half-cell potential and polarization resistance, were used to investigate the corrosion activity of the embedded rebar under the conductive strengthening layer bonded on concrete specimen

Chapter 5, only half-cell potential was used to investigate the corrosion activity of the embedded rebar under the conductive strengthening layer bonded on concrete specimen with longitudinal distribution of chloride content.

Chapter 6, the analytical investigation to understand the behavior of the conductive strengthening layer to the potential distribution on the surface was studied. First, the effect of individual parameters was simple analyzed to indicate which factor has the effect to the potential distribution, or not. After that, the analysis was continuality done to understand how come the potential on the layer from the steel's potential and compare the analytical results to the experimental results.

Chapter 7, the overall results of the research are concluded and the recommendation for its application and future work are stated.

Chapter 2

Theoretical Backgrounds and Literature Reviews

In this chapter the general knowledge, theoretical background of steel corrosion mechanism, corrosion monitoring and also its development are explained at the beginning of the chapter. And later, the previous researches concern fiber-reinforced polymers wraps or bonds are referred.

2.1 Corrosion of Reinforcement

Ordinary reinforcing steel inside the concrete is commonly protected from corrosion by a passive film of iron oxides that form at the steel-concrete interface resulting from the high alkaline environment of concrete pore solution (pH 13 to 13.8). This passive film is only a few nanometers thickness and is composed of hydrated iron oxides varying degree of Fe^{2+} and Fe^{3+}. As long as the oxide film is present, the steel remains intact. But if the oxide film is destroyed for example by Cl^- as shown in Figure 2.1, a difference in electrical potential along the steel in concrete, and electrochemical cell is set up. The anodic and cathodic regions are formed, and connected by the electrolyte in the pore water in harden cement paste. The positive charge ferrous ions, Fe^{2+}, at the anode pass into solution while the negative charge free electron, e^-, pass through the steel into the cathode where they are absorbed with the constituents of electrolyte and combine with water and oxygen to form hydroxyl ions (OH^-). These travel through the electrolyte and combine with the ferrous ions to form ferric hydroxide which is converted by further oxidation to rush. The reactions involved are as follows:

Anodic reactions:

$$Fe \rightarrow Fe^{2+} + 2e^-$$

$$Fe^{2+} + 2(OH)^- \rightarrow Fe(OH)_2 \text{ (ferrous hydroxide)}$$

$$4Fe(OH)_2 + 2H_2O + O_2 \rightarrow 4Fe(OH)_3 \text{ (ferrous hydroxide)}$$

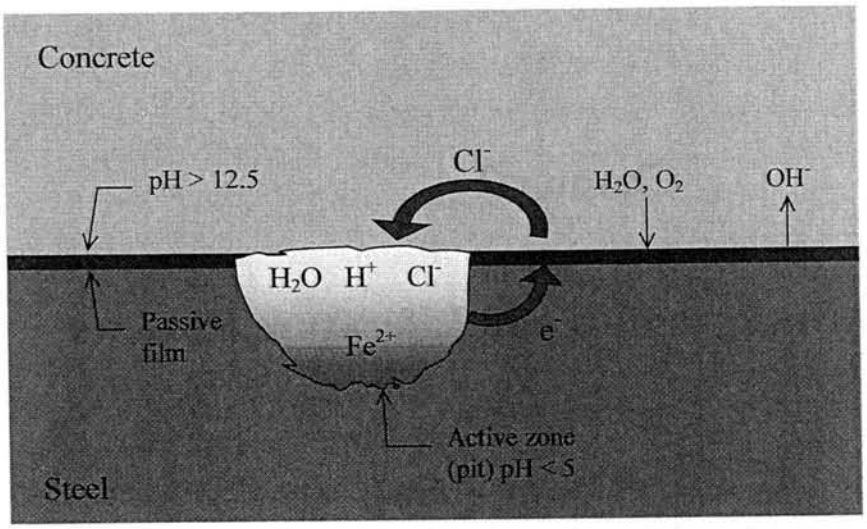

Figure 2.1 Schematic representation of pitting corrosion in concrete.

Cathodic reaction:

$$4e^- + O_2 + 2H_2O \rightarrow \quad 4(OH)^-$$

It can be seen that oxygen is consumed and water is regenerated but it is needed for the process to continue. Thus, there is no corrosion in dry concrete.

The service life of RC structures can be generally divided into 2 phases that are *initiation phase* and *propagation phase*, as shown in Figure.2.2. The former, the reinforcement is usually passive but sometimes some phenomena may lead the reinforcement to lose its passivity, e.g. chloride penetration or carbonation penetration into the concrete taking place. The later the steel starts to be depassivated and over when reaching the limiting state that more corrosion cannot be tolerated.

In the initiation phase, aggressive substances penetrate from outside into the bulk of concrete and then depassivate the reinforcement are carbon dioxide and chloride. The period of initiation phase depends on many factors, e.g. cover depth, concrete quality (porosity and permeability), location of the structure, etc.

In the propagation phase, the corrosion will be able to be taken place in case of the protection film is broken down and water and oxygen are present on its surface. One parameter that can be always used to determine the time taking to reach the maximum acceptable penetration depth of corrosion, in the other way, the minimum acceptable state of structure is "*corrosion rate*", but it need to be kept in mind that the corrosion rate can be changed randomly depends on temperature and humidity.

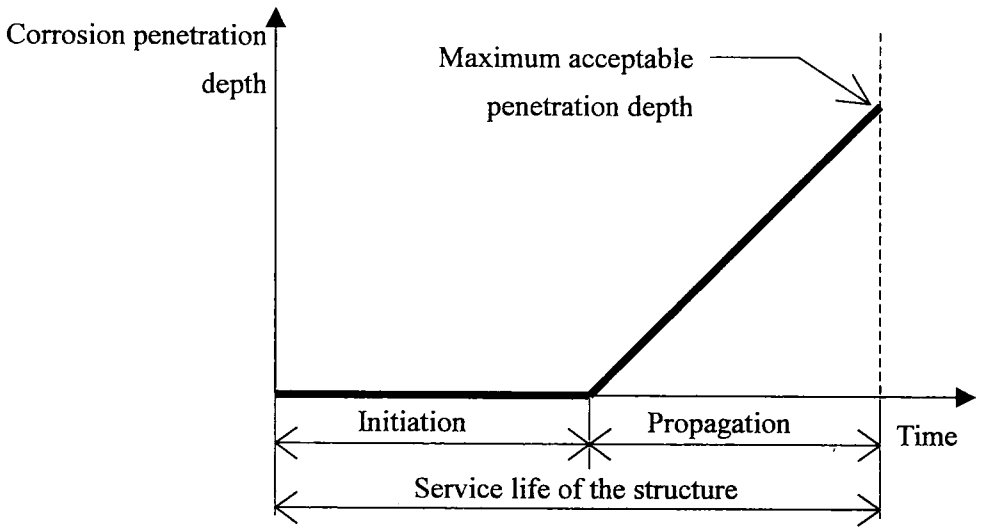

Figure 2.2 Initiation and propagation periods for corrosion in the reinforced-concrete structure

As written in several text books and many literatures, the corrosion induced by carbonation can occur on the whole surface of the steel in contact with carbonated concrete (*general corrosion*), while corrosion induced by chlorides is localize (*pitting corrosion*). In case of the depassivation due to chloride or carbonation just only take place on a small area of reinforcing steel, a phenomenon called "*macrocell*" can be developed between corroding bars and passive bars. This may increase the rate of attack of the reinforcement that is already corroding.

2.2 Corrosion monitoring and development

Two techniques of the electrochemical steel corrosion monitoring, namely half-cell potential and polarization resistance, that quite simple and always be used are explained.

2.2.1 Half-Cell Potentials

The simplest way to assess the severity of steel corrosion is to measure the corrosion potential. The corrosion potential, E_{corr} (half cell reinforcing steel/concrete), is measured as potential difference (voltage) against a reference electrode (half-cell). One can measure the potential difference between a reference electrode placed on the surface of the concrete with the reinforcing steel underneath [1]. Figure 2.3 shows the basis of half-cell potential measurement. The reference electrode is connected to the positive terminal of voltmeter and steel reinforcement to the negative terminal. The technique is very well known, be described in the American National Standards

ASTM C876 [2] that also provides general guidelines for evaluating corrosion probability in concrete structures as outlined in Table 2.1.

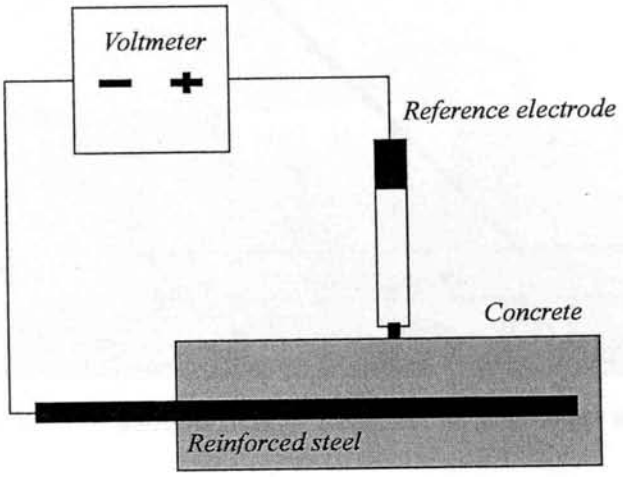

Figure 2.3 Basis of the half-cell potential measurement technique

Table 2.1: Probability of corrosion according to half-cell reading from ASTM C876

Half-cell potential reading vs. $Cu/CuSO_4$	**Corrosion activity**
Less negative than –0.200 V	90% probability of no corrosion
Between –0.200 V and –0.350 V	Corrosion in that area is uncertain
More negative than –0.350 V	90% probability of corrosion

2.2.1.1 Reference Electrodes

It is necessary to quote the reference electrode used for half-cell potential measurements. In practice the following reference electrodes with a defined, constant and reproducible potential versus the standard hydrogen electrode (SHE) are used [3]:

Copper/copper sulfate sat	CSE	+0.318 V SHE
Calomel (Hg/Hg2CL2) KCl sat	SCE	+0.241 V SHE
Silver chloride (Ag/AgCl) KCl sat	SSCE	+0.199 V SHE

For on site work, the saturated copper-copper sulfate electrode is most robust and is sufficiently accurate, although errors may arise due to contamination of the concrete surface with copper sulfate. Calomel and silver chloride electrodes are used more in laboratory work because of high accuracy. The base potential of the reference electrodes depends on the concentration of the electrolyte, thus the care has to be taken to operate in saturated conditions.

Table 2.2: Probability of corrosion according to half-cell reading by silver chloride (Ag/AgCl)KCl saturated electrode (SSCE)

Half-cell potential reading vs. Ag/AgCl	Corrosion activity
Less negative than –0.080 V	90% probability of no corrosion
Between –0.080 V and –0.230 V	Corrosion in that area is uncertain
More negative than –0.230 V	90% probability of corrosion

The silver chloride (Ag/AgCl)KCl sat. (SSCE) was used in this research. Refer to the potential difference between CSE and SSCE, the evaluating corrosion of SSCE in concrete structures was shown in **Table 2.2**.

2.2.1.2 Voltmeters

Voltmeter is a necessary device that is used to obtain the value of half-cell potential. As refer to ASTM C876, "**Voltmeter** - the voltmeter shall have the capacity of being battery operated and have ±3 % end-of-scale accuracy at the voltage ranges in use. The input impedance shall be no less than 10 MΩ when operated at the full scale of 100 mV. The divisions on the scale used shall be such that a potential difference of 0.02 V or less can be read without interpolation."

2.2.1.3 Factor Influencing Half-Cell Potential Readings

Before interpreting half-cell potential data, the factors such as oxygen, chloride concentration, and concrete resistance must be considered. All of these factors have a significant influence on the readings. In simple comparison of half-cell potential obtained data with the ASTM guideline could prove meaningless. For instance, a more negative reading of potential is generally considered to indicate a higher probability of corrosion. But this general rule may not always be valid because many factors can shift the half-cell potential reading towards more positive or negative values but these shifts may not be related to the severity of the steel corrosion. The factors that can influence the potential reading are listed below:

- Oxygen concentration
- Carbonation
- Chloride ion concentration
- Use of corrosion inhibitors
- Epoxy-coated and galvanized reinforcing steel

- Concrete resistance
- Organic coating and sealers
- Temperature
- Water content
- Etc.

2.2.2 Polarization Resistance

Polarization resistance (PR) can be related to the rate of corrosion for metals. PR measurements are an accurate and rapid way to measure the corrosion rate. Real time corrosion monitoring is a common application. The technique can also be used as a way to evaluate alloy, inhibitors, and so forth in order of resistance to corrosion.

In this test method, a sufficiently small potential scan, $\Delta E(t)$, defined with respect to the corrosion potential ($\Delta E = E\text{-}E_{corr}$), is applied to a metal sample. The resultant currents are recorded. The polarization resistance, R_p, of a corroding electrode is define from Eq.2.1 as the slope of a potential versus current density plot at $I = 0$:

$$R_p = \left(\frac{\partial \Delta E}{\partial I} \right)_{I=0, \partial E / \partial t \to 0} \quad \text{.... (2.1)}$$

The current density is given by I. the corrosion current density, I_{corr} is related to the polarization resistance by the Stern-Geary coefficient, K.

$$I_{corr} = 10^6 \frac{K}{R_p} \quad \text{.... (2.2)}$$

The dimension of R_p is ohm square centimeter (Ωcm^2), I_{corr} is ampere per square centimeter (A/cm^2), and K is in volt (V). The Stern-Geary coefficient is related to the anodic, β_a, and cathodic, β_c, Tafel slope as per Eq.2.3.

$$K = \frac{\beta_a \beta_c}{2.303(\beta_a + \beta_c)} \quad \text{.... (2.3)}$$

The unit of the Tafel slopes is volt (V). The corrosion current density, I_{corr} can be converted to the corrosion rate, v as shown in Eq.2.4 by using the 2nd law of Faraday.

$$v = \frac{mI_{corr}}{zF} \quad \ldots(2.4)$$

where

v	*Corrosion rate ($g/cm^2/s$)*
m	*Atomic weight for iron (55.85 g)*
I_{corr}	*Corrosion current density (A/cm^2)*
z	*Metal valences, for iron = 2*
F	*Faraday's constant (96,500 A·s)*

Beside, the corrosion rate is expressed in the unit of mass per unit area per unit time ($g/cm^2/s$). In addition, the corrosion rate is expressed in another unit, called average corrosion depth, by conversion the unit of corrosion current density, I_{corr} from 1 $\mu A/cm^2$ as shown in Eq.2.5 and 2.6 to mm/year as shown in Eq.2.7. (Density of steel = 7.87 g/cm^3) [14]

$$1\ \mu A/cm^2 \rightarrow 2.5\ mdd \quad \ldots(2.5)$$
$$(mmd : mg/dm^2/day)$$

$$1\ \mu A/cm^2 \rightarrow 9.13\ mg/cm^2/year \quad \ldots(2.6)$$

$$\mu A/cm^2 \rightarrow 11.6x10^{-3}\ mm/year \quad \ldots(2.7)$$

In concrete, the main difficulty in use of the technique arises from the irregular distribution of the current applied through the counter electrode of much small dimension than the reinforced concrete structure under test. Therefore an electrical signal seems to be vanished with increasing distance from the counter electrode location. To solve this problem Feliu et al. [5, 6] developed a concept of "transmission line" in order to control the uniform distribution of the signal applied to the reinforcement. Due to the transmission line model, two approaches were derived. The first one uses the response in current resulting from the application of the potential step to the reinforcement with the aid of the smaller counter electrode that placed on the concrete beam. The second one is based on the decrease of the potential applied in this manner in terms of distance from the referred counter electrode.

Feliu et al. [7] proposed the possibility of using guard ring technique that consists of the second counter electrode located concentrically around the first one. Then the signal can be confined to a given area of the structure located below the counter electrode. Figure 2.4 shows the schematic representation of the guard ring

technique. Both counter electrodes are maintained at the same electric potential with respect to the working electrode, which allows measurement of current flowing only from the center electrode. Therefore, while a central auxiliary electrode locally polarizes the bar, another one provides polarization to the rest of reinforcing steel around the area affected by the central one. Finally the central electrode's current is known, as well as the area of the reinforcement affected by it, and then determination of R_p is immediately made.

Nowadays, the guard ring technique is well established and a number of the commercial devices are available. Among these; SRI machine, was used in this research, also employing the guard ring principle for confining the applied current within the area of central counter electrode in order to obtain the local polarization resistance.

At present, the standard for evaluation of polarization resistance of steel in concrete has not been generally established yet. The researchers and/or research institutes are trying to propose the standard for evaluation. Among these, the standard for evaluation of polarization resistance, which is being proposed by Comité Euro-International du Béton (CEB), is shown in Table 2.3. Beside that, the relation between each type of corrosion rate and evaluation of corrosion rate is also shown.

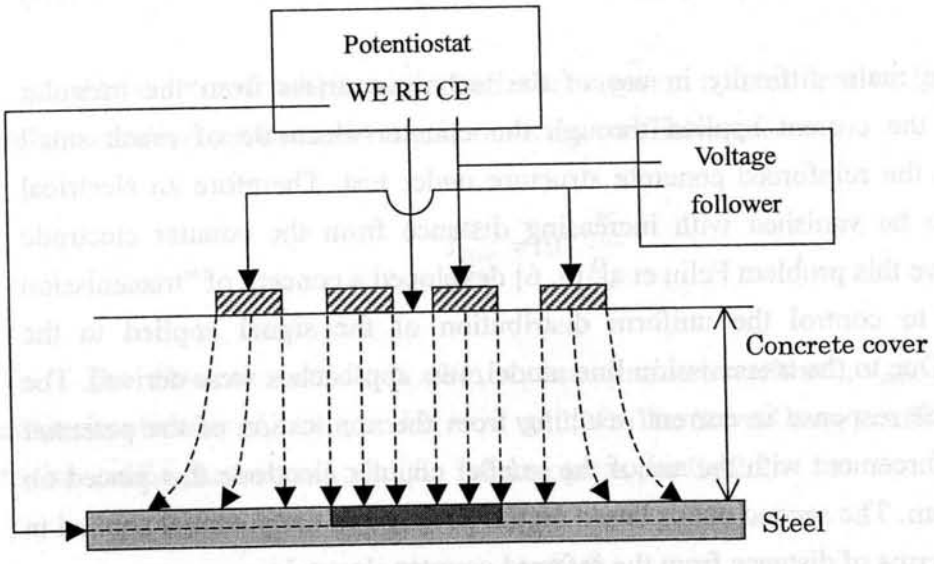

Figure 2.4 Schematic representation of the use of the guard ring. It shows an ideal case, in which the current flowing from the central CE (A) is directed exclusively to polarizing the portion of the rebar beneath it. The discontinuous arrow represents the current lines and direction.

Table 2.3: Standard for Evaluation of polarization resistance (draft) by CEB

Polarization* resistance ($k\Omega \cdot cm^2$)	Estimated value of corrosion rate			Evaluation of corrosion rate
	Corrosion current density I_{corr} ($\mu A/cm^2$)	Corrosion loss* (mg/cm^2/year)	Corrosion depth* PDY (mm/year)	
More than 130	Less than 0.2	Less than 1.8	Less than 0.0023	Non-activated state (no corrosion), or very low rate of corrosion
Between 52 and 130	Between 0.2 and 0.5	Between 1.8 and 4.6	Between 0.0023 and 0.0058	Low to moderate degree of corrosion rate
Between 26 and 52	Between 0.5 and 1	Between 4.6 and 9.1	Between 0.0058 and 0.0116	Moderate to high degree of corrosion rate
Less than 26	More than 1	More than 9.1	More than 0.0116	Severe state, high corrosion rate

** The value of polarization resistance, corrosion loss rate and corrosion depth rate are converted from corrosion current density by using Eq.(2.2) with K=0.026, Eq. (2.6) and Eq.(2.7), respectively.*

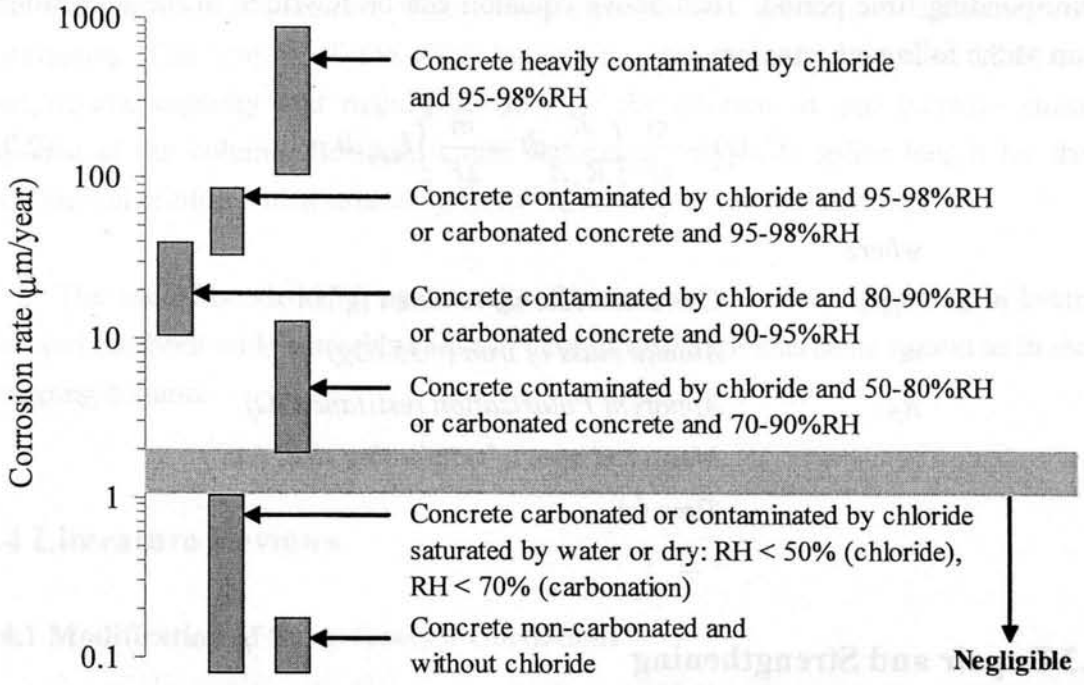

Figure 2.5 Schematic representation of corrosion rate of steel in different concretes and exposure condition

From Table 2.3, the corrosion rate can be considered non-activated state if it is lower than 2.3 μm/y, low to moderate between 2.3 to 5.8μm/y, moderate to high

between 5.8 to 11.6μm/y, and severe state for value bigger that 11.6μm/y. Figure 2.5 shows the typical ranges of variation of the corrosion rate in carbonated or chloride-contaminated concrete as a function of relative humidity (RH) of the environment.

The corrosion losses were calculated using the I_{corr} values from PR data using a K value of 26 mV as in all literature. The following equation (2nd law of Faraday) was used to determine the corrosion weight losses.

$$W_t = (W_a \,.\, I_{corr}.t) / z.F) \qquad \text{....(2.8)}$$

where

W_t	*Corrosion loss of steel (g)*
W_a	*Atomic weight for iron (55.85 g)*
t	*Time (s)*

As each I_{corr} versus time result had been recorded, the total corrosion loses was calculated by adding the incremental corrosion weight loss for each I_{corr} over the corresponding time period. Then above equation can be rewritten in the integration form as the following equation.

$$C_d(t) = \frac{m}{zF}\int_0^t \frac{K}{R_p A}dt = \frac{m}{zF}\int_0^t I_{corr}dt \qquad \text{...(2.9)}$$

where

$C_d(t)$	*Corrosion loss up to time t (g/cm^2)*
m	*Atomic mass of iron (=55.85g)*
R_p	*Apparent Polarization resistance (Ω)*
A	*Measured area of reinforcing steel (cm^2)*
t	*Time (s)*

2.3 Repair and Strengthening

Structural repair of RC structures is becoming an increasingly important option for all deterioration in constructed facility. The earliest applications of external steel plate bonding method were reported in South Africa and France [13], and this method has been used quite extensively around the world. Although steel plate bonding and steel patching and stitching techniques provides a solution for externally reinforcing

concrete structure members, this method also have several disadvantages, which include transportation, handling, and installation of heavy plates, corrosion of plates, limited delivery lengths of plates which necessitates the work and difficulty of welding, the need for massive and expensive scaffold to hold plate in position during adhesive curing, and the need to prepare the steel surface bonding. Thus, the alternative material and techniques are encouraged, such as FRP composite technique.

A recently established technique for strengthening reinforced concrete structures has been much concerned with the application of FRP material both for new constructions and existing structures. The advantages of FRP composites are lightweight, high strength, corrosion resistance and ease of application. The application of the use of FRP can be obviously classified into two groups; which are the use of FRP bars for new RC and PC or external cables, and externally bonded reinforcement (EBR). This EBR has the potential to be one of the most effective repair and strengthening methods in the future, that was confirmed by the major part of the European activities focus on externally bonded FRP reinforcement.

Column wrapping capitalizes on all of the advantage of FRP. The high cost of this material is compensated when comparing to the speed and efficiency of installation. The ability of the FRP to confine the concrete increases both the compressive capacity and mainly ductility of the column. It can increase shear capacity of the column. Besides, it also reduces the required splice length for the longitudinal reinforcement extending from the footing or into the pile cap.

The use of bonded FRP systems for flexural and shear strengthening in beam and wall has been wide spread because of ease of installation as same reason as in the wrapping column.

2.4 Literature Reviews

2.4.1 Modification of Stern-Geary's Coefficient

Baweja et al. (2003) investigated the corrosion rates of steel in concrete by examining long term data on concrete slab partially immersed in 3% NaCl solution by using polarization resistance technique. I_{corr} (corrosion current) values were determined from the polarization resistance R_p data using a range of Stern-Geary Constant K values. The K value of 26 mV usually is widely used. In Baweja's improved method,

the relationships between E_{corr} and I_{corr} were analyzed. Better relationships were obtained when K values were calculated from E_{corr} data using equations developed in his study.

2.4.2 Polarization resistance measurement by AC impedance method and rectangular pulse method

Hattori et al. (2001) conducted the research topic, "Prediction of degradation and performance in RC beams subjected to chloride attack by corrosion monitoring", by considering the corrosion monitoring for chloride attack which measured polarization resistance by rectangular pulse method or AC impedance method. Results in AC impedance method for measuring polarization resistance of the embedded reinforcing steel can better predict corrosion loss rate than rectangular pulse method.

2.4.3 Tendency of corrosion current density

H. Yalcyn et al. (1996) evaluated the reinforcement corrosion by measuring the corrosion potentials and corrosion density using linear polarization resistance (LPR) technique. For polarization measurements, the galvanostatic method was used for obtaining the anodic and cathodic polarization curves. From the cathodic and anodic Tafel plots, β_c and β_a values were determined. The calculation of the steel bars in concrete, Stern-Geary equation was used:

$$I_{corr} = \frac{1}{R_p} \frac{\beta_a \beta_c}{2.3(\beta_a + \beta_c)}$$

where R_p denotes the polarization resistance which was evaluated using the slope of linear part of the measured polarization curve. In conclusion, the corrosion current density was very high at the early stage and decreases by time. And Yalcyn proposed the equation of corrosion rate in the form of exponential quantitative relation between the corrosion rate (I_{corr}) and time (t) as shown below

$$I_{corr} = I_0 \exp(-Ct)$$

where C was termed as concrete corrosion constant having a value of 11×10^{-3} day^{-1} for the types of concrete samples under his consideration

DW. Law et al. (2003) evaluated the corrosion loss of steel reinforcing bars in

concrete using linear polarization resistance (LPR) measurements. LPR was obtained with three conditions of environments that are nitrogen rich environment, chloride exposure, and carbonation exposure. The corrosion rate was rapidly initiated for all specimens in a 2-4 weeks period and then stabilized at mean value of 1-2μA/cm^2 for both the chloride and carbonation specimens. The corrosion rate for carbonation specimens has remained within that range for the duration of the trial period (about 1700days). Moreover, some cycling in the rate is observable which is consistent with seasonal variations in temperature and humidity. Then the specimens in the chloride environment show a significant increase in corrosion rate after 400-500 days; a corrosion rate of up to 10μA/cm^2 being observed. While there is the undercurrent of seasonal fluctuations there is considerably more scatter on these results when compared to the carbonation data. The results show the sensitivity of the measurement to environmental conditions.

2.4.4 Fiber-reinforced polymer wrapped concrete

Maaddaway et al (2006) studied the effect of the fiber-reinforced polymer warps on corrosion activity and concrete cracking in chloride-contaminated concrete cylinders. The study parameters were applied potential, presence of FRP wraps, and reinforcing steel diameter. The results showed that at the same applied potential, FRP wraps cylinders effectively reduced the corresponding current, concrete expansion, and steel mass loss. For the same applied potential, the current density increased as the bar diameter decreased.

Lee et al (2000) conducted the experimental study on the simulation of corrosion in large-scale reinforced concrete columns and their repair using carbon fiber reinforced polymer (CFRP). The accelerated corrosion columns were wrapped with CFRP, and tested to the structural failure or going further for post-repair accelerated corrosion, monitoring, and then testing. Their results indicated that the CFRP repair is greatly improved the repair member strength and also retard the rate of post-repair corrosion.

Wootton et al (2003) have done the research concerning corrosion of steel reinforcement in carbon fiber-reinforce polymer wrapped concrete cylinders. Their study parameters were 13 different surface treatment options by varying types of epoxy, wrap fiber orientation, and number of wrap layers. Their results also indicated that the FRP wrapped specimens was much better than that of just only coated with epoxy. Epoxy type had significant effect on the performance of samples regarding

their resistance to corrosion. Finally, they stated that the carbon FRP wraps were able to confine concrete, slow down the deterioration from cracking and spalling and inhibiting the passage of salt water.

2.4.5 Corrosion monitoring on FPR sheet wrapped concrete

Debaiky et al. (2001) investigated the effect of Carbon Fiber Reinforced Polymer (CFRP) wraps on the corrosion of the reinforcing steel and the response of the cylinders during exposure and under axial compression. The cylinders were wrapped either before exposure or at intermediate stages after 100 and 200 days' exposure. The corrosion activity during exposure was monitored using the three electrodes linear polarization method, half-cell potentials, radial expansion, and crack mapping. Compressive test was done at 100, 200 and 300 days.

Half-cell potential measurement was done by placing the cylinder in tap water at full depth, connecting the steel cage to the +ve terminal of a high impedance portable voltmeter, dipping the electrode in the water adjacent to the cylinder and connecting it to the –ve terminal of the voltmeter as shown in Figure 2.6(b). The potential difference measured was then translated into a probability of corrosion activity.

Polarization resistance, testing was done by a potential sweep using standard equipments (ASTM G59-97), which are potentiostat and X-Y recorder. The interconnected steel cage acted as a +ve terminal while an external galvanized wire mesh placed in the water next to the cylinder worked as the –ve terminal as shown in Figure 2.6(c) and (d). The entire steel surface area was assumed to be polarized during the PR testing.

Debaiky et al. concluded that the half-cell potential readings could be misleading, and perhaps confusing, when used to judge corrosion activity in smaller scale specimen. For LPR measurements can be performed with high accuracy in reinforced concrete specimens using external cathodes. Moreover, the experimental result indicated that the CFRP significant decreased in corrosion activity and chlorides ingression for the wrapped cylinders, and the number of CFRP layers applied had no affect in these aspects.

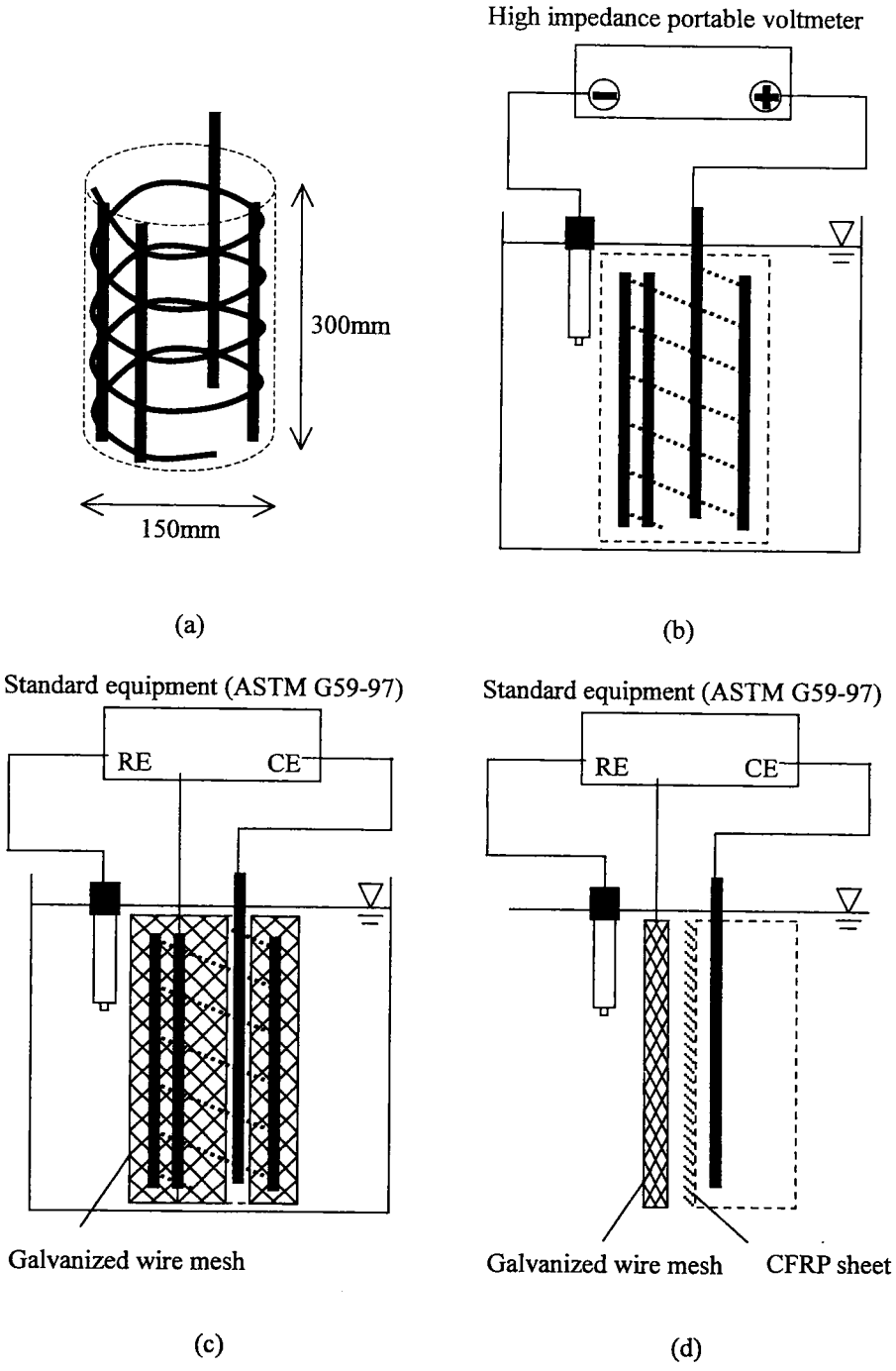

Figure 2.6 Debaiky's experiment detail; (a) Schematic of the cage, (b) Half-cell potential measurement details, (c) LPR measurement details and (d) Simplification of LPR measurement

2.4.6 Analysis on Half-Cell Potential Measurement and Current Flow

Kobayashi (2001) studied the characteristic of the double rectangular pulse method and the AC impedance method, and also the quantitative estimation of corrosion loss of reinforcing steel. In this research, the Laplace's equation was used and employed

the different method in 2D analysis. The results showed the different of half-cell potential distribution and current flow pattern due to three different methods, which are double rectangular pulse method, AC impedance method with double counter electrode, and AC impedance method with only center electrode.

Leelalertkiet (2004) also made the same study as Kobayashi in the half-cell potential measurement and current flow by boundary element method in 3D analysis, and also sequence researches on the analysis of hale-cell potential distribution.

Chapter 3

Properties of Conductive Strengthening Layer

In this chapter consists of the experiment for measurement the resistivity of conductive strengthening layer before and after expose to three exposure environments and the anode/cathode classification between the conductive strengthening layer and reinforcing steel.

3.1 Resistivity and Durability of Conductive Strengthening Layers

Many ASTM standards are provided for electrical resistivity measurement, for example, ASTM C611-98 (Reapproved 2005): Standard Test Method for Electrical Resistivity of Manufactured Carbon and Graphite Article at Room Temperature, ASTM D6120-97 (Reapproved 2002): Standard Test Method for Electrical Resistivity of Anode and Cathode Carbon Material at Room Temperature, ASTM D2739-97 (Reapproved 2004): Standard Test Method for Volume Resistivity of Conductive Adhesives. But they are not applicable to this test. Therefore, The report of Osaka Research Center of Konishi public company was used as the original guideline to the resistivity measurement of this research. In the report, the resistivity of the conductive epoxy resins was calculated from the resistance measured at 25V by the digital insulation resistance reading 2426 model (Yokogawa Instrument Co.,Ltd) on the 130x20x1mm size of sample work piece (conductive epoxy resin) as showed in the Figure 3.1. The numbers (1) to (4) indicated the electrical line connection position of positive and negative electrode when measured.

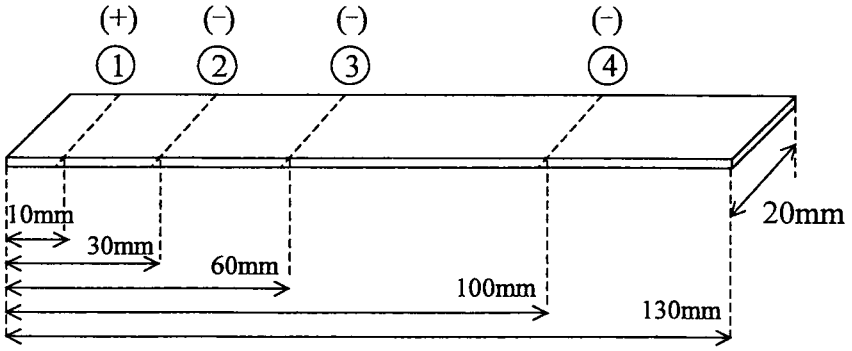

Figure 3.1 The conductive epoxy resin sample work piece

From the Figure 3.2, x-axis indicates measure distance and y-axis indicates the measured resistance value. The resistance at 0cm of measure distance of the graph is the connection resistance. Then, the volume resistivity can be calculated by the Eq. (3.1).

$$\textit{Volume resistivity } (\Omega m) = \frac{(\textit{measured resistance} - \textit{connection resistance}) \times \textit{sheet thickness}}{\textit{measured distance}} \qquad (3.1)$$

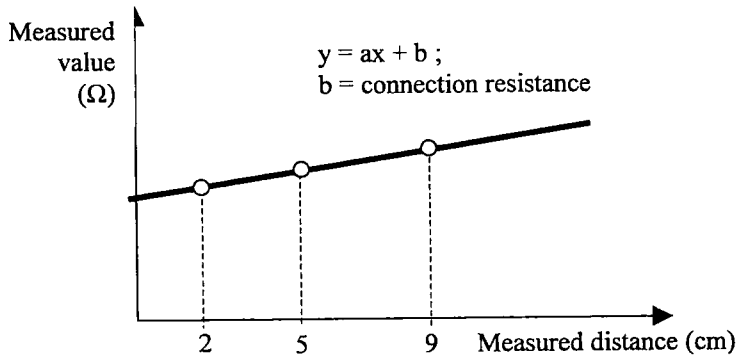

Figure 3.2 Plot of measured results

In this experiment, the volume resistivity of the conductive strengthening layers, both before and after expose to the aggressive condition such as temperature, humidity, chloride environment, was examined.

3.1.1 Experimental Program

3.1.1.1 Factors

The parameters used in the experiment are type of layer, exposure conditions, and applied voltage.

Type of layer: Two types of conductive epoxy resin were employed in order to investigate the resistivity of various types of conductive strengthen layer. The first one is conductive epoxy resin with 5% carbon black that has low conductivity but good workability, and the other one is conductive epoxy resin with 8% carbon black that has high conductivity. Two strengthening material, which are carbon fiber sheet (CF) and aramid fiber sheet (AF), are used in the test. Hence, 6 types of conductive strengthening layers used in the experiment can be listed below.

1. 5% carbon black epoxy resin
2. 5% carbon black epoxy resin with 1 ply of CF sheet
3. 5% carbon black epoxy resin with 2 plies of CF sheet
4. 8% carbon black epoxy resin
5. 8% carbon black epoxy resin with 1 ply of CF sheet

6. 8% carbon black epoxy resin with 1 ply AF sheet

Exposure Conditions: Three conditions, which used for the investigation of the endurance of the material when subject to the environment, were selected in order to, as listed below.

1. Air at 40°C, 60%RH
2. Cycle of 3% NaCl solution at 20°C
3. Cycle of 3% NaCl solution at 40°C

Apply voltage: Three values of voltage, which are DC 3V, DC 10mV and AC 10Hz 10mV, were used to measuring the resistance of the conductive strengthening layer.

Table 3.1 Properties of conductive epoxy resin

Properties	Type of conductive epoxy resin		Unit	Test method
	5%CB	8%CB		
Viscosity	17	> 2000	Pa.s	JIS K6833
Working time	69	67	min.	
hardening time	17.4	15.9	hrs.	RCI Drying Recorder
Density	1.17	1.17		JIS K7112
Tensile strength	36.7	31.5	N/mm^2	JIS K7113
Tensile elastic modulus	1700	1550	N/mm^2	
Compressive strength	71.9	76.9	N/mm^2	JIS K7208
Compressive elastic modulus	2500	2750	N/mm^2	JIS K7208
Pull off strength	-	3.26	N/mm^2	
Bending strength	62.4	52.4	N/mm^2	JIS K7203
Tensile shear bonding strength	15.7	14.4	N/mm^2	JIS K6850
Hardness by meter type D	85	85	HDD	JIS K7215
Volume resistivity	$6x10^5$	$5x10^3$	Ω.cm	

Table 3.2 Properties of fiber sheets

Properties	Carbon Fiber sheet[*1]	Armid Fiber sheet[*2]
Thickness (mm)	0.11	0.193
Unit weight (g/mm^2)	200	280
Density (g/cm^3)	1.80	1.45
Tensile strength (N/mm^2)	3430	2060
Young's Modulus ($x10^5 N/mm^2$)	2.3	1.18
Elongation	0.015	0.017
Volume resistivity (Ω.cm)	$5.0x10^6$	$8.8x10^{14}$

*[*1] Torayca Co,Ltd, UT 70-20, [*2] Fibex Co,Ltd, AK-40/K-49*

3.1.1.2 Materials and Equipments

The properties of material and the equipments used in the experiment are as follows:

Epoxy resin: Two types of conductive epoxy resin were used and their properties are shown in Table 3.1. These epoxy resins are mixed with two agents called main agent and hardening agent in a ratio of 224/100 and 215/100 for the epoxy added with carbon black powder of 8% and 5%, respectively.

Fiber sheet: Carbon fiber (CF) sheet and aramid fiber (AF) sheet were used and their properties are shown in Table 3.2.

Stainless steel plate: The 0.5mm-thickness stainless steel plate with the dimension of 1x7cm was used as the electrical connection between the sample work piece and the measurement machine.

Plastic plate: The plastic plate of the dimension 16x6cm was used as the base of the sample work piece. This plate consists of two layers of 1.0mm-thickness (lower-base) and 0.5mm-thinkness (upper-base). The 0.5mm-thickness plates is cut with the size of 1.05x5.5cm at 1, 5, 8, and 14cm from the left end, then the 0.5mm thickness plastic plate is bonded on the 1.0mm-thickness plate. To finish the base of work piece, four stainless steel plates are buried in the cutting space of 0.5mm-thickness plate above 1.0mm-thickness plate, as shown in Figure 3.3.

Equipments: The machine called "***LCR meter***" was employed in this measurement.

3.1.1.3 Sample Work Pieces

Test sample: The test sample with size of 140x50mm with various thickness *(t)*, which depends on type of layer and application method, were applied on the plastic plate base buried with stainless steel, as shown in Figure 3.4. The value of 50mm-width was selected as same as the width of the specimen making in chapter 4, section 4.2.

Type of Layer: As written in the previous section 3.1.1, 6 conductive strengthening layers were applied on the prepared plastic bases. Table 3.3 shows the number of sample in each type of layer and the exposure conditions to test the durability of the layers. The total amounts of sample in each series are shown in the last column, in each series the samples are divided into 3 groups of exposure conditions.

Application of Conductive Strengthening Layer: Figure 3.5 shows the strengthening materials application procedure. The procedure to apply the conductive strengthening layer in each series is explained in detail here.

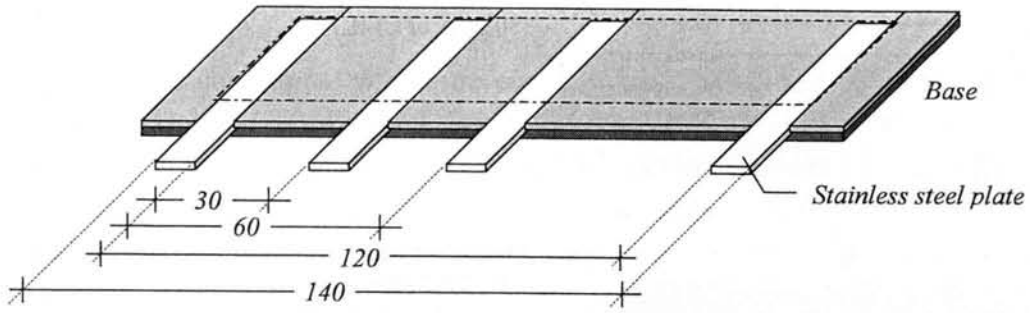

Figure.3.3 Base of sample work piece

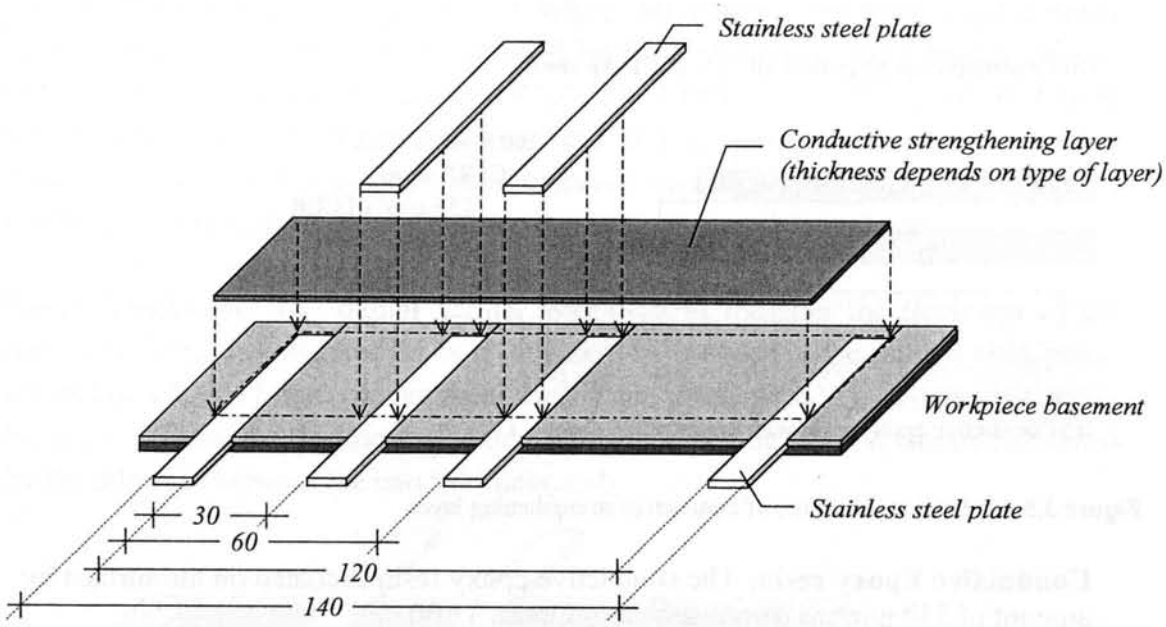

Figure 3.4 Sample work piece

Table 3.3 Types of layer and number

	Type of layer	Exposure conditions			Total
		Air	3%NaCl solution		
		40°C	20°C	40°C	
1	5% carbon black added epoxy resin	4	4	4	12
2	5% carbon black added epoxy resin with 1 ply of CF sheet	4	4	4	12
3	5% carbon black added epoxy resin with 2 plies of CF sheet	2	2	2	6
4	8% carbon black added epoxy resin	4	4	4	12
5	8% carbon black added epoxy resin with 1 ply of CF sheet	4	4	4	12
6	8% carbon black added epoxy resin with1 ply of AF sheet	2	2	2	6

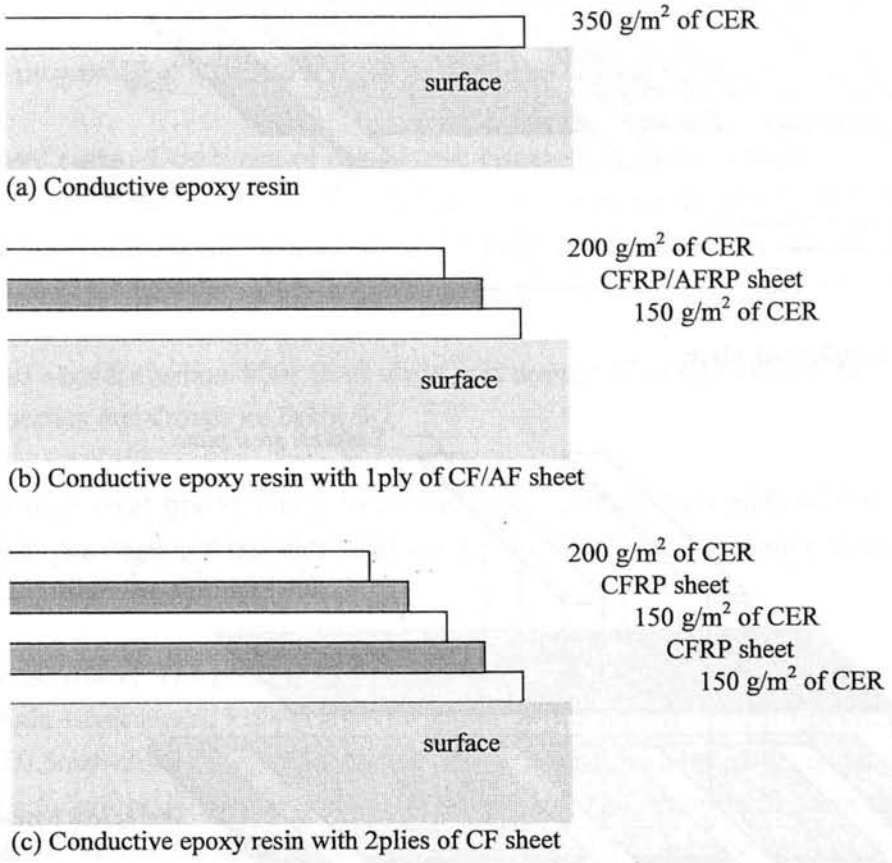

(a) Conductive epoxy resin

(b) Conductive epoxy resin with 1ply of CF/AF sheet

(c) Conductive epoxy resin with 2plies of CF sheet

Figure 3.5 Application procedure of conductive strengthening layer

Conductive Epoxy resin: The conductive epoxy resin is coated on the surface by amount of 350 g/m^2 as demonstrated in Figure 3.5(a).

1 ply of CF sheet or AF sheet: The conductive layer could be divided into 3 sub-layers, the lower conductive epoxy resin sub-layer, CF or AF sheet, and the upper conductive epoxy resin sub-layer as shown in Figure 3.5(b). The 150 g/m^2 and 200 g/m^2 were used for lower and upper conductive epoxy resin, respectively.

2 plies of CF sheet: The conductive layer could be divided into 5 sub-layers, the lower conductive epoxy resin sub-layer, CF sheet, middle conductive epoxy resin sub-layer, CF sheet, and the upper conductive epoxy resin sub-layer as shown in Figure 3.5(c). The 150g/m^2, 150g/m^2 and 200 g/m^2 were used for lower, middle and upper conductive epoxy resin, respectively.

After the layer application, the samples were left for 1 week to let the conductive epoxy resin set and dry.

3.1.1.4 Exposure Conditions

Three expose conditions, which are cured in air at 40°C and 60%RH, subjected to 3%NaCl solution wetting and drying cycle at 20°C and 40°C, were used to accelerated the deterioration of the sample. Due to the shortage of time, only 30 days of exposure was done for the durability test. In case of sample subjected to 3%NaCl solution, 6hr-wet and 18hr-dry cycle was employed.

3.1.1.5 Measurements

Electrical Resistance: The resistance between two measurement point was measured both in longitudinal and vertical direction by LCR meter machine with 3 values of voltage control measurement that are DC 3V, DC 10mV and AC 10Hz 10mV at room temperature. The resistance values were read at 1 minute after the measure started. Figure 3.6 shows the positive and negative connection to the LCR meter in longitudinal and vertical direction of the conductive strengthening layer.

Layer Thickness: The digital vernier was used to measure the thickness of the sample work piece at 0.5 and 15.5cm (thickness of the base of the sample work piece, t_1), and at 3.5, 7, 11.5cm (thickness of the sample work piece, t_2), as demonstrated in Figure 3.7. Then, the thickness of conductive strengthening layer, t, can be calculated by the different between the two thickness, t_2-t_1.

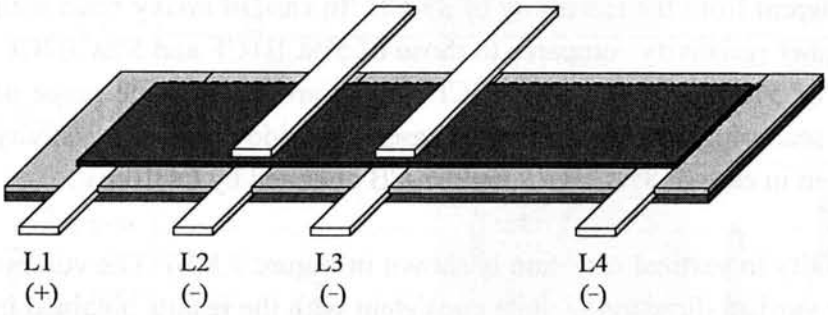

(a) Measurement setting in longitudinal direction

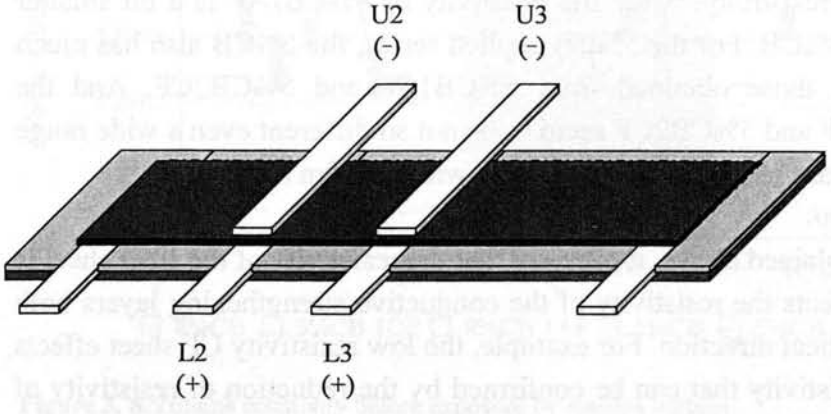

(b) Measurement setting in vertical direction

Figure 3.6 LCR meter connection

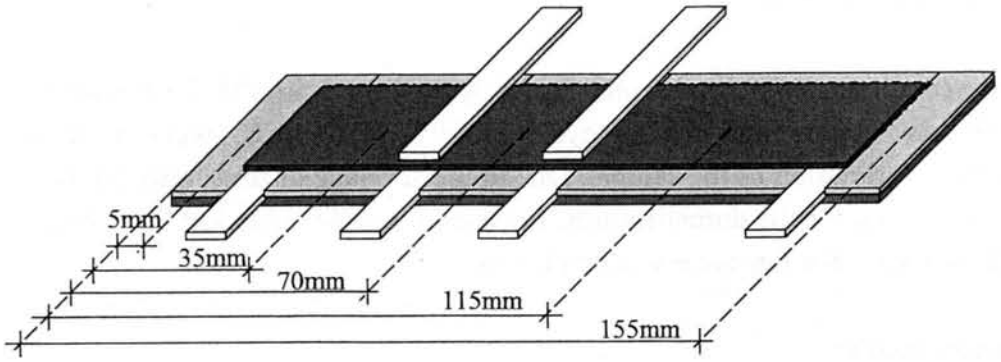

Figure 3.7 Thickness measuring position

3.1.2 Experimental Results

3.1.2.1 Volume Resistivity Before Exposure

Figure 3.8(a) and (b) shows the value of volume resistivity classified by the applied voltages in longitudinal and vertical directions, respectively.

From Figure 3.8(a), the values of volume resistivity measured in longitudinal direction are consistent to each other in all applied voltages. In case of the surface applied with 8%CB added epoxy resin, 8%CB1CF has lowest resistivity compares to those of 8%CB and 8%1AF applied surface. And, the resistivity of 8%CB1AF seems to be not so much different from the resistivity of 8%CB. In case of epoxy resin with 5%CB, 5%CB has higher resistivity compares to those of 5%CB1CF and 5%CB2CF. While, the resistivity of 5%CB1CF and 5%CB2CF almost are in the same range of resistivity even some scatterings occurred in some cases. A wide range of resistivity (1000times) can be seen in case of 8%CB1CF and 5%CB obtained by DC10mV.

The volume resistivity in vertical direction is shown in Figure 3.8(b). The volume resistivity obtained in vertical direction is quite consistent with the results obtained in the longitudinal direction. In the 8%CB conductive epoxy resin applied series, 8%CB1CF has lowest resistivity, while the resistivity of 8%CB1AF is a bit smaller than the resistivity of 8%CB. For the 5%CB applied series, the 5%CB also has much bigger resistivity than those obtained from 5%CB1CF and 5%CB2CF. And the resistivity of 5%CB1CF and 5%CB2CF seem to be not so different even a wide range of data can be seen in case of 5%CB2CF measured with DC10mV.

From the results explained above, it may say that the resistivity of the fiber sheet is an important factor affects the resistivity of the conductive strengthening layers both in longitudinal and vertical direction. For example, the low resistivity CF sheet effects in the reduction of resistivity that can be confirmed by the reduction of resistivity of 8%CB1CF compares to that of 8%CB, and of 5%CB1CF and 5%CB2CF compare to that of 5%CB. But for the high resistivity AF sheet does not give much effect

compares to CF sheet. In the 5%CB series, the number of applied layers also does not give any obviously different resistivity between 5%CB1CF and 5%CB2CF.

In the previous report by Osaka Research Center of Konishi public company, the resistivity of 8%CB and 5%CB epoxy resin are $5x10^3$ Ω-cm and $6x10^5$ Ω-cm respectively while the wide range of value is obtained in this research. The obtained value range of the resistivity of 8%CB and 5%CB epoxy resin are 40 to 5,400Ω-cm and 500 to 15000Ω-cm, respectively. Then, it cannot be identify the reason why such different occurred.

(a) Longitudinal direction

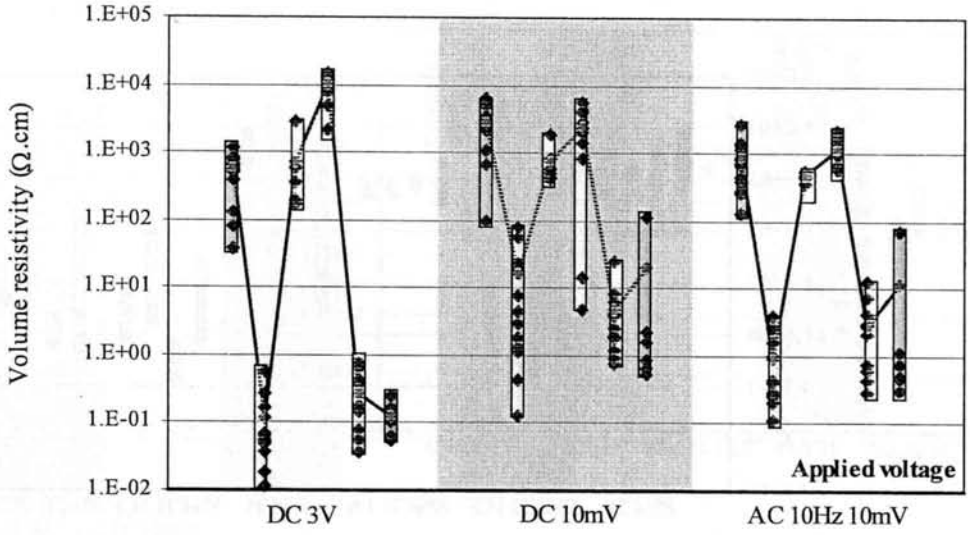

(b) Vertical direction

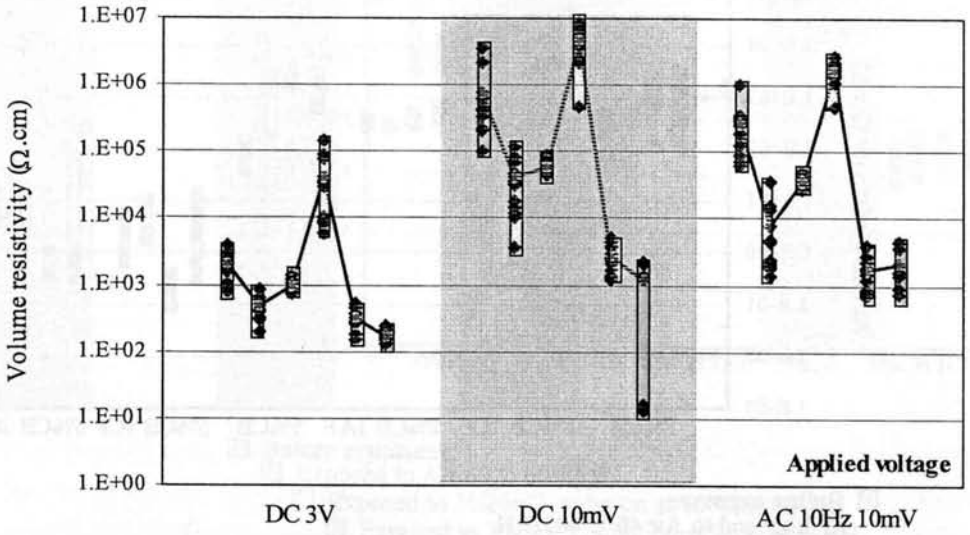

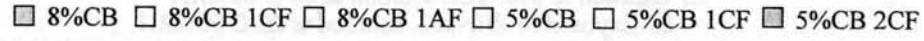

Figure 3. 8 Volume resistivity before exposure by applied voltage

(a) DC 3V

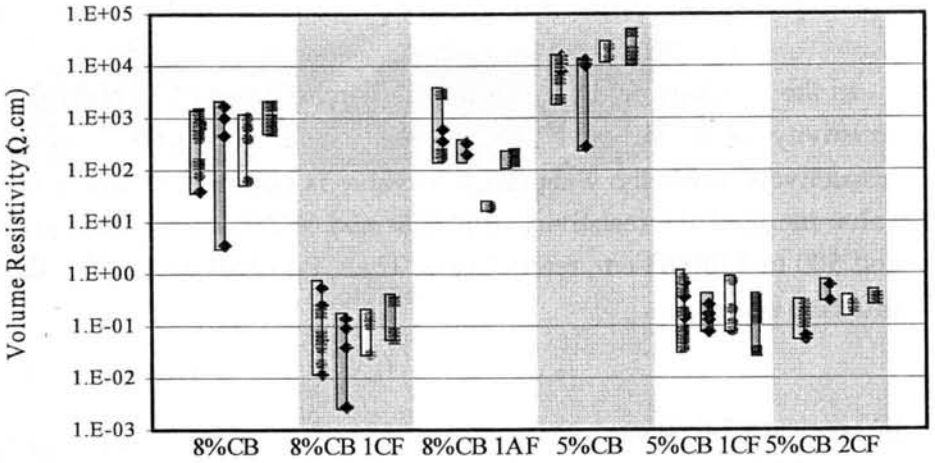

(b) DC 10mV

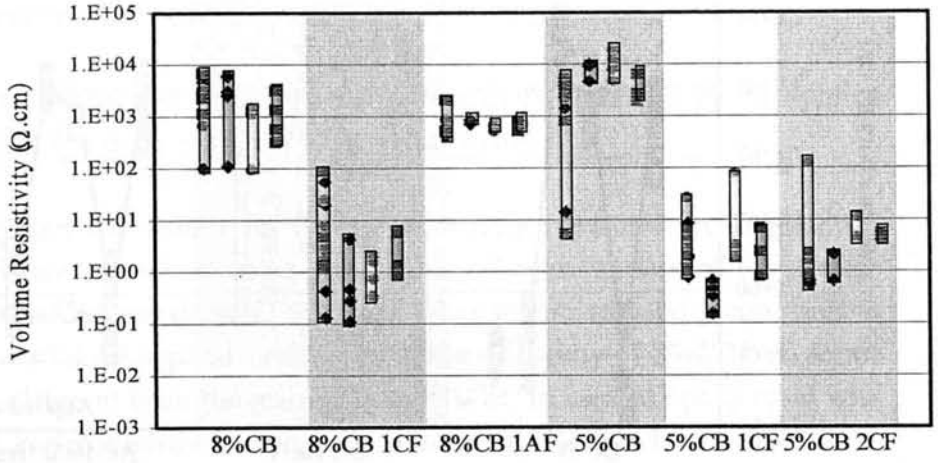

(c) AC 10Hz 10mV

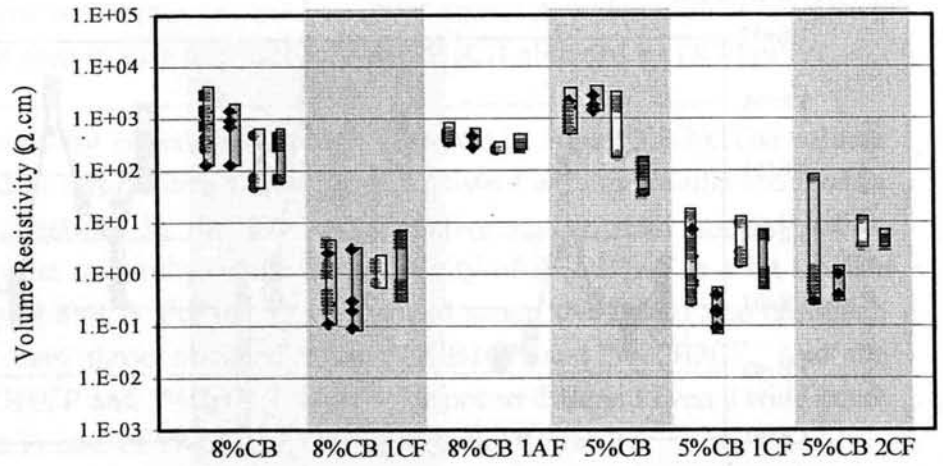

Before exposure
Exposed to Air 40'C 60%RH
Exposed to 3%NaCL solution at 40'C 60%RH
Exposed to 3%NaCL solution at 20'C 60%RH

Figure 3.9 Volume resistivity in longitudinal direction after exposure

(a) DC 3V

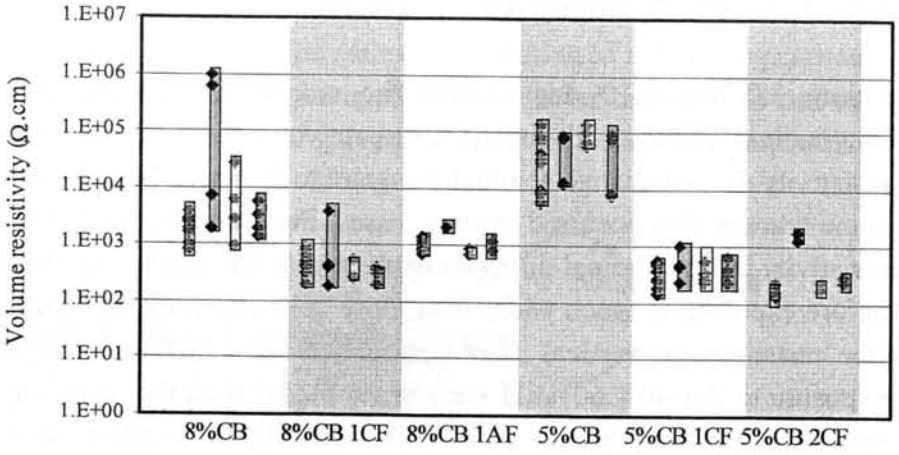

(b) DC 10mV

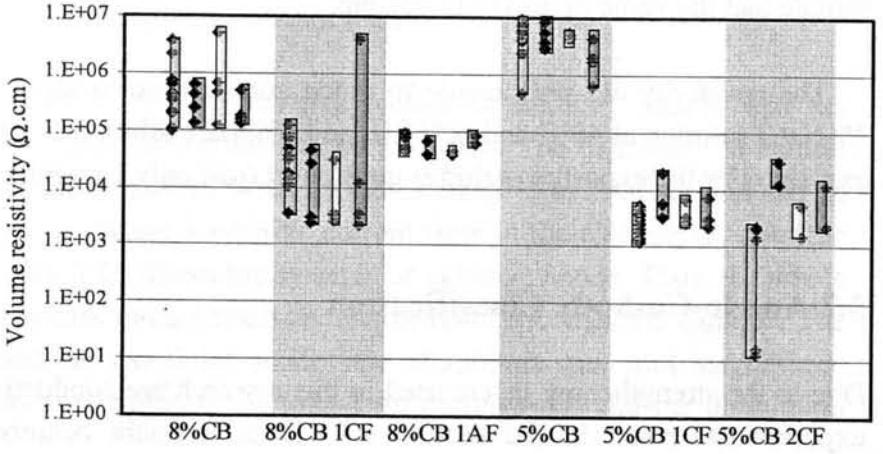

(c) AC 10Hz 10mV

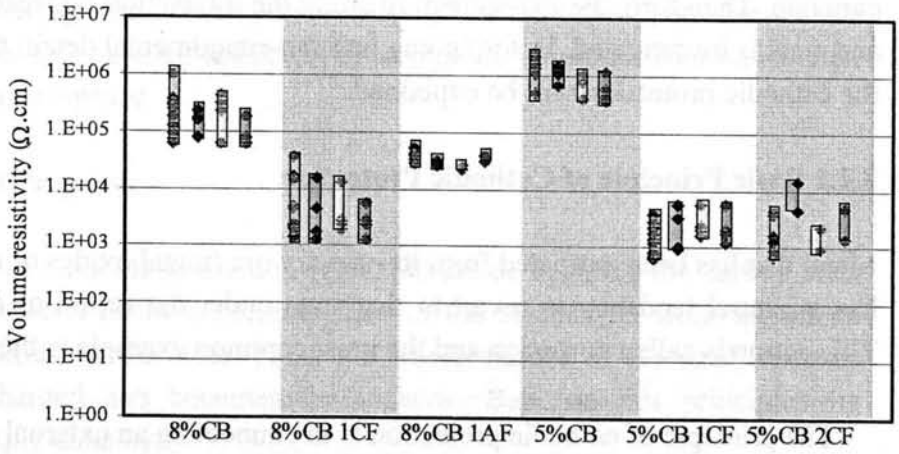

Before exposure
Exposed to Air 40'C 60%RH
Exposed to 3%NaCL solution at 40'C 60%RH
Exposed to 3%NaCL solution at 20'C 60%RH

Figure 3.10 Volume resistivity in vertical direction after exposure

3.1.2.2 Volume Resistivity After Exposure

Figure 3.9 and 3.10 demonstrate the comparison of the volume resistivity in longitudinal and vertical direction, respectively. Most of the results showed that the resistivity did not change so much compare to the value before exposure. Even though some scatters also occurred in some cases. For example, 5%CB in Figure 3.9(b) (the resistivity in longitudinal direction applied with DC10mV) that the range of resistivity before exposure is much wider than those after exposure, or 8%CB in Figure 3.10(a) (the resistivity in vertical direction applied with DC 3V) that the resistivity after exposure to Air 40'C60%RH were much bigger than the resistivity before exposure, or 8%CB1CF in Figure 3.10(b) (the resistivity in vertical direction applied with DC10mV) that the resistivity after expose to 3%NaCl solution at 20'C60%RH some sample had the value up to 10^6 Ω-cm, etc.

The resistivity did not change so much after expose to air at 40'C and 60%RH, 3%NaCl solution at 40'C and 60%RH, and 3%NaCl solution at 20'C 60%RH may be explained by the exposure period is quite short (just only 1 month).

3.2 Anode-Cathode Classification

Due to the strengthening layers used in this research are conductive as seen from the experimental result in the section 3.1. Then, a doubt occurred that the layers' conductivity might affect to induce or retard the corrosion of the embedded rebar in concrete. Therefore, the experiment to study the interaction between conductive layer and steel is investigated. Before going into the experimental detail, the background for the cathodic protection will be explained.

3.2.1 Basic Principle of Cathodic Protection

Metal that has been extracted from its primary ore (metal oxides or other free radicals) has a natural tendency to revert to that state under the action of oxygen and water. This action is called corrosion and the most common example is the rusting of steel.

The principle of cathodic protection is in connecting an external anode to the metal to be protected and the passing of an electrical DC current so that all area of the metal surface become cathodic and therefore do not corrode. The external anode may be a galvanic anode, where the current is a result of the potential different between the two metals, or it may be an impressed current anode, where the current is impressed from an external DC power source. In electrochemical terms, the electrical potential between the metal and the electrolyte solution with which it is in contact is made more negative, by the supply of negative charge electrons, to a value at which the corroding (anodic) are stifled and only cathodic reactions can take place. In general, it

is assumed that the metal to be protected is carbon steel, which is the most common material used in construction. Therefore, the cathodic protection of reinforcing carbon steel in reinforced concrete structure can be applied in a similar manner that can be achieved in two ways which are the use of galvanic (sacrificial) anodes, or impressed current.

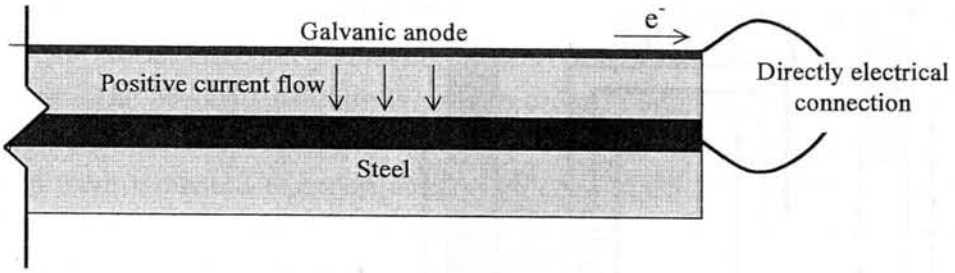

Figure 3.11 Schematic representation of galvanic anode systems

Galvanic anode systems employ reactive metals as auxiliary anodes that are directly electrically connected to the steel to be protected. The difference in natural potentials between the anode and the steel, as indicated by their relative positions in the electrochemical series, causes a positive current flow in the electrolyte, from the anode to the steel. Figure 3.11 shows the systems of galvanic anode. Thus, the whole surface of the steel becomes more negatively charged and becomes the cathode. The metals commonly used, as sacrificial anodes are aluminum, zinc and magnesium. These metals are alloyed to improve the long-term performance and the dissolution characteristic.

Impressed-current systems employ inert (zero or low dissolution) anodes and use an external source of DC power (rectified AC) to impress a current from an external anode onto the cathode surface.

3.2.2 Experimental Program

From the principle of cathodic protection (galvanic anode system), the carbon steel will be protected when a positive currents flow in the electrolyte, from the anode (another metal material) to the steel. Thus, the whole surface of the steel becomes more negatively charged and becomes the cathode. Base on this principle, the experiment was simply done by;

(1) Comparison the relative potential of carbon steel and conductive strengthening layers by respecting to the using reference electrode: The background on the electrochemistry is applied in order to roughly define the flow direction of positive and negative charge. The simple example is the reaction between zinc and copper cell.

$$Zn \rightarrow Zn^{2+} + 2e^- \quad : -0.762V$$
$$Cu \rightarrow Cu^{2+} + 2e^- \quad : +0.342V$$

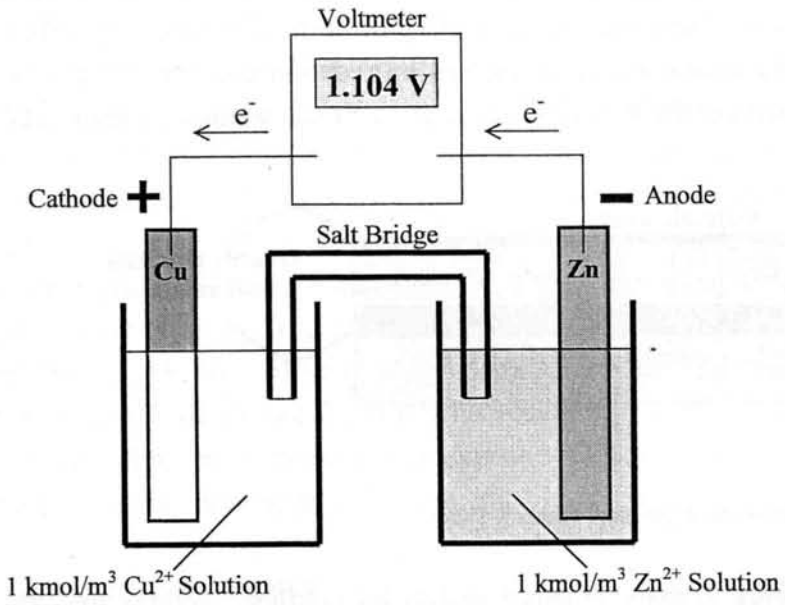

Figure 3.12 Schematic represent the potential different measurement between two electrodes

Figure 3.12 demonstrates the potential different for Cu and Zn. The Zn has weaker reduction potential therefore it will be oxidized that means Zn will loose e^- to Cu in the connection lead wire. Thus, the direction of current flow can be known that is opposite to the flow direction of electron.

(2) Investigate the value and direction of current flow when steel and conductive strengthening layer are electrically connected. The measure value is use to calculate the corrosion current density while the direction indicates that the steel is loose or gain the electron. In the experiment, the positive and negative connections of ampere meter are connected to the steel and conductive strengthening layer, respectively to order to simulate the galvanic anode systems (assume steel is protected). If the measure current is positive value, it means the positive current flow from the layer to steel in the medium (the concept of galvanic anode system) and behave like cathode. Then, the steel is protected by the conductive strengthening layer. But in the other way, if the measure current value is negative, it means the positive current flow from steel to the layer in the medium (opposite to the concept of galvanic anode system), and behaves like anode. Then, it gets corroded.

3.2.2.1 Factors

Two parameters considered in this experiment are type of conductive strengthening layer and test conditions.

Type of conductive strengthening layer: Six conductive strengthening layers were used because of the difference in their conductivity, or resistivity.

Test condition: Four test conditions, which are sample test in 3%NaCl solution, sample test in the alkaline solution, dry-condition concrete and wet-condition concrete, were considered in order to investigate the interaction between conductive strengthening layer and reinforcing steel. These two solutions are selected according to *NACE standard test, TM0294-2001: Testing of Embeddable Impressed Current Anodes for use in Cathodic Protection of Atmospherically Exposed Steel-Reinforced Concrete*. The 3%NaCl solution is used in order to simulate the seawater (chloride) environment while the alkaline solution is used for simulating the concrete pore solution environment. The experiments were done in Cl^- free and Cl^- mixed concrete specimen both dry and wet condition to investigate the effect of humidity in concrete to the current flow characteristic.

3.2.2.2 Materials and Equipments

Materials: Materials used in this section are as same as needed in section 3.1. Only difference is the preparation of the plastic plate. The plastic plate consists of 2 layers that are 160x60x1mm plastic plate (lower plate) and 160x60x0.5mm plastic plate (upper). The upper one was cut at 10mm from the end with the size of 10x55mm to bury the stainless steel in the plastic plate for connecting the electrical lead wire from the conductive strengthening layer, as shown in Figure 3.11(b).

Equipments: The corrosion meter was used to obtain the potential reading for roughly indicate the flow direction. The ampere meter was used to obtain the current flow to calculate the current density of the simulating system.

3.2.2.3 Testing in Solution

Sample Preparation

Steel: Non-corroded 15cm-lomg carbon steels were connected to the electrical lead wire at one end, and then was wrapped by the rubber-gum tape and coated with the epoxy on both two tips (the tip with the soldered connection between steel and connection wire, and another free tip that has no black-steel (FeO_2) cover at the cutting edge) to effect to the natural current flow in the measurement and to prevent galvanic corrosion, as shown in Figure 3.13(a).

Conductive Strengthening Layer: The conductive strengthening layers were made on the prepared plastic plate as shown in Figure 3.13(b). Type of conductive strengthening layer used in the experiment corresponding to Chapter 4 and 5 are written in Table 3.4. The layer type and application procedure for each type of layer are demonstrated in Table 3.4 and Fig. 3.5, respectively.

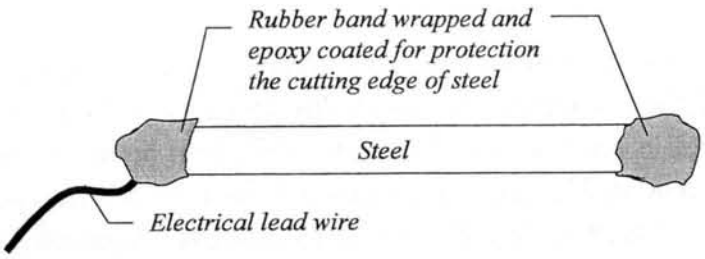

(a) Steel test sample

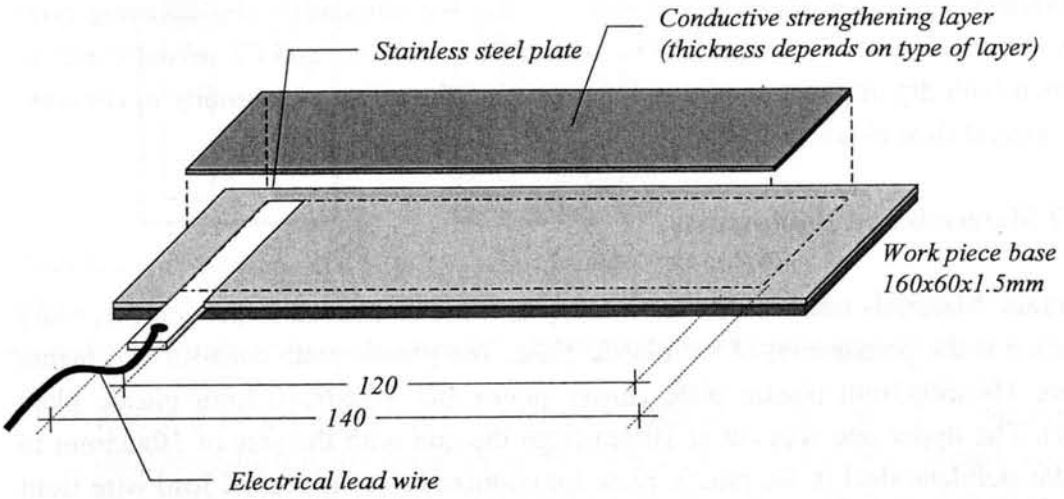

(b) Conductive strengthening layer test sample

Figure 3.13 Test samples

Solution Preparation

3%NaCl Solution: The 30g of NaCl is weighed and added to 970ml of water, and the solution must be stirred in the container until all NaCl crystals are totally dissolved.

Alkaline Solution: Refer to the NACE 0294-2001, 4 chemical substances, which NaOH, KOH, KCl, $Ca(OH)_2$ are used to make the alkaline solution or the concrete pore solution. But the one used in this experiment is excluded the KCl for simulating the concrete pore solution without Cl^-. Therefore the mix for the alkaline solution used in this test followed the previous one used in the previous work of Hattori and Miyagawa. Their alkaline solution consists of NaOH 10g/l, KOH 14g/l, $Ca(OH)_2$ 2g/l and mixing with water. Then, 10.42g of solid NaOH pellets (96% NaOH reagent) are weighed out as 100% NaOH and slowly added to 974 ml of water. After that 16.47g of KOH pellets (85% KOH reagent) are weighed out as 100% KOH and slowly added to the solution. Finally 2.10g of 95% $Ca(OH)_2$ reagent is weighed out and added to the solution. Fresh solution is used for each current flow test.

Table 3.4 Types of layer and number of sample and specimen used in each test condition

	Type of layer	Code	Using in section		Test in Solution		Concrete specimen*1	
			Chapter 4	Chapter 5	3%NaCl	Alkaline Sol.	Cl^- free	Cl^- mixed
1	5%CB CER	5%CB	-	Yes	2	2	-	-
2	5%CB CER and 1ply of CF sheet	5%CB 1CF	-	Yes	2	2	2*2	2*2
3	5%CB CER and 2plies of CF sheet	5%CB 2CF	-	Yes	2	-	-	-
4	8%CB CER	8%CB	Yes	Yes	2	2	-	-
5	8%CB CER and 1ply of CF sheet	8%CB 1CF	Yes	Yes	2	2	2*2	2*2
6	8%CB CER and 1ply of AF sheet	8%CB 1AF	Yes	-	2	-	2*3	2*3

*1 *Concrete specimens in each series were tested in both dry and wet condition to vary the effect of concrete resistance to the current flow test*
*2 *Specimen size is 1200x50x75mm.*
*3 *Specimen size is 1200x50x50mm.*

Experiment Setting

Figure 3.14 demonstrates the experiment setting for the anode-cathode classification test. The prepared steel and conductive strengthening layer plate were set by using the epoxy to fasten them at the bottom of container in vertical direction and 2cm apart from each other by using plastic spacer. The electrical lead wires from steel and conductive strengthening layer were then connected to the positive (red line) and negative (black line) connection of the ampere meter, respectively. Next, the test solution was filled in the test container up to 10cm of the steel length, and started the measure the current.

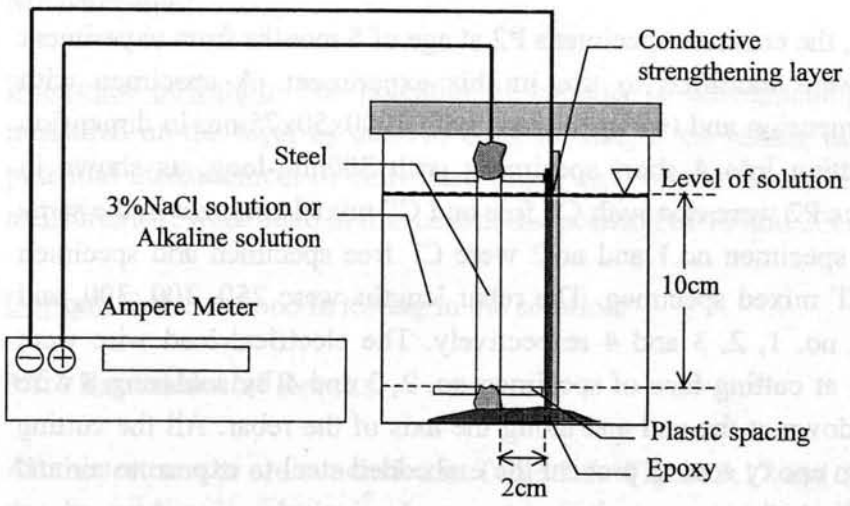

Figure 3.14 Schematic representation the experimental setting for anode-cathode classification in solutions

Measurement

Reference potential: The corrosion meter (7635machine, Ag(AgCl(KCl)) sat. electrode) was employed to measure the potential of conductive strengthening layer and steel to roughly indicate the current flow direction of the system before layer and steel were set into the test for current flow measurement. The potential was measured by placing the reference electrode on the wet cotton at 2.5, 5 and 7.5cm from the lower tip of both conductive strengthening layer and steel.

Current: Ampere meter was used to measure the current value at every minute in the first two hours and every five minutes for the next two hours, totally four hours measurement for each test sample. The period of four hours was selected because of the result of preliminary test that 4 hours is a period that the current going to be in the steady state and after that seem to be constant or gradually decrease with time.

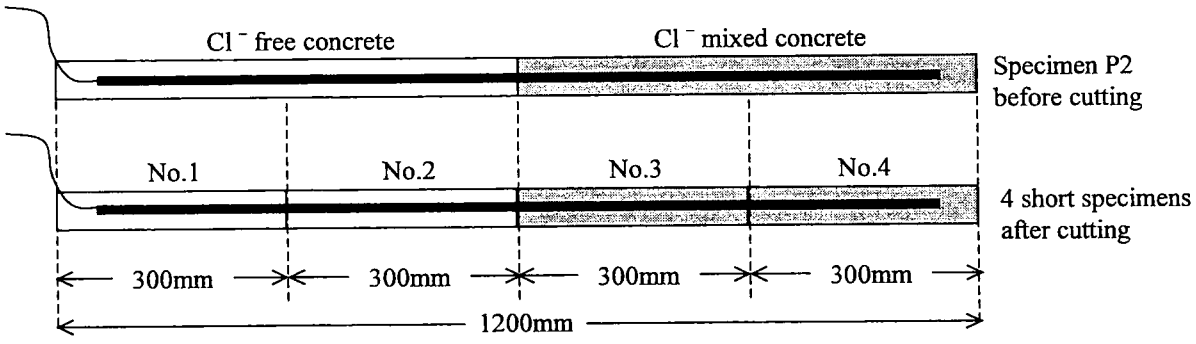

Figure 3.15 Modification of Specimen P2

3.2.2.4 Testing in concrete specimen

Specimen preparation

Due to time limitation, the concrete specimens P2 at age of 5 months from experiment done in Chapter 5 were modified to use in this experiment. A specimen with 1200x50x50mm in dimension and two specimens with 1200x50x75mm in dimension were modified by cutting into 4 short specimens with 300mm-long, as shown in Figure 3.15. Specimens P2 were cast with Cl^- free and Cl^- mixed concrete in the same length. After cutting, specimen no.1 and no.2 were Cl^- free specimen and specimen no.3 and no.4 were Cl^- mixed specimen. The rebar lengths were 250, 300, 300, and 250mm for specimen no. 1, 2, 3 and 4 respectively. The electrical lead wire were connected to the steel at cutting face of specimen no. 2, 3 and 4 by soldering a wire lead into a hole drill down at the end and along the axis of the rebar. All the cutting faces were cover by an epoxy coat to prevent the embedded steel to expose to air and water during the experiment.

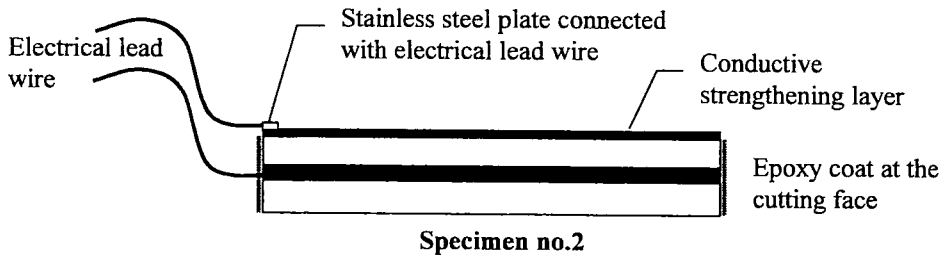

Figure 3.16 Example of completely modified specimen

The prepared specimens were then bonded with the conductive strengthening layer as written in table 3.6 from the side of 2mm-cover thickness. Two 1200x50x75mm specimens were bonded with 5%CB 1CF and 8%CB 1CF while a 1200x50x50mm specimen was bonded with 8%CB 1AF. The procedure of layer application shows in Figure 3.5(b), epoxy and 1ply of fiber sheet. At the end of the layer application, the 70x10x0.5mm stainless steel, which already connected with the lead wire, was fastened at the tip of the conductive strengthening layer. A week after leaving the layer set and dry, the stainless steel plate was covered by an epoxy coat. Figure 3.16 demonstrates the example of completely modified specimen, specimen no.2.

Experiment Setting

The positive (red line) and negative (black line) connections of the ampere meter were connected to cord connected to the rebar and conductive strengthening layer, respectively. The modified specimens were used in the current flow measurement both in dry and wet condition. Testing the specimen in wet, the specimens were submerged into the water up to the level just 5mm below top surface that bonded by the conductive strengthening layer for 1 weeks after testing in dry condition, and then wrapped with the plastic wrap to keep constant the condition of testing specimen.

Measurement

Reference potential: The potential of conductive strengthening layer was directly measured on the layer as same as done in case of the testing in the solution, but the potential measurement of embedded rebar was done on concrete surface. Two points measurement were done in this case at the position of 10 and 20cm.

Current: Same as done in testing in the solution.

3.2.3 Experimental Results

All the test results are concluded in Table 3.5. Figure 3.17 and 3.18 show the current density reading in solution and concrete specimen respectively. Figure 3.17(a) shows the current density reading in 3%NaCl solution. The obtained current densities of all

conductive strengthening layers are negative. It means steel will be faster corrode by all types of conductive strengthening layer. Moreover, it also shows that the fiber sheet applied conductive strengthening layer (8%CB1CF, 8%CB1AF, 5%CB1CF and 5%CB2CF) has bigger current density than one without sheet (8%CB and 5%CB) both 8%CB series and 5%CB series. The current density ranking from high to low is 8%CB1CF, 8%CB1AF, 8%CB in case of 8%CB series, and 5%CB1CF, 5%CB2CF, 5%CB in case of 5%CB series. The average value of the current density (of 2 samples in each type of layer) shows the current density of 8%CB1CF and 8%CB1AF are 8.8 and 2.5 times bigger than that of 8%CB, respectively. For 5%CB series, the current density of 5%CB1CF and 5%CB2CF are 230 and 86 times bigger than that of 5%CB. Regarding in the %CB contain in epoxy resin, the current density of 8%CB series is bigger than that of 5%CB series in both the layer with CF sheet and without CF sheet. By using the value of 0.2 $\mu A/cm^2$ (non-activated state or very low rate of corrosion, CEB) as criteria to indicate the applicable of the material, only the corrosion current density of 5%CB is smaller than 0.2 $\mu A/cm^2$.

Figure 3.17(b) shows result obtained in alkaline solution. All of the obtained current density is negative as same as in case of testing in 3%NaCl solution. And the current density of the conductive strengthening layer applied with CF sheet also has bigger value compare to that of conductive strengthening layer without sheet. 8%CB1CF is 18 times bigger than 8%CB while 5%CB1CF is 41.5 time bigger than 5%CB. Again, the current density of 8%CB series is bigger than that of 5%CB series in both the layer with CF sheet and without CF sheet. All obtained values of current density are negative but smaller than 0.2 $\mu A/cm^2$ that mean all can be applicable.

From Figure 3.17(a) and (b), the test done in Cl^- environment give higher current density than the test done in alkaline solution. It explains that chloride ion affects to increase the current flow between conductive strengthening layer and steel.

Figure 3.18(a) demonstrates the current density testing in dry condition of concrete specimens. The current density came out both in positive and negative value. All Cl^- mixed specimens and some of Cl^- free specimens (8%CB1AF no.2 and 5%CB1CF no.2) gave the negative current density that means they induce steel to be corroded. But in opposite case, the specimens that gave the positive value, the steel is protected to be corroded. From Figure 3.18(a) for those that gave the negative value, the Cl^- mixed concrete specimens have bigger current density than Cl^- free concrete. But those values are smaller than 0.2 $\mu A/cm^2$ that indicate non-activated state or very low rate of corrosion. Then all are applicable.

Figure 3.18(b) shows the results of the current density testing in wet condition of concrete specimens. All specimens gave the negative value of current density that means they all induce the steel to be corroded. The Cl^- free specimens have lower

current density than the Cl^- mixed specimens and also lower than 0.2 $\mu A/cm^2$ that specify they are applicable.

From Figure 3.18(a) and (b), the concrete in wet condition give higher current density than the concrete in dry condition. It proves that the concrete humidity also play an important role to the current flow between the layers and embedded steel.

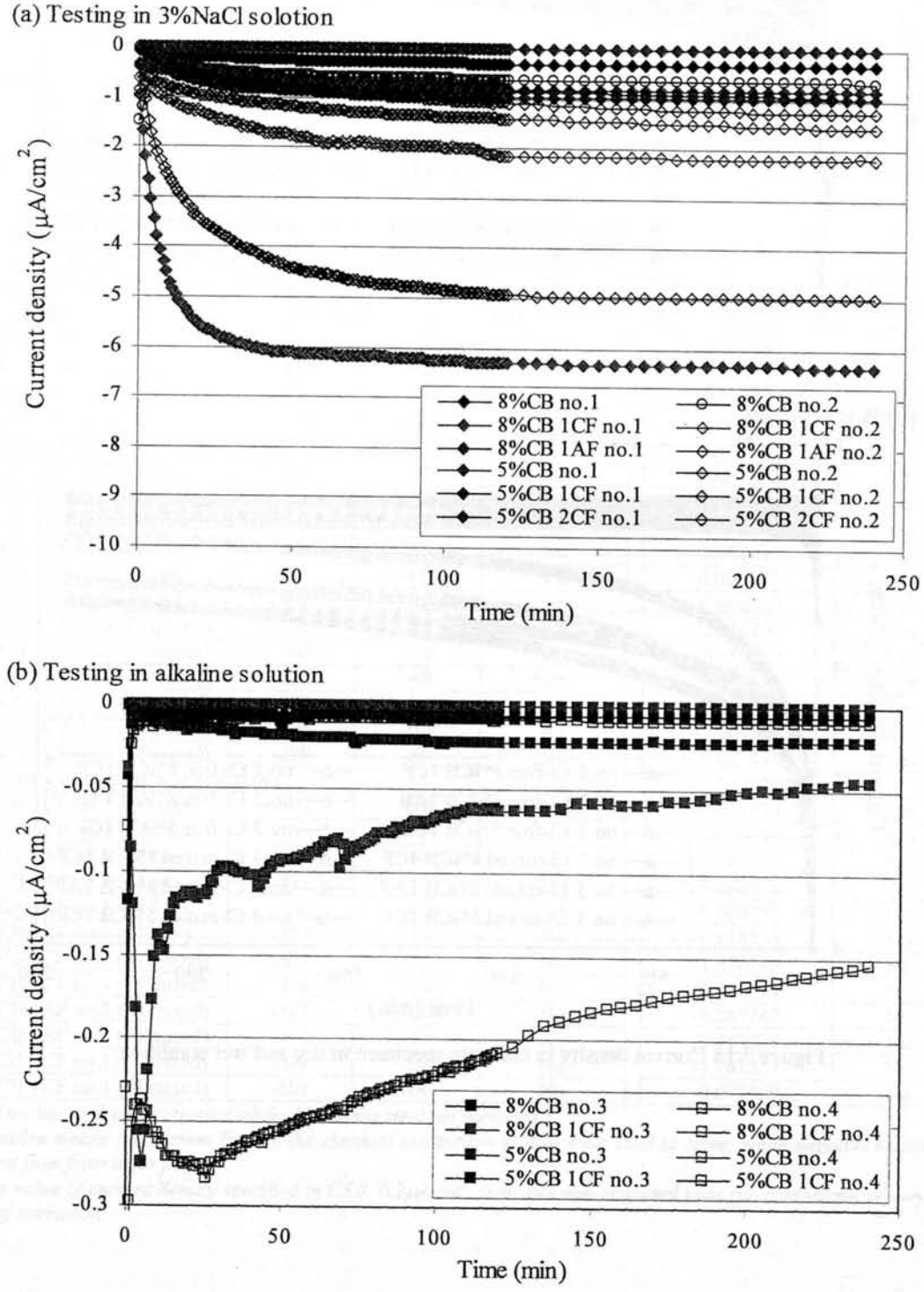

Figure 3.17 Current density of test sample in 3%NaCl solution and alkaline solution

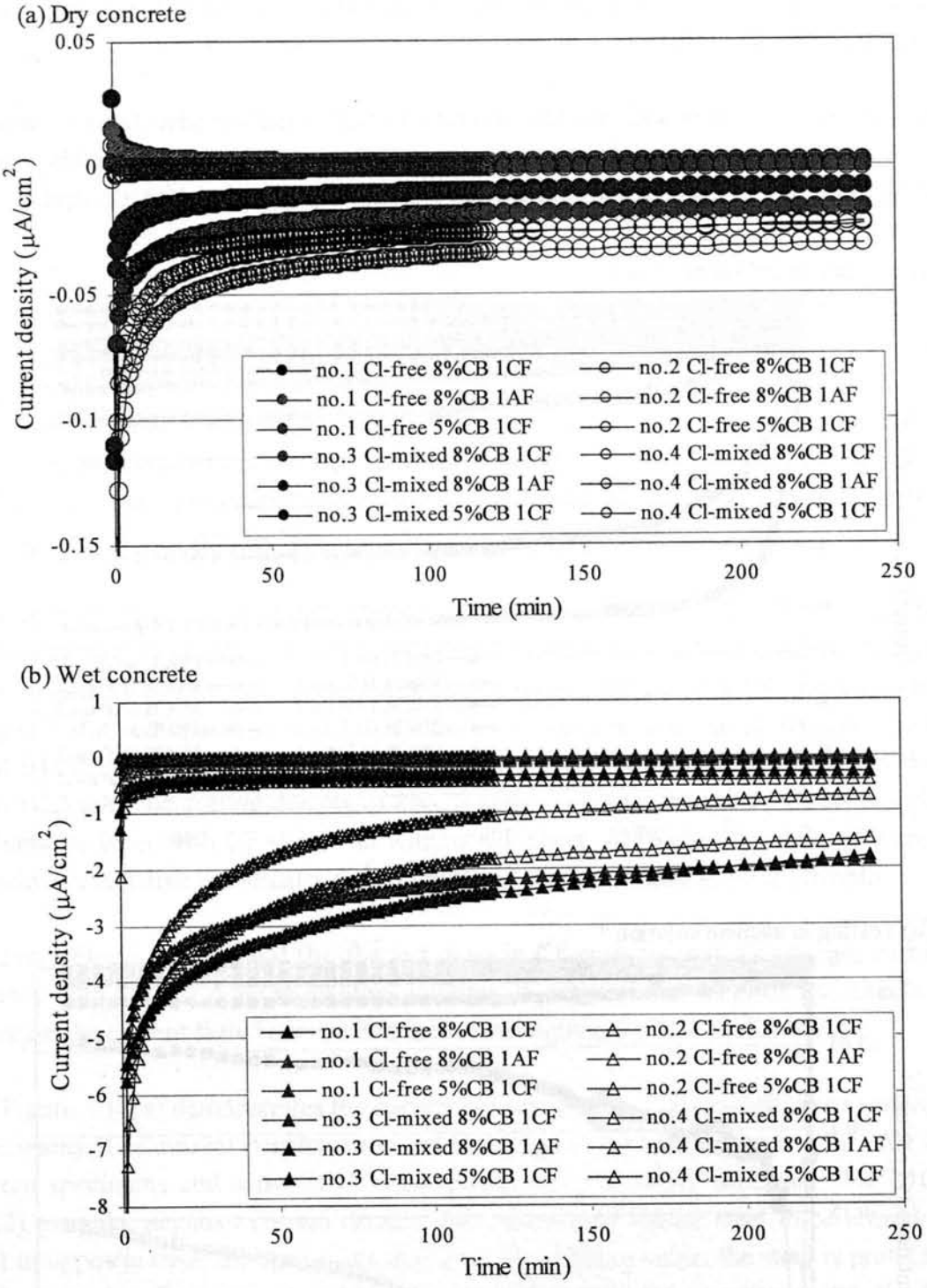

Figure 3.18 Current density in concrete specimen in dry and wet condition

Table 3.5 Experimental results of the anode-cathode classification

Testing condition	Potential reading respected to SSCE (mV)		Galvanic anode systems[*1]	Current density at 4 hr[*2] ($\mu A/cm^2$)	Applicable[*3]
	Steel	layer			
Testing in 3%NaCl solution					
8%CB no.1	-255	-30	No	-0.300607	No
8%CB no.2	-292	-28	No	-0.668017	No
8%CB 1CF no.1	-240	-57	No	-6.379558	No
8%CB 1CF no.2	-292	-69	No	-2.171054	No
8%CB 1AF no.1	-275	-53	No	-0.835021	No
8%CB 1AF no.2	-340	-151	No	-1.576519	No
5%CB no.1	-274	-100	No	-0.012058	Yes
5%CB no.2	-473	-28	No	-0.014028	Yes
5%CB 1CF no.1	-254	-63	No	-0.968624	No
5%CB 1CF no.2	-298	-59	No	-4.976723	No
5%CB 2CF no.1	-334	-30	No	-0.968624	No
5%CB 2CF no.2	-285	-18	No	-1.269231	No
Testing in alkaline solution					
8%CB no.3	-305	-77	No	-0.005277	Yes
8%CB no.4	-294	-61	No	-0.005778	Yes
8%CB 1CF no.3	-213	-48	No	-0.045759	Yes
8%CB 1CF no.4	-276	-75	No	-0.154646	Yes
5%CB no.3	-317	-25	No	-0.000481	Yes
5%CB no.4	-345	9	No	-0.000254	Yes
5%CB 1CF no.3	-326	-45	No	-0.021377	Yes
5%CB 1CF no.4	-273	-40	No	-0.009118	Yes
Concrete specimen in dry condition					
8%CB 1CF no.1 (Cl^-free)	18	-72	Yes	0.001552	Yes
8%CB 1CF no.2 (Cl^-free)	-34	-100	Yes	0.000802	Yes
8%CB 1AF no.1 (Cl^-free)	31	-65	Yes	0.001202	Yes
8%CB 1AF no.2 (Cl^-free)	-82	-66	No	-0.000512	Yes
5%CB 1CF no.1 (Cl^-free)	22	-140	Yes	0.000067	Yes
5%CB 1CF no.2 (Cl^-free)	-54	-104	Yes	-0.000657	Yes
8%CB 1CF no.3 (Cl^-mixed)	-277	-73	No	-0.016700	Yes
8%CB 1CF no.4 (Cl^-mixed)	-260	-78	No	-0.030595	Yes
8%CB 1AF no.3 (Cl^-mixed)	-238	-89	No	-0.008128	Yes
8%CB 1AF no.4 (Cl^-mixed)	-279	-71	No	-0.022485	Yes
5%CB 1CF no.3 (Cl^-mixed)	-295	-101	No	-0.008551	Yes
5%CB 1CF no.4 (Cl^-mixed)	-299	-80	No	-0.023514	Yes
Concrete specimen in wet condition					
8%CB 1CF no.1 (Cl^-free)	-161	-30	No	-0.036474	Yes
8%CB 1CF no.2 (Cl^-free)	-147	-40	No	-0.010577	Yes
8%CB 1AF no.1 (Cl^-free)	-39	-64	Yes	0.000433	Yes
8%CB 1AF no.2 (Cl^-free)	-485	-15	No	-0.090739	Yes
5%CB 1CF no.1 (Cl^-free)	-72	-47	No	-0.000779	Yes
5%CB 1CF no.2 (Cl^-free)	-257	-71	No	-0.018593	Yes
8%CB 1CF no.3 (Cl^-mixed)	-602	-43	No	-1.870446	No
8%CB 1CF no.4 (Cl^-mixed)	-576	-92	No	-1.482997	No
8%CB 1AF no.3 (Cl^-mixed)	-523	-140	No	-0.287247	No
8%CB 1AF no.4 (Cl^-mixed)	-544	-45	No	-0.442227	No
5%CB 1CF no.3 (Cl^-mixed)	-592	-66	No	-1.781377	No
5%CB 1CF no.4 (Cl^-mixed)	-601	-64	No	-0.697409	No

*[*1] **Yes** means steel get protection while **No** means steel get corroded.*

*[*2] **Positive** means the current flow in the electical conttection is flow from steel to layer, while **negative** means the current flow from layer to steel*

*[*3] The value of current density specified in CEB, 0.2 $\mu A/cm^2$, indicates non-activated state (no corrosion), or very low rate of corrosion.*

3.3 Summary

In the former part, the volume resistivity of conductive strengthening layers and the effect of the layers to steel was investigated. The value obtained in this experiment is in a wide range from 40 to 5400Ω-cm for 8%CB epoxy and 500 to 15000Ω-cm for 5%CB epoxy. The conductive strengthening layer with CF sheet has much lower resistivity than that with out CF sheet that can be seen both 8%CB series and 5%CB series. But the resistivity of conductive strengthening layer with AF sheet is not obviously different compare to the layer without sheet. The exposure conditions does not affect the resistivity of the conductive strengthening layer that may be the period of exposure is quite short.

In the later part, the experiment to classify anode and cathode of two materials in the simulated galvanic anode system is investigated. At this stage, the results show that the steel will be safe in the alkaline environment, in dry condition both Cl^- mixed and Cl^- free concrete specimen, and in wet condition for Cl^- free concrete.

Chapter 4

Electrochemical Corrosion Monitoring on Concrete Specimens with Uniform Chloride Content

As written in the introduction chapter, after the columns and/or members are repaired and strengthened by wrapping or bonding with the strengthening materials, it is unable to identify the corrosion activity under those strengthening materials.

This chapter demonstrates the main objective for the research that investigated on the effect of the conductive strengthening layers to the electro-chemical corrosion monitoring. The conductive epoxy resin was used as adhesive material instead of the usual epoxy resin in order to make many types of strengthen layers to be conductive. Two electro-chemical corrosion monitoring technique, half-cell potential and polarization resistance (hereafter, HCP and PR), were employed.

In this section, the uniform chloride content concrete specimens were cast. The specimen's surface was then bonded with strengthening material by using conductive epoxy resin. Three types of strengthening materials, CF sheet, AF sheet and steel plate, were used in the experiment. Beside that, the effect of blister/gab under CFRP/steel plate on concrete surface were also considered, where the plastic plate was used to make an artificial blister/gab. Two corrosion-monitoring techniques, HCP and PR, were employed. For PR measurement, 2 methods, which are double rectangular pulse method and AC impedance method, were used.

4.1 Factors

The considered factors in this research were listed below.

Water cement ratio, *w/c* - two values of water cement ratio, which are 0.45 and 0.65, were used in order to compare the obtained value while water content and sand to total aggregate content (s/a) were same for all specimens. The concrete specimen with lower *w/c* may give a better state of corrosion (such as noble half-cell potential, higher polarization resistance, lower corrosion current density, and lower corrosion loss) than one with higher *w/c*. Because of the lower *w/c* concrete has the good properties such as high density, capacity to prevent the ingression of aggressive substance, etc.

Strengthening material using conductive epoxy resin with CF sheet, AF sheet and steel plate - three types of strengthening material were employed in this research because the difference in conductivity of them. The degree of conductivity can be graded from high conductive, moderate conductive and non-conductive, which are steel, CF sheet and AF sheet, respectively. Therefore, they were used to make 7 types of testing surface.

Gap under CF sheet or steel plate above the concrete surface – this factor was taken into account in order to find out whether the gab/blister/air bubble under the strengthening material can be detected by 2 methods of corrosion monitoring or not. Therefore, the plastic plate was used to make the artificial gap.

4.2 Materials and Equipments

The properties of materials and the equipments used in this research are as follows:

Portland cement: Ordinary Portland cement (Sumitomo Osaka cement) The physical properties of the cement are shown in Table 4.1.

Fine aggregate: Natural river sand. The physical properties are shown in Table 4.2.

Coarse aggregate: Limestone aggregate was used. The physical properties are shown in Table 4.3.

Epoxy resin: Conductive epoxy resin was used and its properties are shown in Table 3.4. This epoxy will be mixed with main agent and hardening agent in a ratio of 224/100 and added with carbon black powder of 8% (additional mix).

Fiber sheet: CF sheet's properties and AF sheet's properties are shown in Table 3.5

Steel plate: 2mm-thickness steel plates were used

In addition, 2mm-thickness stainless steel plates and 2mm-thickness plastic plates were also used in this research as conductive layer-electric cord connection and artificial gap, respectively.

Equipments: *Auto-Range Corrosion Meter 7635* (see Figure 4.1) and *SRI CM Portable Rebar Corrosion Meter* (see Figure 4.2) were used in the test.

Table 4.1 Physical properties of Portland cement type I

Physical properties	Specific gravities	Stability	Setting time(hr:min)		Specific surface area (cm^2/g)	Compressive strength (N/mm^2)		
			Initial	Final		3days	7days	28days
	3.15	Good	2:08	3:12	3410	28.7	44.3	61.7

Table 4.2 Physical properties of fine aggregate

Physical properties	Specific gravities (dry-cont)	Water absorption (%)	Sieve retaining (%)							Finess modulus
			1.29 mm	0.80 mm	0.62 mm	0.32 mm	0.23 mm	0.11 mm	<0.11 mm	
	2.62	1.68	0	3.01	26.99	29.84	22.31	11.74	6.11	2.69

Table 4.3 Physical properties of coarse aggregate

Physical properties	Specific gravities (dry-cont)	Water absorption (%)	Sieve retaining (%)						Finess modulus
			15.9 mm	9.52 mm	4.76 mm	2.38 mm	1.19 mm	<1.19 mm	
	2.7	1.15	0	34.25	62.98	2.51	0.14	0.11	6.31

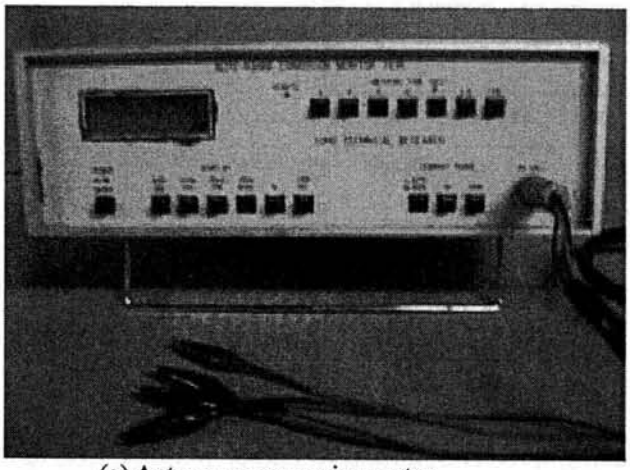

(a) Auto-range corrosion meter

(b) Reference electrode (Ag/AgCl)KCl sat.

Figure 4.1 Auto-range corrosion meter 7635

4.3 Specimens

4.3.1 Dimensions

The specimens with the dimension of 400x100x50mm specimens were cast by placing a reinforcing steel of D10x30cm at the center, as shown in Figure 4.3.

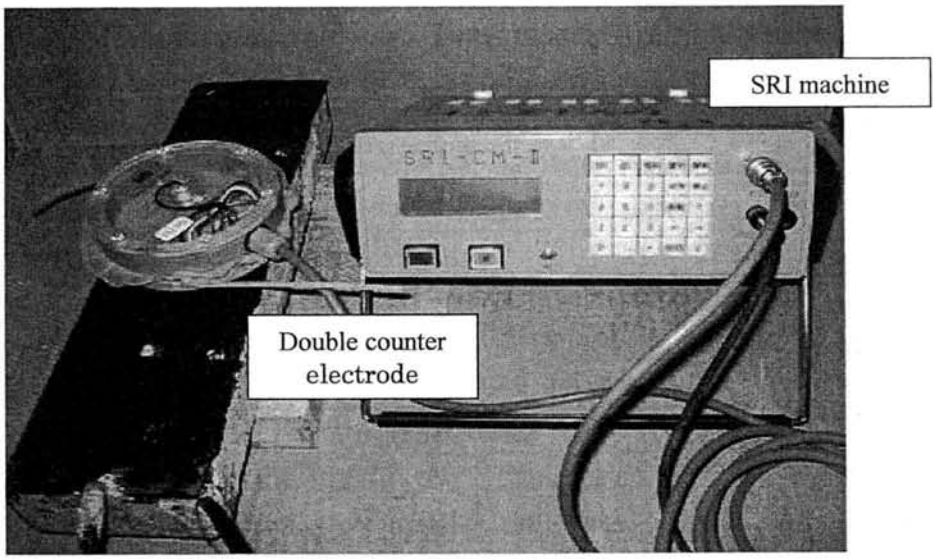

Figure 4.2 SRI portable rebar corrosion meter

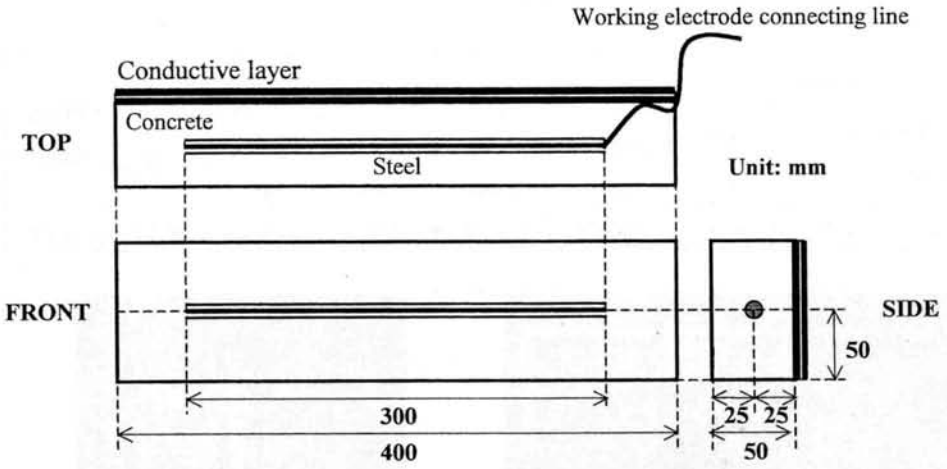

Figure 4.3 Specimen with uniform chloride content

4.3.2 Conditions of specimen

The concrete specimens were bonded with three strengthening materials, which are CF sheet, AF sheet and steel plate, by using 8%CB conductive epoxy resin (CER) as the adhesive material. Therefore, 7 surface's types were made as lists below:

1. Concrete
2. 8%CB CER
3. 8%CB CER and 1ply of CF sheet
4. 8%CB CER and 1ply of AFsheet
5. 8%CB CER and a steel plate
6. 8%CB CER and a steel plate + artificial blister
7. 8%CB CER and 1ply of CF sheet + artificial blister

Table 4.4: Conditions and number of testing specimen

Cl^- content in concrete and curing condition		Cl^- 3.0 kg/m^3 + wet&dry cycle of 3%NaCl solution							
W/C		0.45				0.65			
Type of specimen		Breaking period[i] for photo/sketch			HCP and PR meas.	Breaking period[i] for photo/sketch			HCP and PR meas.
		28mths	3mths	6mths		28days	3mths	6mths	
1	Concrete	2[ii]	2[ii]	2[ii]	2[iii]	2[ii]	2[ii]	2[ii]	2[iii]
2	8%CB CER	----	----	----	----	----	----	----	2[iii]
3	8%CB CER with 1ply of CF sheet	2[ii]	2[ii]	2[ii]	2[iii]	2[ii]	2[ii]	2[ii]	2[iii]
4	8%CB CER with 1ply of AFsheet	----	----	----	----	----	----	----	2[iii]
5	8%CB CER with a steel plate	----	----	----	2[iii]	----	----	----	2[iii]
6	8%CB CER with a steel plate and artificial blister	----	----	----	----	----	----	----	2[iii]
7	8%CB CER and 1ply of CF sheet and artificial blister	----	----	----	----	----	----	----	2[iii]
Total		18 specimens				26 specimens			

[i] *The number of breaking specimens was reduced by assuming the corrosion activity is the same for all types of specimen, then only specimen type A and C were made.*
[ii] *HCP and PR were measured once a month for breaking specimens.*
[iii] *HCP and PR were measured once a week in the first month and once for two weeks in the following months.*

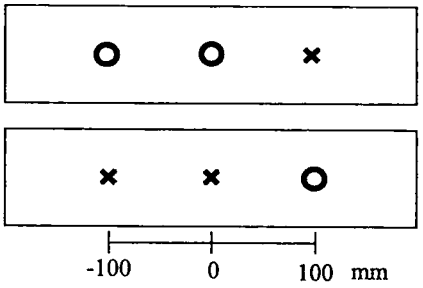

O: 6mm-diameter drilled hole on conductive layer to concrete surface,
X: No-hole

Figure 4.4 Drilled hole of specimens in series 2 to 7 (For series 6 and 7, the hole at the center in specimen no.1 was not drilled)

Conditions and number of specimens are shown in Table 4.4. Each type of surface consists of 2 specimens. The first specimen has two holes on the strengthening material's surface and the second one has a hole as shown in Figure 4.4. These holes were made in order to compare the reading on strengthening material and the reading at drill hole on strengthening material concrete surface. If the hole exists, the measurement on the conductive layer may be similar to the measurement directly on concrete surface to some extent. The specimen Type 6 and 7, a 60x60x2mm size of

plastic plate was buried in the concrete surface layer for making the artificial blister/gap as shown in Figure 4.5.

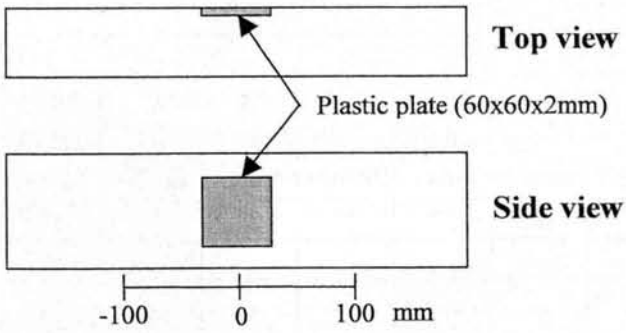

Figure 4.5 Artificial gap by burying plastic plate on concrete surface layer

4.3.3 Mix proportion, casting, curing

The concrete mix proportion used in the experiment was shown below and mix-design was shown in Table 4.5.

Mix design;

Water cement ratio (w/c)	0.45 and 0.65
Water content (W)	170 kg/m^3
Air content (air)	4.50%
Sand to total aggregate ratio (s/a)	49%
Cl^- content	3 kg/m^3 (NaCl content is 4.94 kg/m^3)

Table 4.5: Mix proportions of concrete specimen used in the experiment

w/c	W	C	S	G	NaCl	AE*1 no.303	WRA*2 no.70	Slump (cm)	Compressive strength	Young's Modulus
	kg/m^3					ml/m^3			N/mm^2	
0.45	170	378	834	916	5	2520	944	4.2	36.4	4.00E+04
0.65	170	262	901	967	5	1744	654	24.0	14.9	2.79E+04

*1 *AE: Air entraining agent*

*2 *WRA: Water reducing agent*

A day after casting, specimens were demolded and were cured by keeping in the plastic bag for 28 days. In order to accelerate the corrosion of embedded steel, 3.0kg/m^3 of Cl^- (approximately 5 kg/m^3 of NaCl) was mixed to the concrete and wetting and drying cycle was employed during this research. The detail of wetting and drying cycle was written in section 4.4 Immersion.

(a) Epoxy resin or Fiber sheet

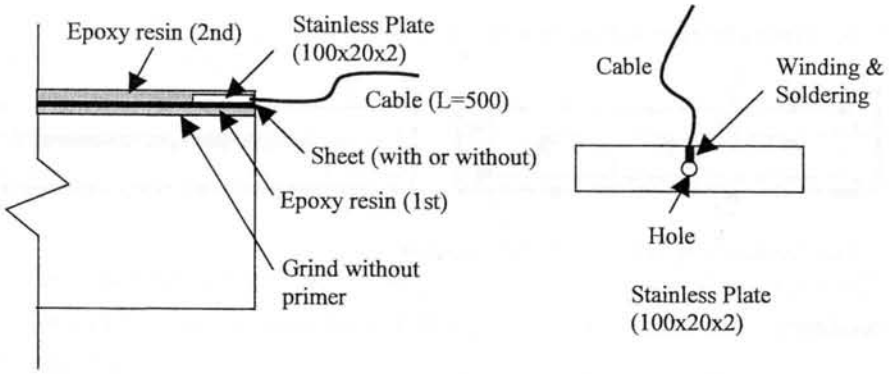

(b) Steel plate

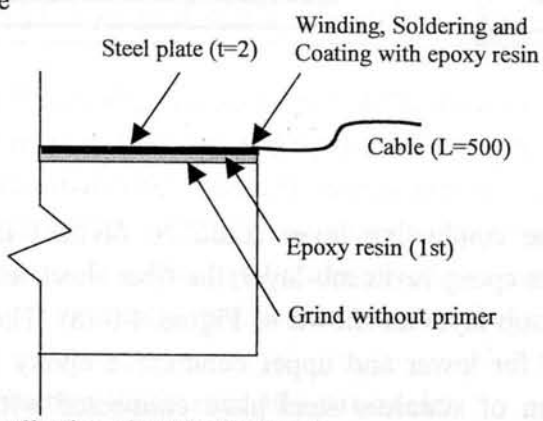

Figure 4.6 Application of conductive layers

4.3.4 Application of Conductive Layers

Figure 4.6 shows the bonding method of the strengthening materials that were used as the counter electrode in double rectangular pulse method. In case of conductive epoxy resin (type 2) and fiber sheet (type 3, 4 and 5), the layer application procedure are shown in Figure 3.5(a) and (b) of Chapter 3, but before apply the upper-epoxy the prepared 2x10x100mm stainless steel that already connected with the lead wire was placed at the end of each specimen. And in case of steel plate (type 6 and 7), the lead wire was directly soldered to the steel plate. The application of conductive layer in each types of material is explained here again in detail below.

Epoxy resin: The conductive layer could be divided into 2 sub-layers, lower and upper conductive epoxy resin sub-layers as shown in Figure 4.6 (a). The 150 g/m^2 was used for lower conductive epoxy resin and 200 g/m^2 for upper conductive epoxy resin. The 100x20x2mm of stainless steel plate connected with the lead wire was placed at the end of the specimen on lower conductive epoxy resin sub layer before apply the upper conductive epoxy resin sub-layer.

(a) Wet condition (steel immersion)

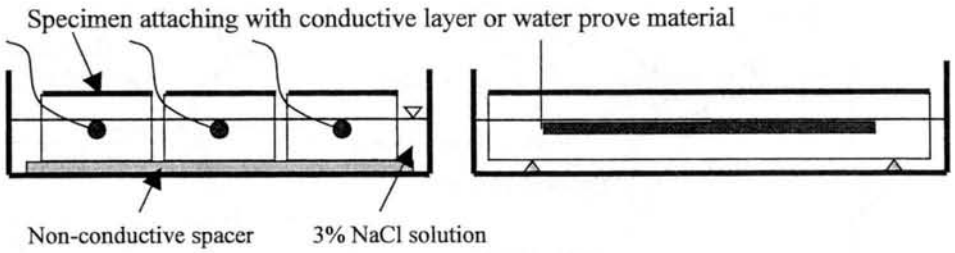

(b) Dry condition

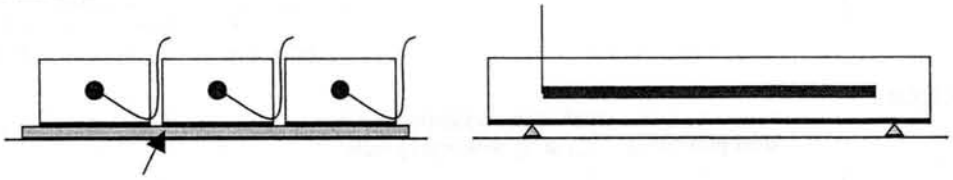

Figure 4.7 Wetting and drying cycle

CF sheet and AF sheet: The conductive layer could be divided into 3 sub-layers, the lower conductive epoxy resin sub-layer, the fiber sheet, and the upper conductive epoxy resin sub-layer as shown in Figure 4.6 (a). The 150 g/m^2 and 200 g/m^2 were used for lower and upper conductive epoxy resin, respectively. The 100x20x2mm of stainless steel plate connected with the cable was fastened at the end of the fiber sheet before apply the upper conductive epoxy resin sub-layer.

Steel plate: The conductive layer could be divided into 2 sub-layers, the conductive epoxy resin sub-layer and steel plate as shown in Figure 4.6 (b). The 150 g/m^2 was used for conductive epoxy resin, and the prepared steel plate that already connected with the cable.

4.4 Immersion

In the experiment, the specimens were placed at the basement without temperature and humidity control. In order to accelerate the corrosion of the steel, wet & dry cycle curing condition was applied. A wet & dry cycle consists of 3 days in 3% of NaCl solution, 1 dry day for measurement and 3 dry days as shown below.

1 week →	1	2	3	4	5	6	7
	wet	wet	wet	dry/measurement	dry	dry	dry

The wetting and drying cycle is shown in Figure 4.7. In the cycle, specimen type 1 were attached with 400x100x10mm of polystyrene form on top surface in order

to make the same condition for all types of concrete specimen in the wet and dry cycle. For other type of specimen, the small size of cotton was inserted into hole in order to prevent the evaporation of water.

4.5 Measurements

Electrochemical steel corrosion monitoring techniques that were employed in this research are half-cell potential and polarization resistance. The measurement details are shown in Table 4.6.

4.5.1 Half-Cell Potential Measurement

The half-cell potential was measured at the distance 0, 100, -100 mm from the center of the specimen on both top and bottom by using SRI portable rebar corrosion meter. The bottom (concrete surface) measurement may be regarded as the usual measurement for RC without any surface protection. The saturated silver chloride reference electrode locates at the center of the censor. At the same time, half-cell potential is automatically measured when the PR is measured.

4.5.2 Polarization Resistance Measurement

The PR was measured by 2 methods that are double rectangular pulse method and AC impedance method.

For double rectangular pulse method, auto-range corrosion meter 7635 was employed, where dual frequency of 0.1 Hz and 800Hz were set every 10 seconds with a current intensity automatically ranging 10 μ A to 1mA. The positions of the reference electrode were 0, 100 and −100 mm from the center of specimen on both top and bottom. On top surface of specimen type B to type G, the measurement was done at position of o-o-x (hole, hole and no-hole) in specimen no.1 and x-x-o (no-hole, no-hole and hole) in specimen no.2 as shown in Figure 4.4. In this measurement, the counter electrode was introduced. The copper plate was used as counter electrode for specimen type A. For the other, the external conductive layer itself was used as the counter electrode. In this research, the saturated silver chloride reference electrode (Ag(AgCl)KCl sat.) was used. Figure 4.8 shows the connecting line and experiment setting of 7365. The reinforcing steel inside concrete specimen is a working electrode and the copper plate/conductive layer is a counter electrode as shown in Figure 4.8.

Table 4.6 Measurement details

w/c	Test methods		Number of measurement							
			AC Impedance method						Double rectangular pulse method	
			HCP		PR-Gon		PR-Goff		PR	
	Position of measurement		Top	Bottom	Top	Bottom	Top	Bottom	Top	Bottom
0.45	1	Concrete	3*1	3*1	3*1	1 (0)*2	3 (0)*3	1 (0)*2	3	3 (0)*2
	2	8%CB CER	-	-	-	-	-	-	-	-
	3	8%CB CER with 1ply of CF sheet	3*1	3*1	3*1	1 (0)*2	3 (0)*3	1 (0)*2	3	3 (0)*2
	4	8%CB CER with 1ply of AFsheet	-	-	-	-	-	-	-	-
	5	8%CB CER with a steel plate	3*1	3*1	3*1	1 (0)*2	3 (0)*3	1 (0)*2	3	3 (0)*2
	6	8%CB CER with a steel plate and artificial blister	-	-	-	-	-	-	-	-
	7	8%CB CER and 1ply of CF sheet and artificial blister	-	-	-	-	-	-	-	-
0.65	1	Concrete	3*1	3*1	3*1	1 (0)*2	3 (0)*3	1 (0)*2	3	3 (0)*2
	2	8%CB CER	3*1	3*1	3*1	1 (0)*2	3 (0)*3	1 (0)*2	3	3 (0)*2
	3	8%CB CER with 1ply of CF sheet	3*1	3*1	3*1	1 (0)*2	3 (0)*3	1 (0)*2	3	3 (0)*2
	4	8%CB CER with 1ply of AFsheet	3*1	3*1	3*1	1 (0)*2	3 (0)*3	1 (0)*2	3	3 (0)*2
	5	8%CB CER with a steel plate	3*1	3*1	3*1	1 (0)*2	3 (0)*3	1 (0)*2	3	3 (0)*2
	6	8%CB CER with a steel plate and artificial blister	3*1	3*1	3*1	1 (0)*2	3 (0)*3	1 (0)*2	3	3 (0)*2
	7	8%CB CER and 1ply of CF sheet and artificial blister	3*1	3*1	3*1	1 (0)*2	3 (0)*3	1 (0)*2	3	3 (0)*2

Note HCP: Half-cell potential measurement, PR: Linear polarization resistance measurement
HCP: HCP by AC Impedance method with SRI machine in 2 frequencies mode
PR-Gon: PR by AC Impedance by using SRI machine in 2 frequencies mode and turn guard on.
PR-Goff: PR by AC Impedance by using SRI machine in 2 frequencies mode and turn guard off.
PR: PR by Double Rectangular Pulse Method with 7635 machine when reinforcing steel is WE and conductive layer or attached cupper plate is CE. (see Figure 3.8)
Top: Top surface in wet cycle; with conductive layer (B-G)Bottom: Bottom surface in wet cycle

*1 Points of measurement which is 100, 0, -100mm from center (In case of top surface is o, o, x in specimen 1 and x, x, o in specimen 2 of specimen type B to E and is o, x, x in specimen no.1 and x, x, o in specimen no.2 of specimen type F and G)
*2 Points of measurement and maybe stop the measurement if the value obtained from bottom is equal to one obtained from top.
*3 Points of measurement and maybe stop the measurement if the value obtained from guard off is equal to one obtained from guard on.

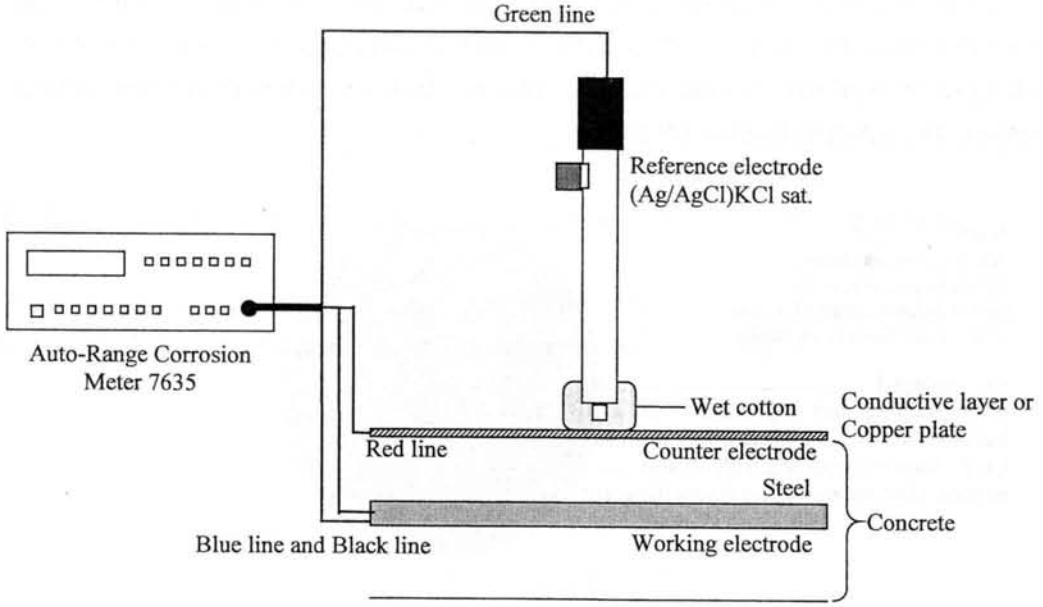

Figure 4.8 Schematic representation of the use of auto-range corrosion meter 7635 to measure polarization resistance

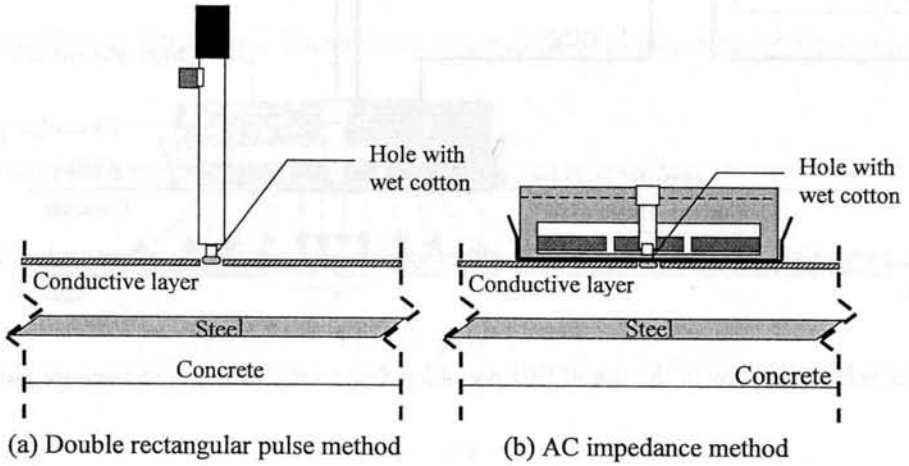

Figure 4.9 Measurement at hole, top surface

In order to connect the reference electrode and concrete surface, the small size of wet cotton was inserted into the hole in the case of top surface measurement as shown in Figure 4.9(a).

In AC impedance method, the 2-frequencies mode of SRI portable rebar corrosion meter was used and 3 points measurement at the distance 0, 100, -100 mm from the center of the specimen was done both top and bottom. Guard's effect also was taken into account. Therefore in the experiment, guard was switched both on and off. In case of guard-on, the 2-frequencies and applied peak voltage were 10Hz, 20mHz and $10mV_{p-p}$, respectively. For guard-off, the 2-frequencies and applied peak voltage were 10Hz, 20mHz and $1mV_{p-p}$, respectively because the machine asked to

use small value of current intensity when guard-off was tested. Figure 4.10 shows the use of SRI machine. In order to connect the reference electrode and concrete surface, the small size of wet cotton was inserted into the hole in the case of top surface measurement as shown in Figure 4.9 (b).

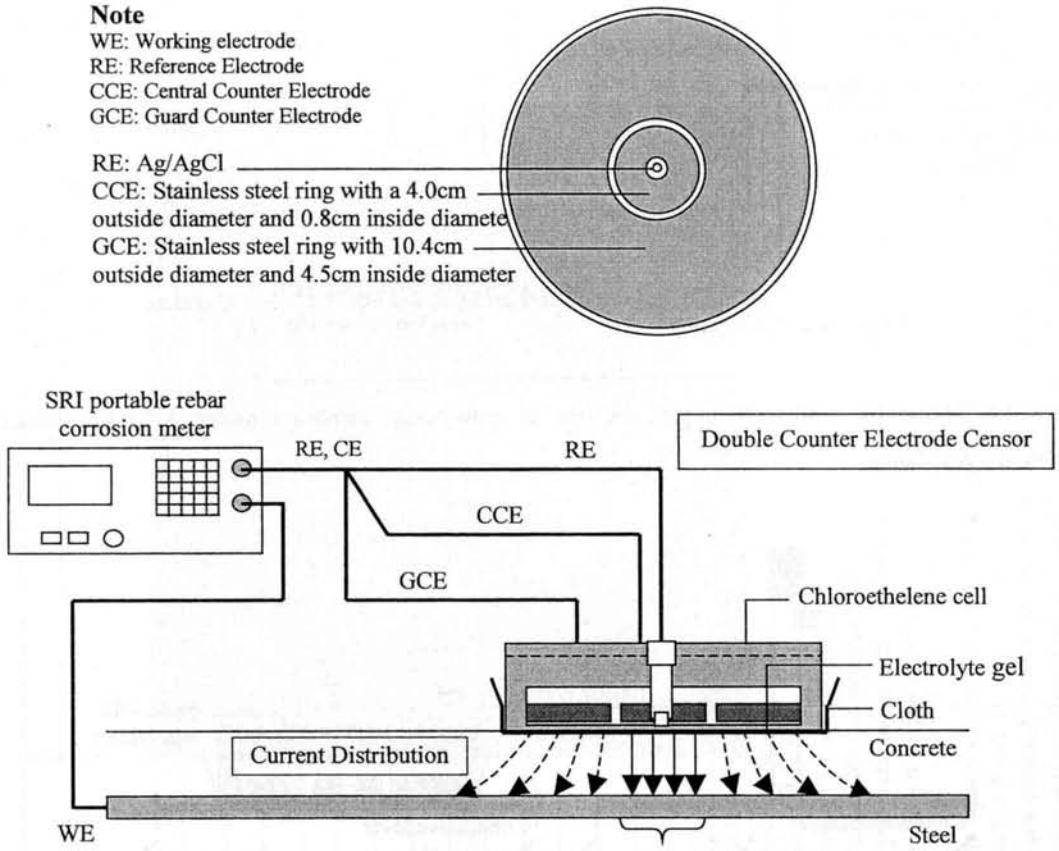

Figure 4.10 Schematic view of the use of SRI portable rebar corrosion meter to measure polarization resistance

4.5.3 Corrosion Loss Measurement

After 28 days for curing and 1 week of conductive layer bonding (totally 35 days of the specimen's preparation), corrosion loss will be weighed at the age of 6months and at the age of 2years and 9 months. Before weighing, the corroded steel cleaning procedure was done by following the JIS-SC1. The procedure is done by breaking the concrete specimen by hammering, take the reinforced steel out, remove the pieces of concrete from the reinforcing steel surface by brushing, submerge the reinforcing steel in 10% of di-ammonium hydrogen citrate at 60°C for 24-hour, wash with water, blow with cool wind until dry, and then weigh the corroded rebar.

4.6 Calculations

The current density and corrosion loss were calculated. The obtained values of PR were converted to those two parameters by using the two equations as follow.

4.6.1 Conversion of polarization resistance to corrosion current density

Refer to chapter 2, the corrosion current density, I_{corr} is related to the polarization resistance by the coefficient, K as shown in the equation below:

$$I_{corr} = \frac{K}{R_p.A} \qquad (4.1)$$

where

I_{corr}	*Corrosion current density (A/cm^2)*
K	*Constant (general value = 0.026V)*
R'_p	*Apparent polarization resistance (Ω)*
A	*Measured area of reinforcing steel (cm^2)*

Eq.4.1 is different from Eq.2.2 as shown in chapter 2, because the different in unit of R_p.

4.6.2 Conversion of polarization resistance to corrosion loss

The expression to calculate the corrosion loss for PR is shown in Eq.4.2.

$$C_d(t) = \frac{m}{zF}\int_0^t \frac{K}{R_p A}dt = \frac{m}{zF}\int_0^t I_{corr}\,dt \qquad (4.2)$$

where

$C_d(t)$	*Corrosion loss at t (g/cm^2)*
m	*Atomic mass of iron (=55.8g)*
z	*Valence electron of iron (=2)*
F	*Faraday constant (96,500A.s)*
K	*Constant (general value = 0.026V)*
R'_p	*Apparent polarization resistance (Ω)*
A	*Measured area of reinforcing steel (cm^2)*
t	*Time (s)*
I_{corr}	*Corrosion current density (A/cm^2)*

Figure 4.11 shows the example of the plot of corrosion current density, I_{corr} vs. time, t. where i_n is corrosion current density at time t_n, and A_n is an area of individual time interval (t_n-t_{n-1}).

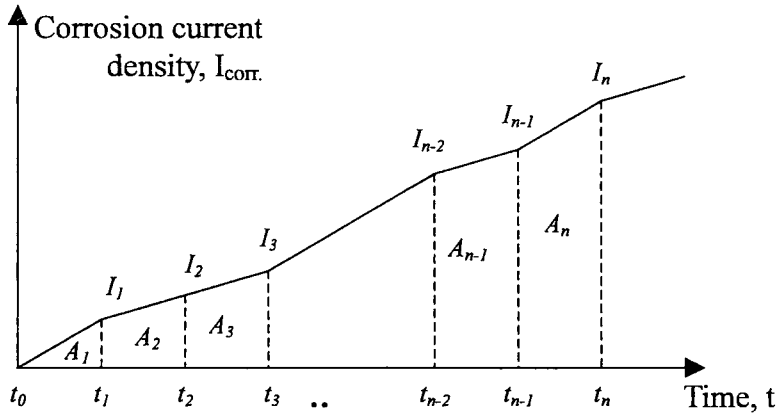

Figure 4.11 Plot of corrosion current density vs. time

The integration means the total area under the curve. Hence, Eq.4.2 means the total area under the corrosion current density curve multiply by *m/zF*. Moreover, the obtained value of corrosion current density is in the discrete form, not in the continuous form, then, the integration sign should be changed to the summation sign as shown in Eq.4.3.

$$C_d(t=t_n)=\frac{m}{zF}\sum_{n=1}^{n}A_n \qquad (4.3)$$

where A_n is the trapezoidal area under the line between two points of I_{n-1} and I_n at time t_{n-1} and t_n, respectively. Eq.4.4 shows the mathematical formula of the trapezoid.

$$A_n=\frac{1}{2}(I_n+I_{n-1})(t_n-t_{n-1}) \qquad (4.4)$$

Therefore Eq.4.2 can be rewritten in the form of summation sign as shown in Eq.4.5, by substitution of Eq.4.4 into Eq.4.3.

$$C_d(t=t_n)=\frac{m}{zF}\sum_{n=1}^{n}\frac{1}{2}(I_n+I_{n-1})(t_n-t_{n-1}) \qquad (4.5)$$

In case of the double rectangular pulse method, the apparent polarization resistance is obtained that is in the unit of ohm (Ω). Therefore, Eq.4.1 was employed in order to calculate corrosion current density, I_{corr}. The measured area of reinforcing steel *A*, which equal to half reinforcing steel's surface as shown in Figure 4.12, was used in the calculation.

In case of AC impedance method, the value of polarization resistances, which had been automatically calculated by the SRI machine, was used in order to calculate corrosion current density (I_{corr}) only in case of guard-on. Because the measured area of steel that automatically calculated by the machine is 157 cm^2 in case of guard-off that was larger than the actual one. Thus, the apparent polarization obtained in this case was multiplied by actual measured area of steel that is equal to 47.124 cm^2. Then these calculated values were used to calculate corrosion current density.

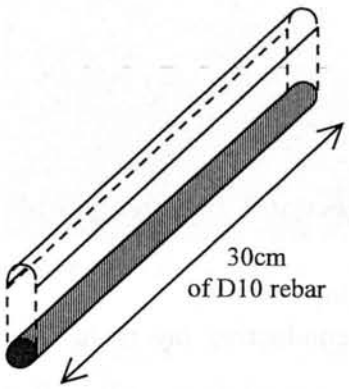

A = half of perimeter of D10 rebar x length
= πrl
= 3.141592 x 0.5 x 30
= 47.124 cm^2

Figure 4.12 Measured area of reinforcing steel

Finally, Eq.4.5 was employed to calculate corrosion loss by substitute all known parameters of *m, z, F* as 55.85g, 2 and 96500A.s, respectively.

4.7 Notation

Notation used to represent type of specimen

"0.45w/c Con ", "0.65w/c CF" or "0.65w/c CFG"

The number represents w/c,
where 0.45 = 0.45w/c
0.65 = 0.65w/c

The alphabet represents specimen's type,

where Con : Specimen type 1 (non-bonding),
CER : Specimen type 2 (8%CB CER)
CF : Specimen type 3 (8%CB CER with 1ply of CF sheet)
AF : Specimen type 4 (8%CB CER with 1ply of AF sheet)
ST : Specimen type 5 (8%CB CER with a steel plate)
STG : Specimen type 6 (8%CB CER with a steel plate and artificial blister)
CFG : Specimen type 7 (8%CB CER and 1ply of CF sheet and artificial blister)

Example;

"0.45w/c Con" means 0.45w/c of specimen type 1.
"0.65w/c CF" means 0.65w/c of specimen type 3.
"0.65w/c CFG" means 0.65w/c of specimen type 7.

Notation used in the label boxes

The meaning of notation used is listed below;

Top	: Top surface in wet cycle
Bottom	: Bottom surface in wet cycle
Con	: Obtained data on concrete surface (bottom) in each types of specimen
CER, CF, AF, ST	: Obtained data on conductive layers (top surface)
CER-hole, CF-hole, AF-hole, ST-hole	: Obtained data in drilled hole on conductive layers to the concrete surface (top surface)
ST-gap, CF-gap	: Obtained data on conductive layer at the position of buried plastic plate (top surface)

4.8 Experimental Results and Discussions

4.8.1 Visual observation

There was no evidence of crack showed up on he concrete surface even the experiment has been done for 2 years and 9 months. But it can obviously observed the white crystal of NaCl on the concrete surface. One another problem is the corrosion of the steel plate that bonded on the specimen in the ST and STG series. The corrosion of the steel plate has started since the week 16 of the observation (Figure 4.13). Moreover, the debonding of steel plate from the specimen and cutting off of the electrical lead wire from strengthening layer also occurred in long-term observation.

4.8.2 Half-Cell Potential

The criteria to indicate the probability of corrosion according to half-cell reading by silver chloride saturated electrode ((Ag/AgCl)KCl sat. or SSCE) is –80mV and –230 mV as written in chapter 2. The potential nobler than –80mV indicates 90% probability no corrosion, the potential poorer than –230mV indicates 90% probability of corrosion. If the potential between these two values indicates uncertain corrosion in the measure area.

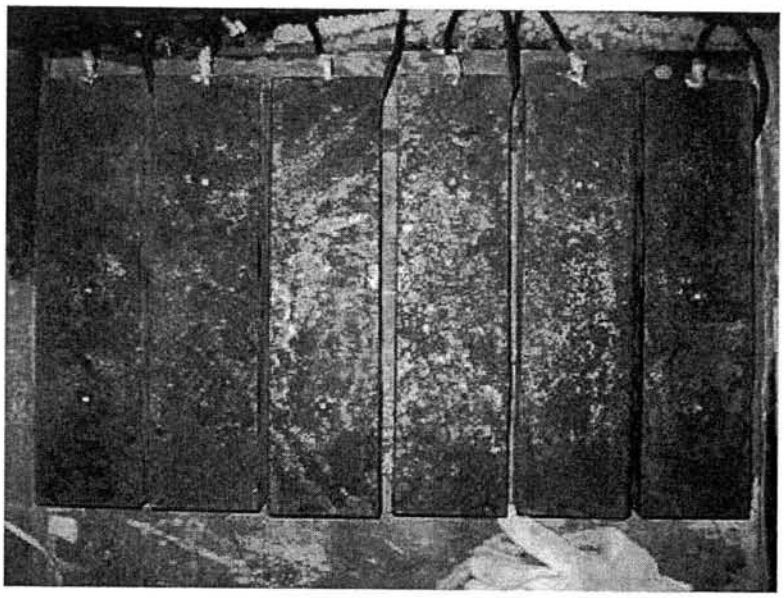

Figure 4.13 Corrosion of steel plate bonded on concrete specimen

Figure 4.14 shows the results of HCP obtained on conductive strengthening layers both 0.45w/c and 0.65w/c. The potential reading in 0.45w/c is poorer than –230mV at week 44, 36 and 44 of Con, CF and ST respectively. But the potential reading of 0.65w/c is poorer than –230 since a couple weeks after observation. The tendency of HCP readings of 0.45w/c series gradually decreases with time while that of 0.65w/c sharply decreases. It can be explained by the different in w/c have effect to HCP reading. The low w/c (0.45w/c) concrete has low porosity than one with high w/c (0.65w/c) that resists the ingression of chloride ion into concrete, and lower corrosion activity may be obtained. Therefore, it is clearly explained that concrete with 0.45w/c has nobler potential than concrete with 0.65w/c concrete.

Figure 4.14(a) and (d) compare the value obtained on non-bonding specimen. It demonstrates that the HCP obtained from both side of these control specimens are equal to each other and can be used to compare the HCP reading between conductive strengthening layer's surface (top in wet phase cycle) and concrete surface (bottom in wet phase of cycle) in the other type specimen.

The potential readings on the conductive strengthening layer's surface and concrete surface are shown in Figure 4.14(b), (c) and (e) to (j). The potentials obtained on the layer are quite equal from concrete surface in case of CER, CF and AF, except in case of ST plate that the potential reading on the layer is a bit obviously different from the potential from concrete surface. It may say the reason that the difference in potential reading on steel plate is the corrosion of steel plate.

Three measure conditions, which are layer without hole, layer with hole and artificial gap, do not give any obviously different from each other. Therefore, we may conclude that all conditions give the same potential reading.

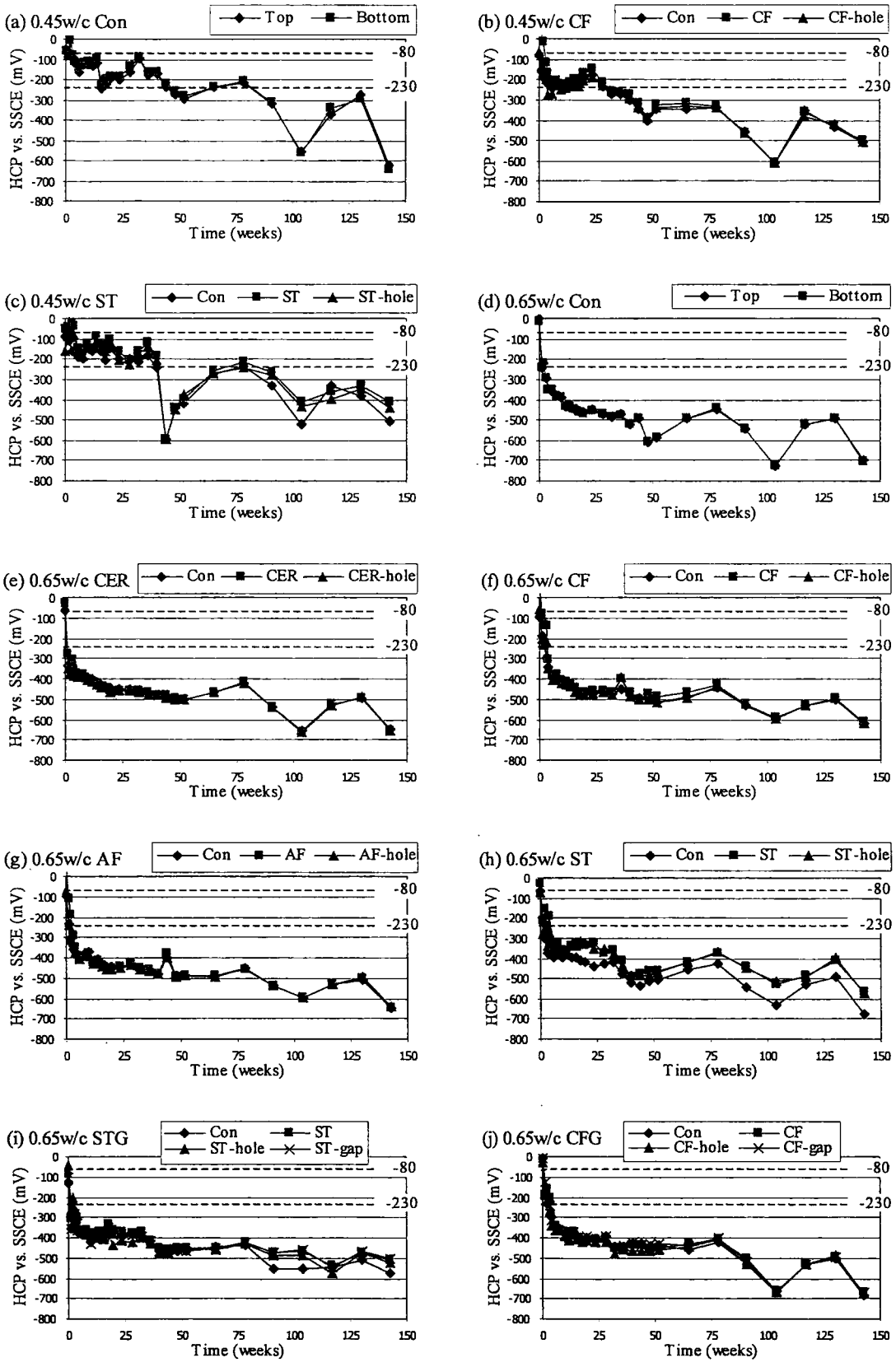

Figure 4.14 Half-cell potential reading

4.8.3 Polarization Resistance, Corrosion Current Density and Corrosion Loss

4.8.3.1 AC Impedance Method

In this section the obtained PR (R_p) by AC impedance method by using SRI portable rebar corrosion meter in 2-frequency mode with switching guard on and off, are explained together. Moreover, the corrosion current density (I_{corr}) and corrosion loss (C_d), which are calculated from the obtained polarization resistance, are also explained in this section.

1) Polarization resistance

Before going in to explain the results of obtained PR, we have to make clear and keep in mind that the actual obtained PR values randomly came out negative, or even enormous. Therefore, the negative values and enormous values are omitted before plotting and using in calculate the value of corrosion loss. The value of PR should be positive because the value of corrosion current density will be positive and corrosion loss will increase gradually. If not, the value of corrosion current density will be negative and corrosion loss will be decrease that is not impossible in the real situation.

Figure 4.15 and 4.16 illustrate the adjusted value of PR obtained by AC impedance method guard-on and guard-off, respectively. The PR of 0.45w/c is higher than the PR of 0.65w/c both guard-on and guard-off. That can be explained by the same reason as in section of HCP; lower w/c has lower porosity, lower ingression of chloride ion and presents more PR. The criteria to evaluation PR are shown in Table 2.3. The obtained PR values of 0.65w/c no both guard-on and guard-off, and those of 0.45 in case of guard off are lower than 26kΩ.cm^2 while the most obtained value of 0.45w/c in case of guard on are larger. From the criteria, PR lower than 26kΩ.cm^2 indicates high rate corrosion, and bigger can indicate moderate, low and very low rate of corrosion.

In those figure case (a) and (d) show the value obtained on no-bonding specimens (0.45w/c Con and 0.65w/c Con). The values obtained on top surface are quite equal to the values obtained from the bottom surface. Even though some difference between them come out, e.g., Figure 4.15(a) at the period of 50 to 75 weeks and 104 to 130 weeks. However, we have to use these obtained values of PR from bottom surface (concrete) to compare with those obtained on top surface (conductive strengthening layer) in another cases.

The comparisons of PR obtained on conductive strengthening layer and concrete surface are in Figure 4.15 and 4.16 (case (b), (c) and (e) to (j)) The PR reading on the conductive layer without hole and conductive layer with artificial gap are not stable at the beginning, but become stable in the long term. The values PR obtained on conductive layer are in the same tendency, some (AF and ST) equal to those obtained

on the concrete surface, and some (CER and CF) fluctuation and much bigger than to those obtained on the concrete surface. However, some evidence shows up. PR obtained of the layer with hole give the value closer to PR obtained on concrete surface than that of the layer without hole, which can be seen in many figures, but still several time bigger in magnitude.

For the over all results, PR obtained on the same type conductive layer but different w/c, or obtaining by guard-on and guard-off are not consistency. Finally, the clear relation between those values of conductive layer and one of concrete cannot be found.

2) Corrosion current density

Figure 4.17 and 4.18 show the corrosion current density that calculated from the obtained PR by AC impedance method with guard-on and guard-off, respectively. As written in Eq.4.1, I_{corr} is inversely proportional to R_p, then, the results of I_{corr} will be related to the obtained PR but opposite in magnitude and tendency. For example, the results of 0.65w/c CER with guard-on, PR (Fig 4.15(e)) showed that the values obtained on the conductive layer were much bigger than the value obtained on concrete surface and its tendency was gradually decreased while I_{corr} (Fig. 4.17(e)) showed that the values obtained on the conductive layer was much smaller than the value obtained on concrete surface and its tendency was gradually increased.

From Figure 4.17 and 4.18, I_{corr} calculated from PR obtained on conductive layer and I_{corr} calculated from PR obtained on concrete surface are compared. For CER and CF, I_{corr} of conductive layer (with hole and without hole) were several times lower than that of concrete surface and sometimes the fluctuations occurred. For AF and ST, the calculated I_{corr} were quite equal to I_{corr} of concrete surface both in case of guard-on and guard-off, and were much steady than the results of CER and CF. even some cases in guard-on were not.

3) Corrosion Loss

Figure 4.19 and 4.20 demonstrate the calculated results of C_d from PR obtained by guard-on and guard-off, respectively. Because of C_d was also calculated from obtained PR, therefore, the results of C_d were much similar to the results of PR as same as in case of I_{corr}.

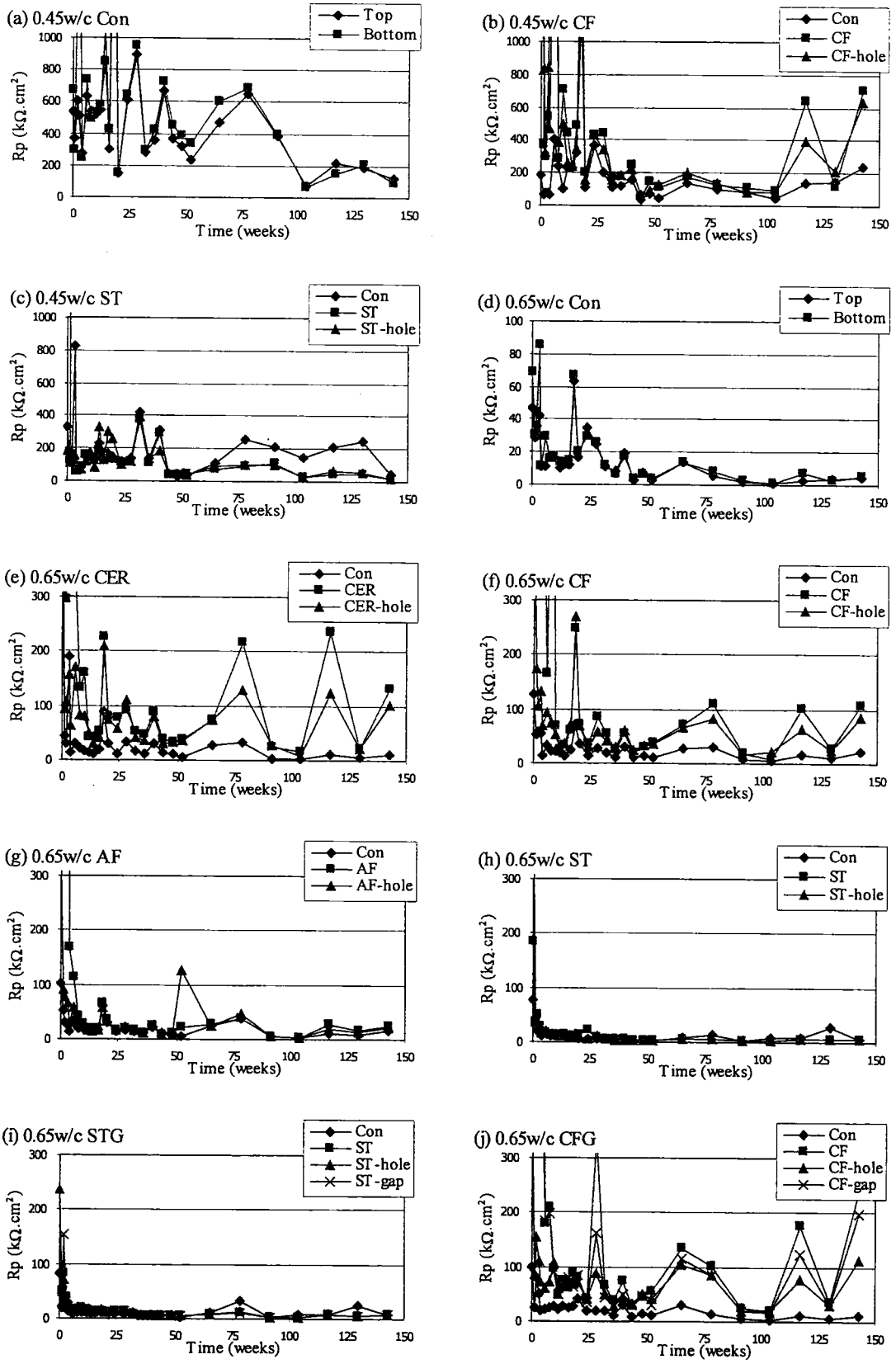

Figure 4.15 Polarization resistance reading by AC impedance method with guard-on

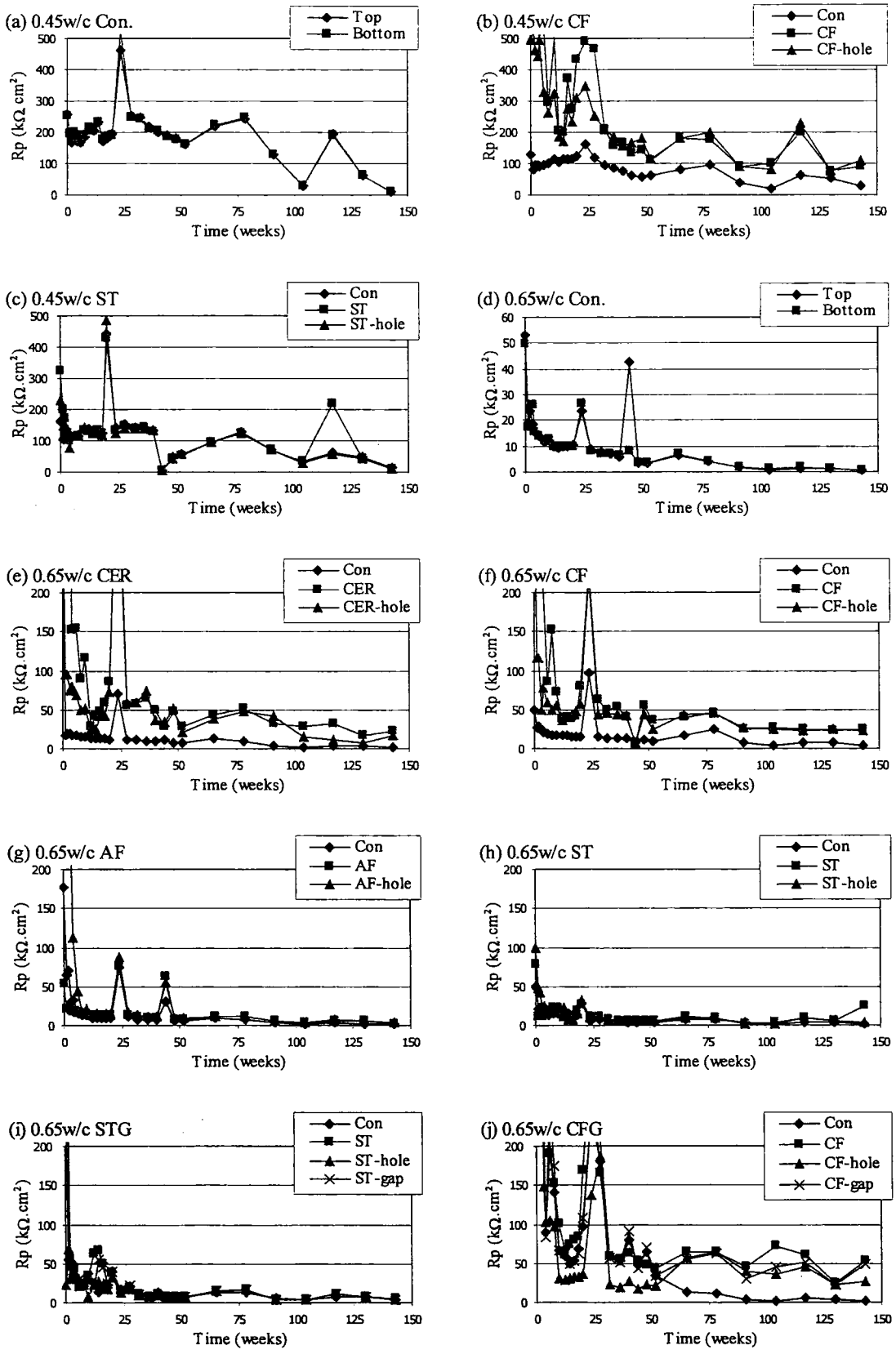

Figure 4.16 Polarization resistance reading by AC impedance method with guard-off

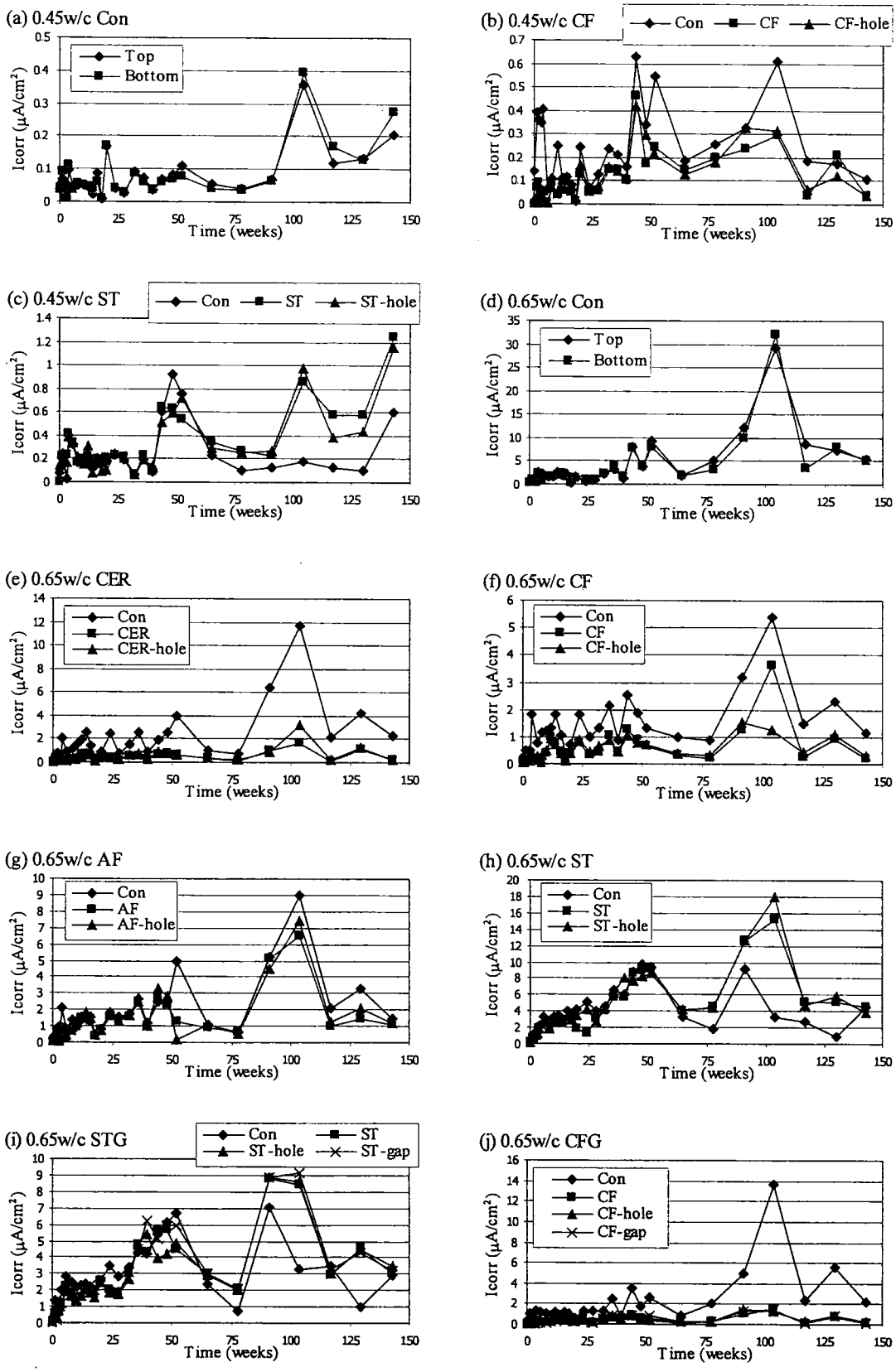

Figure 4.17 Corrosion current density calculated from polarization resistance reading by AC impedance method with guard-on

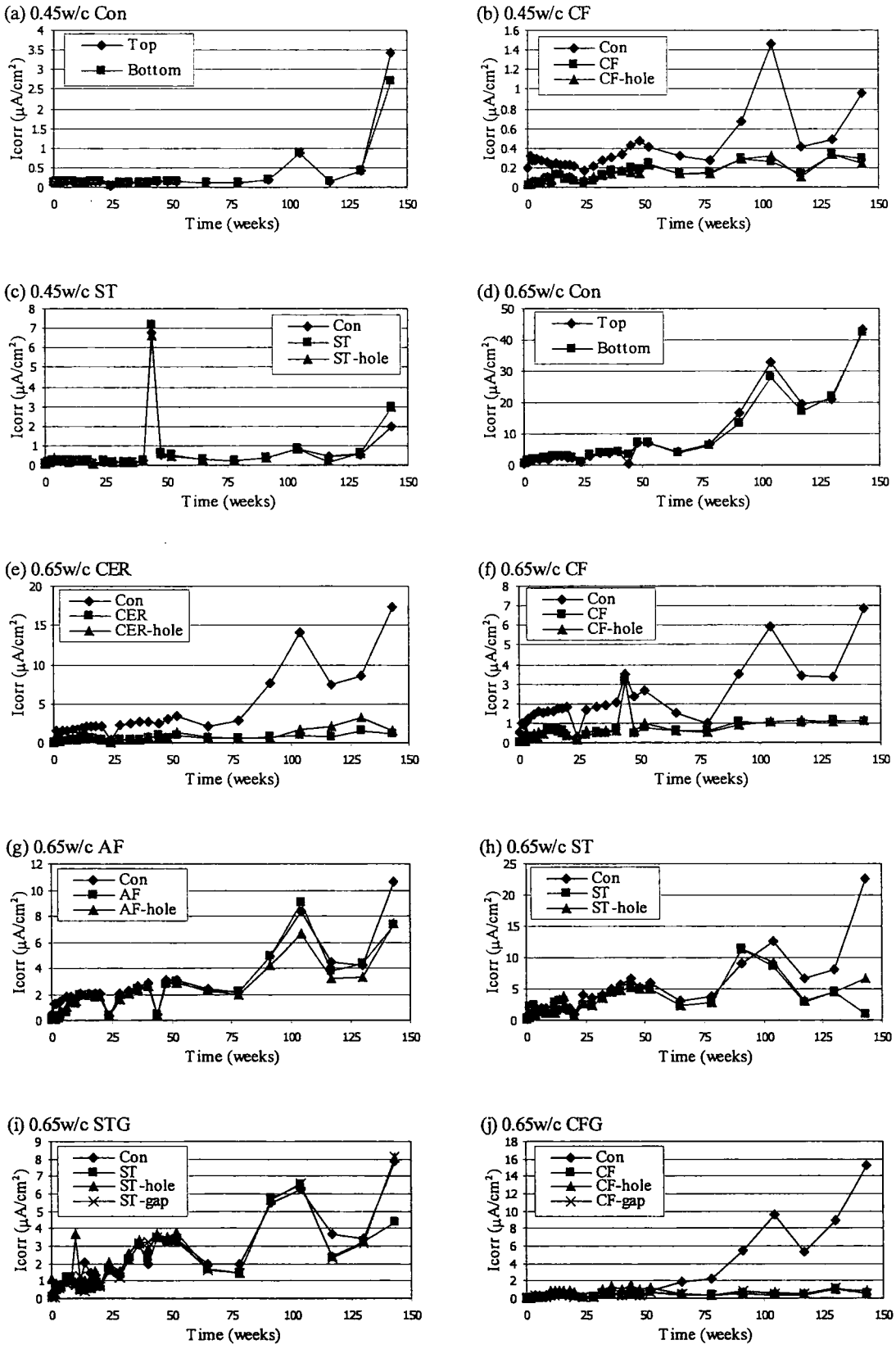

Figure 4.18 Corrosion current density calculated from polarization resistance reading by AC impedance method with guard-off

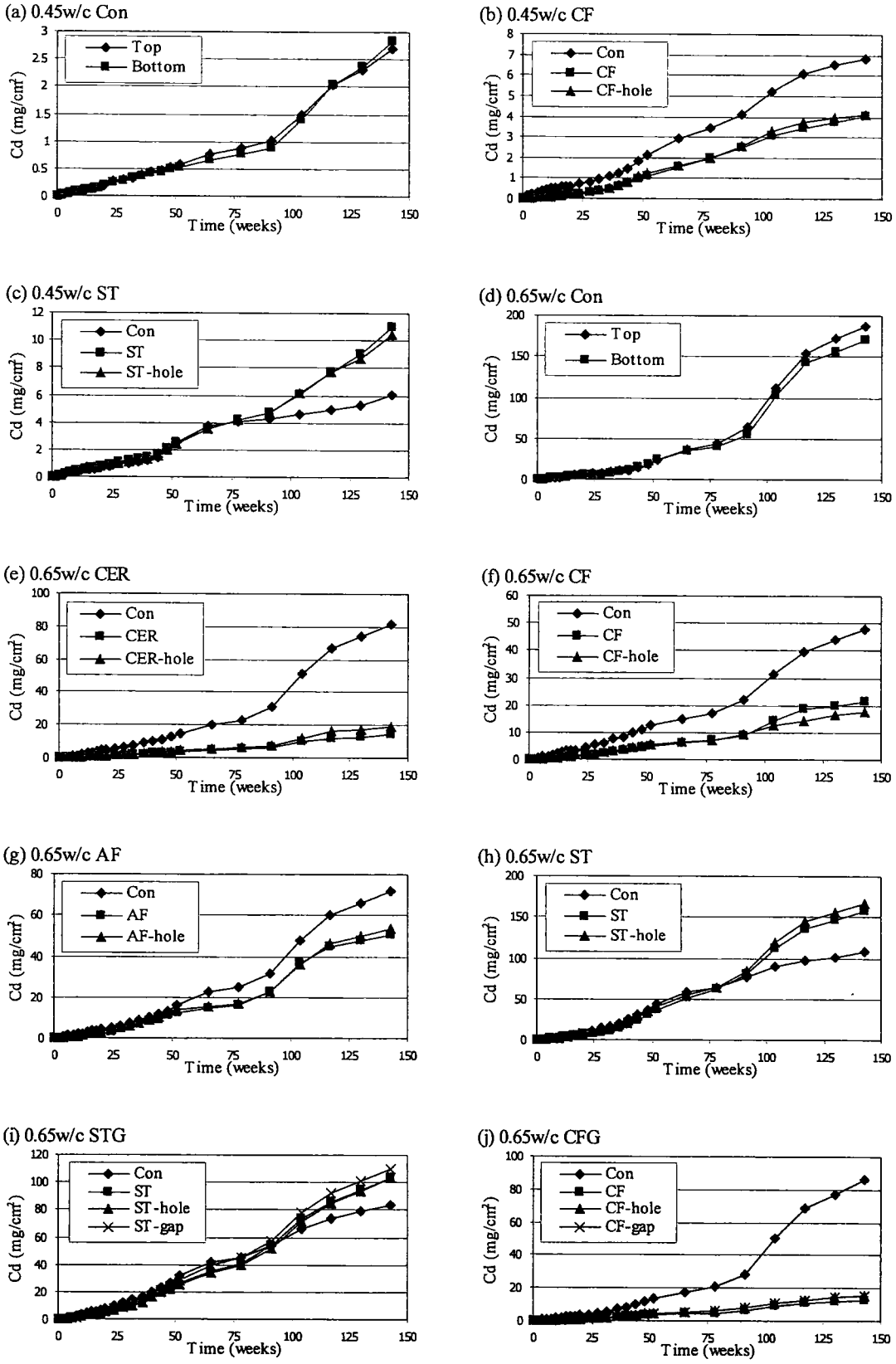

Figure 4.19 Corrosion loss calculated from polarization resistance reading by AC impedance method with guard-on

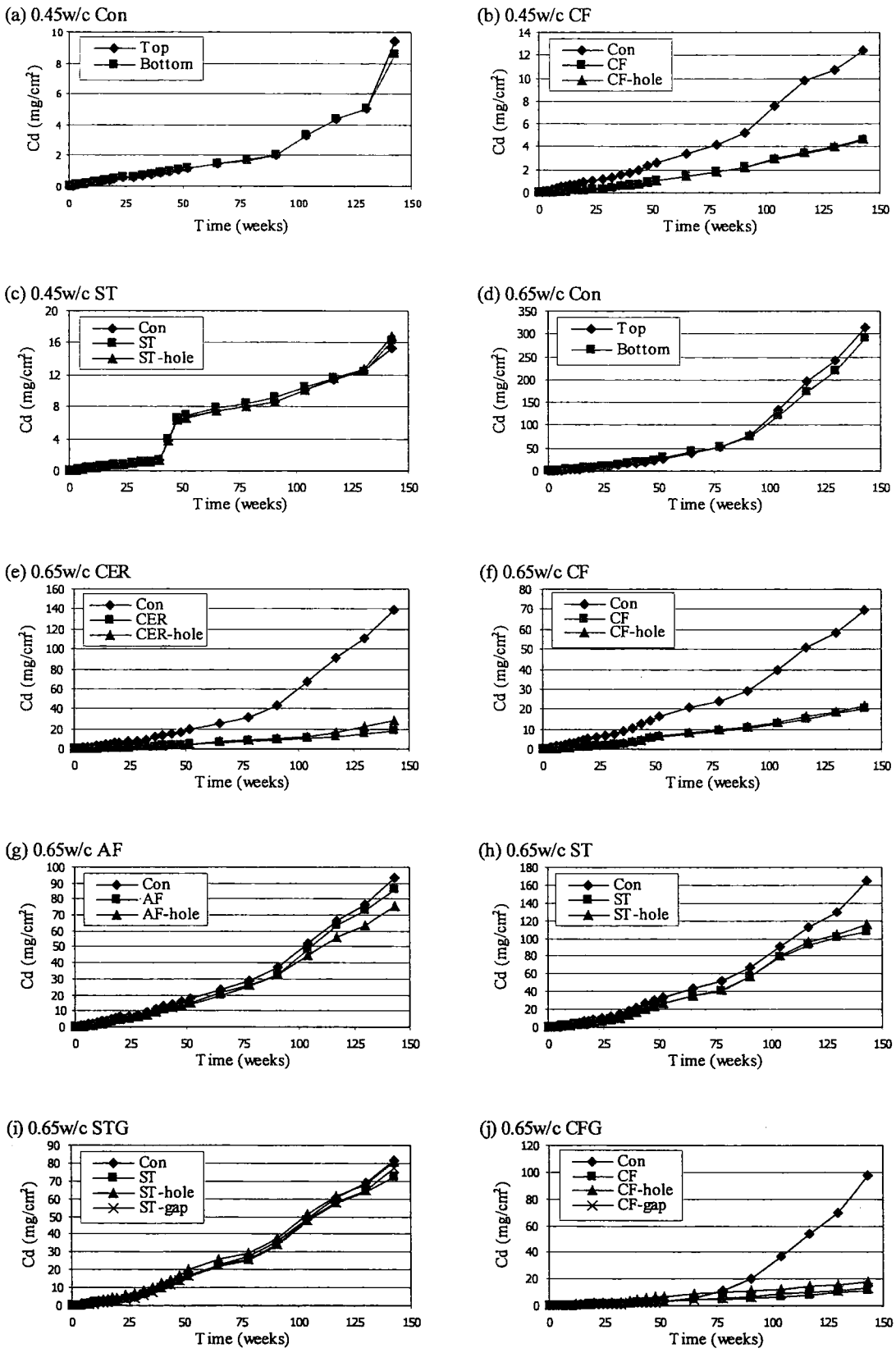

Figure 4.20 Corrosion loss calculated from polarization resistance reading by AC impedance method with guard-off

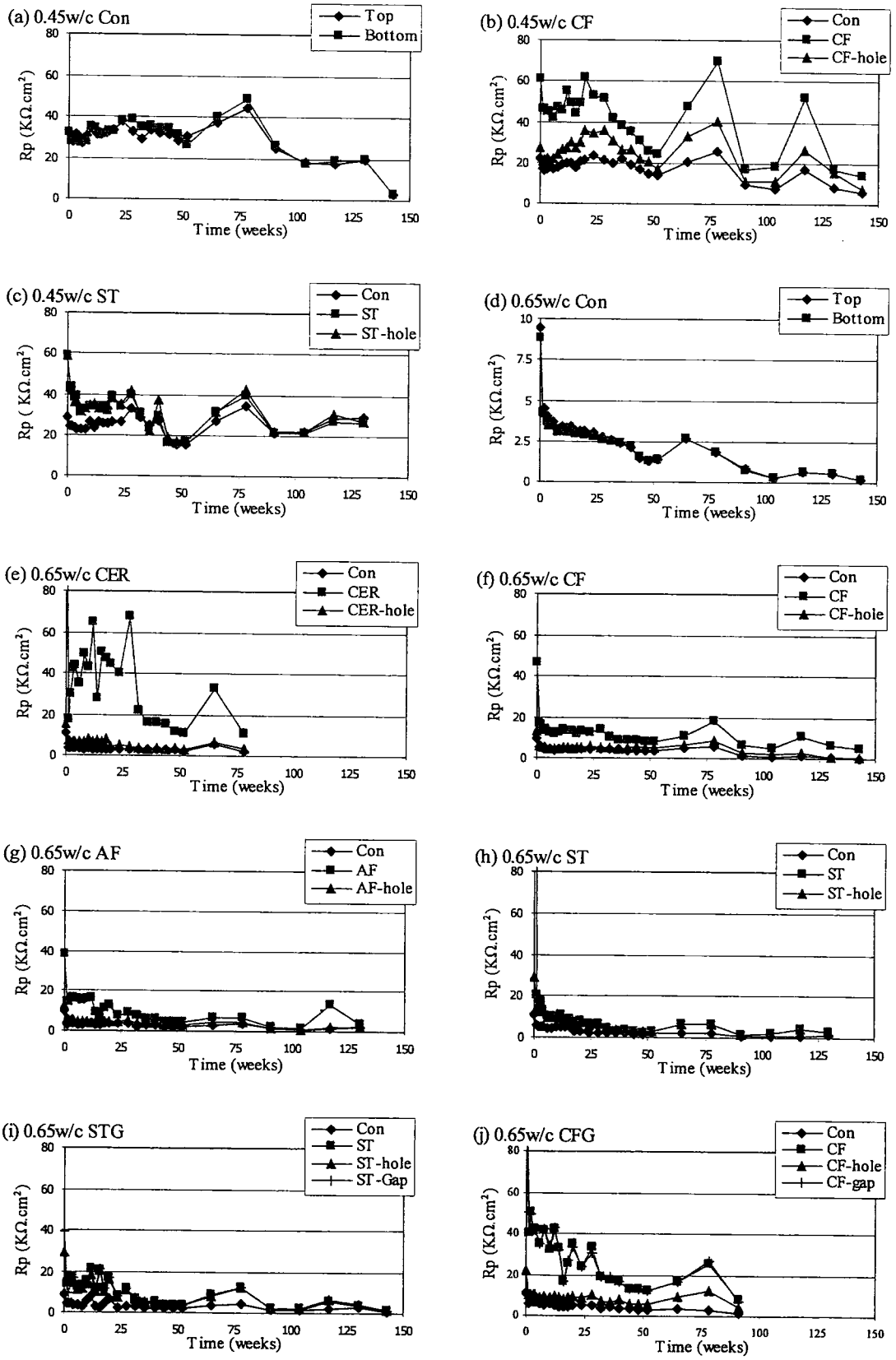

Figure 4.21 Polarization resistance obtained by double rectangular pulse method

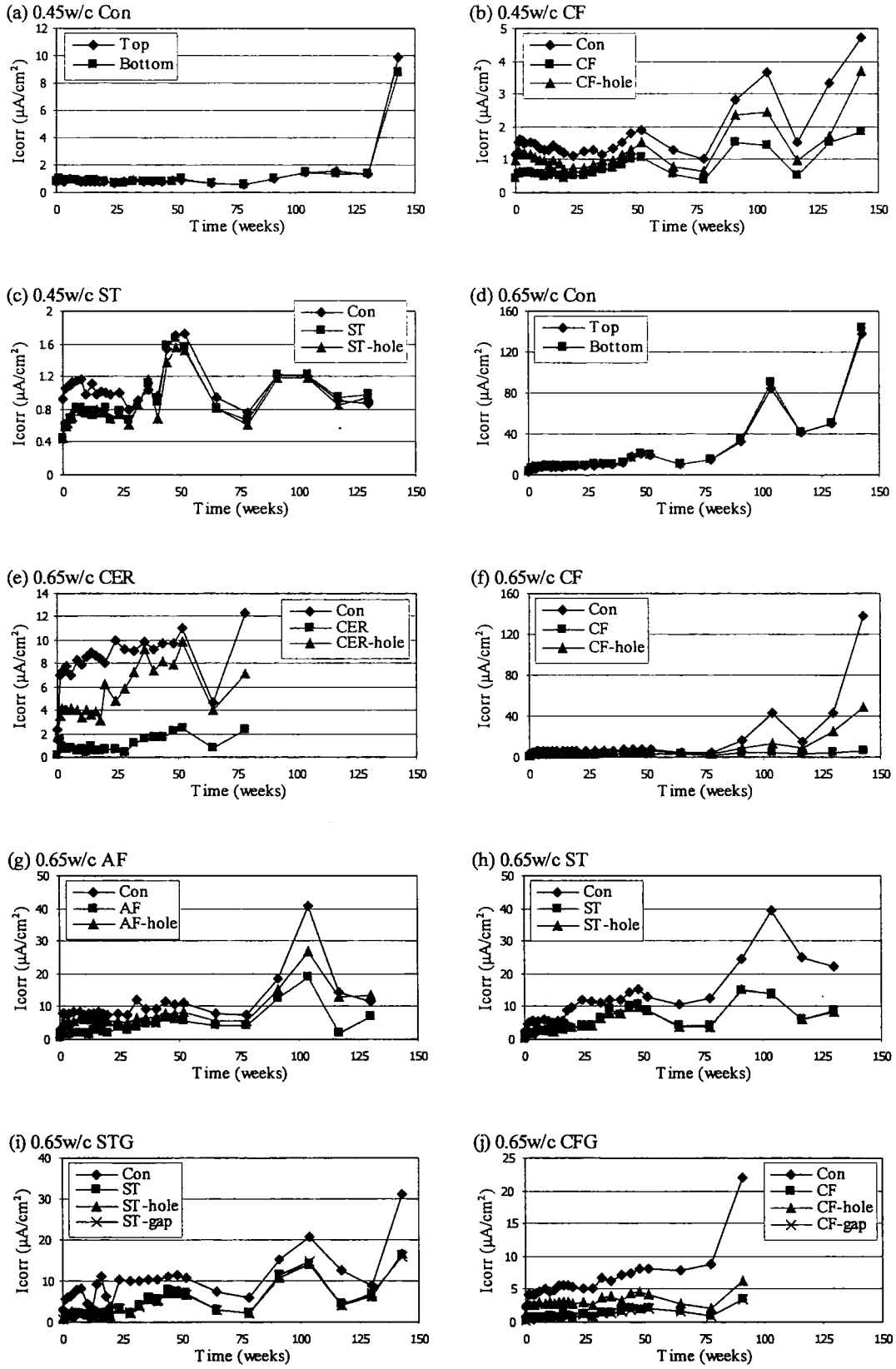

Figure 4.22 Corrosion current density calculated from polarization resistance reading by double rectangular pulse method

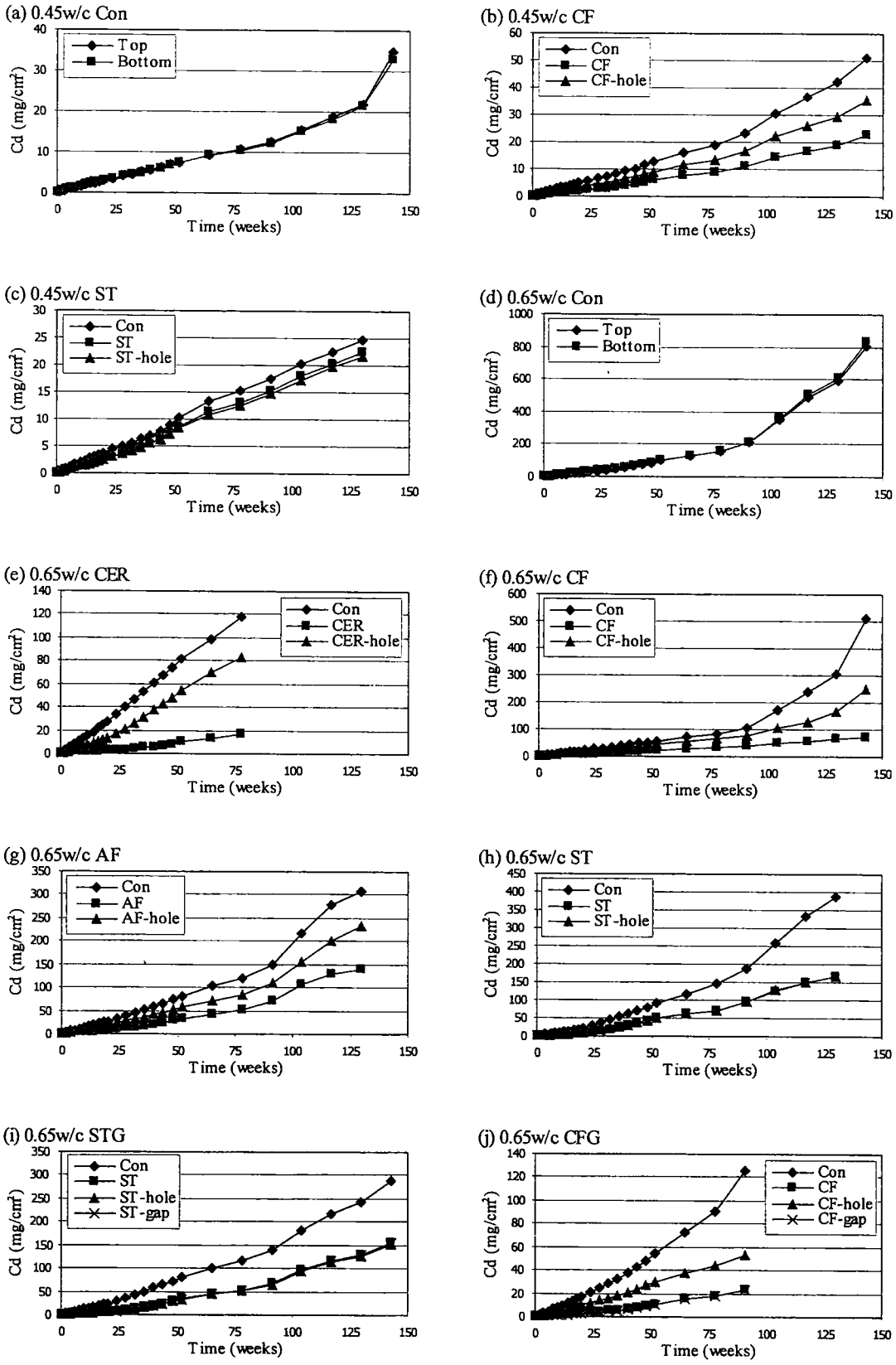

Figure 4.23 Corrosion loss calculated from polarization resistance reading by double rectangular pulse method

4.8.3.2 Double Rectangular Method

1) Polarization resistance

Figure 4.21 illustrates the experimental results of PR reading by double rectangular pulse method. In some cases, the results were obtainable until the breaking down of the connection lead wire from the conductive strengthening layer and the measurement could not be obtained anymore. Refer to Table 2.3, the criteria to evaluate PR, PR obtained in 0.65w/c series has lower value than 26kΩ.cm^2 indicate the severe state of high corrosion. PR obtained in 0.45w/c series has bigger value 26kΩ.cm^2 that can be indicate moderate, low and very low rate of corrosion depends on the range of obtained PR in each cases.

Figure 4.21 (a) and (d) shows the comparison of PR reading from top and bottom surface of non-bonding specimens. From the figure, the readings from both surfaces are quite equal to each other, even slightly different in magnitude, or even one point in 0.65w/c Con is much different occurs at week 44.

The PR readings on conductive strengthening layers compare to concrete surface are demonstrated in Figure 4.21(b), (c), and (f) to (j). PR readings on conductive layer are in the same tendency with one reading from concrete surface, but only different in magnitude. Moreover, the clear relation between the layer without hole, with hole, and gap can be found. PR obtained on the layer with hole is much steady and closer than PR obtained on layer with out hole in most cases, except in case of steel plate than the reading on both conductive layer without hole and with hole are quite the same. In addition, the PR reading on conductive layer at gap is quite equal to PR reading on conductive layer without hole both in case of conductive CF sheet and steel plate.

There are some doubts that PR reading on concrete surface and PR reading on conductive layer with hole, which should be equal, are not equal. Because the reading in both cases are done by directly placing the reference electrode with the wet cotton on the concrete surface. Therefore, some interactions may happen when the connection occurs between the wet cotton and surrounding conductive layer.

The PR reading on steel plate without hole is quite equal to the reading at hole while the readings on the other conductive layer are much different. It may be said that the steel plate is only material that can be obtained PR directly on the plate.

2) Corrosion Current Density

Figure 4.22 shows the value of I_{corr} calculated from PR obtained by double rectangular pulse method. Again, because of I_{corr} calculated from PR by Eq. 4.1, then, the results of I_{corr} will be related to the obtained PR but opposite in magnitude and

tendency. For example, the results of 0.65w/c CER, the PR value (Figure 4.21(e)) obtained on the conductive layer without hole was much larger than the value obtained on concrete surface while the value of I_{corr} (Figure 4.22(e)) of conductive layer without hole was much smaller than the value of concrete surface. The conductive layer with hole also gave closer value to the concrete surface than the conductive layer without hole in almost cases, except in case of steel plate as same as obtained in the results of PR.

3) Corrosion Loss

Figure 4.23 demonstrates the calculated results of C_d from PR obtained by double rectangular pulse method. Again, because of C_d was also calculated from obtained PR, therefore, the results of C_d were much similar to the results of PR as same as in case of I_{corr}.

Table 4.7 Actual corrosion loss at age of 2 years and 9 months

Specimen	Corrosion Loss (mg/cm^2)			
	Actual	AC Impedance method		Double reactangular pulse method
		Guard-on	Guard-off	
0.45w/c Con1	36.82	6.53	20.25	55.86
0.45w/c Con2	39.47	1.83	6.03	24.69
0.45w/c CF1	46.37	7.26	14.63	51.17
0.45w/c CF2	41.49	7.39	11.67	n/a
0.45w/c ST1	32.26	n/a	n/a	n/a
0.45w/c ST2	39.79	11.31	26.04	n/a
0.65w/c Con1	53.26	177.72	266.49	716.57
0.65w/c Con2	76.61	194.35	361.45	981.29
0.65w/c CER1	41.49	76.93	119.03	n/a
0.65w/c CER2	47.85	92.70	184.50	n/a
0.65w/c CF1	45.20	94.38	123.46	543.68
0.65w/c CF2	30.13	38.19	52.83	n/a
0.65w/c AF1	28.33	59.35	73.31	n/a
0.65w/c AF2	32.57	96.56	132.31	n/a
0.65w/c ST1	70.35	n/a	n/a	n/a
0.65w/c ST2	51.35	110.53	164.94	n/a
0.65w/c STG1	20.80	80.81	83.88	230.85
0.65w/c STG2	21.65	87.28	92.99	411.37
0.65w/c CFG1	62.18	82.74	104.36	n/a
0.65w/c CFG2	54.22	82.29	121.21	n/a

4.9 Actual Corrosion Loss

Figure 4.24 shows the photo of corroded steel of concrete specimen with 0.65w/c at age about 1000days (2 years and 9 months). Table 4.7 shows the actual corrosion loss of individual specimen. In case of 0.45w/c, the results show that the calculated values

of corrosion loss from AC impedance method both guard-on and guard-ff are underestimation while in double rectangular pulse method, some is over estimation but some is underestimation. In case of 0.65 w/c, the calculated corrosion loss from all methods is overestimation.

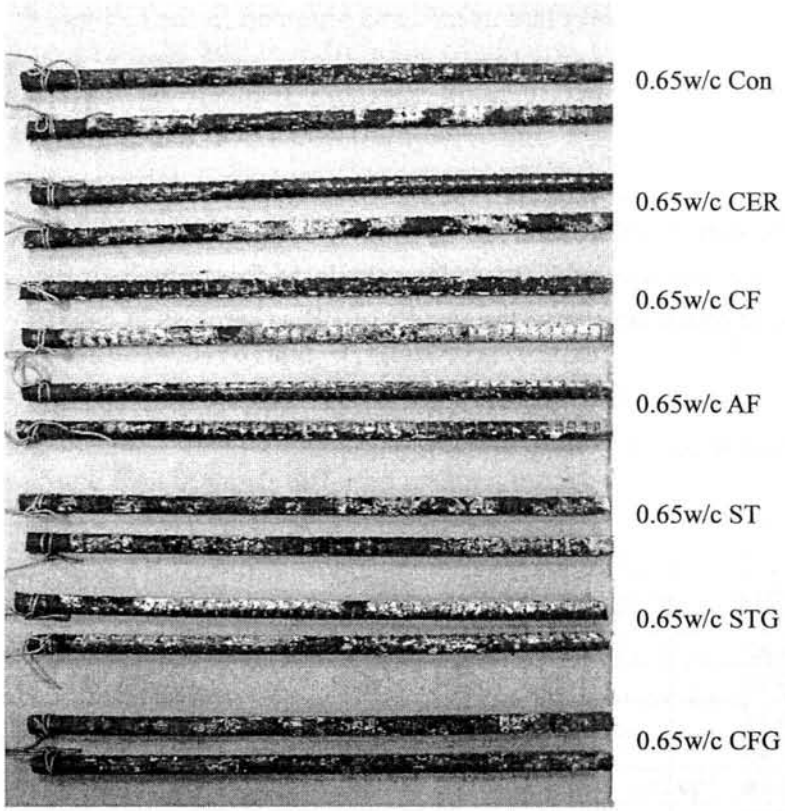

Figure 4.24 Corrosion of steel embedded in concrete specimen with 0.65w/c at age of 1000 days

4.10 Summary

From the experimental results obtained in this Chapter, HCP measurement can be effectively used to investigate the corrosion activity of embedded rebar under the conductive strengthening layer in concrete with uniform chloride content. For PR measurement seems to be not successful and also have the effect to the corrosion current density and corrosion loss. For the results of HCP, the question comes up that these HCP reading represents the local value, or average value over the whole surface, or just takes the effect of distant corrosion area from a measure position. This question leaded us to do the next experiment.

Chapter 5

Half-Cell Potential Measurement on Concrete Specimen with Longitudinal Distribution of Chloride Content in Concrete

From the experimental results in Chapter 4, it brings us the question what is the obtained HCP value really represented. It represents the local HCP value, or the average HCP over the whole specimen, or even it takes the effect from HCP reading of the other point close to/far from the measure position. Then the experiment done in this chapter aims to study the effect of conductive strengthening layer to half-cell potential reading on concrete specimen with longitudinal distribution of chloride content in concrete which may give the different potential between each region.

5.1 Factors

The factors considered in this section were listed below.

Longitudinal distribution of Chloride content: Two concrete mix-proportions, which are Cl^- free and Cl^- mixed concrete, were used in order to make the difference in potential in concrete specimen. The Cl^- mixed concrete will give the lower value of potential than the Cl^- free concrete, as written in literatures, and also have an ability to accelerate corrosion of the steel.

Concrete cover: Two values of cover thickness were used to investigate its effect to the HCP reading.

Conductive strengthening layers: Five types of conductive strengthening layer were made in the experiment by varying type of conductive epoxy resin and number of layer. Therefore, their resistivity can be graded and be compared their effect to HCP reading.

5.2 Materials and Equipments

The properties of materials and the equipments used in this research are as follow:

Cement: Ordinary Portland cement (Sumitomo Osaka Cement), the physical

properties of the cement are shown in Table 4.1.

Mixing water: Tap water, supplied in Kyoto University Yoshida Campus, was used for all mixes.

Fine aggregate: Natural river sand was used. The physical properties are shown in Table 5.1.

Coarse aggregate: Limestone aggregate was used. The physical properties are shown in Table 5.2.

Epoxy resin: Two types of conductive epoxy resin were used; their properties are shown in Table 3.1. These epoxies are mixed by 2 agents, which are main agent and hardening agent, in a ratio of 224/100 and 215/100 for 8%CB CER and 5%CB CER, respectively.

Fiber sheet: Carbon fiber sheet's properties are shown in Table 3.2.

Equipments: SRI Portable Rebar Corrosion Meter (Figure 4.2) was used for measurement.

Table 5.1 Physical properties of fine aggregate

Physical properties	Specific gravity (dry condition)	Water absorption (%)	Sieve retaining (%)							Finess modulus
			5.0 mm	2.5 mm	1.2 mm	0.6 mm	0.3 mm	0.15 mm	<0.15 mm	
	2.6	1.2	0	4.9	31.98	24.95	21.54	10.45	6.18	2.81

Table 5.2 Physical properties of coarse aggregate

Physical properties	Specific gravity (dry condition)	Water absorption (%)	Sieve retaining (%)						Finess modulus
			15.0 mm	10.0 mm	5.0 mm	2.5 mm	1.2 mm	<1.2 mm	
	2.69	0.7	0	43.63	51.69	4.04	0.65	0	6.38

5.3 Specimens

5.3.1 Dimensions

The specimens with the dimension of 1200x50x50mm and 1200x50x75mm specimens were cast by placing of 1100mm-long D10 reinforcing steel at the center. All the details of the testing specimen are demonstrated in Figure 5.1. Three standard cylindrical specimens with (10cm-diameter with 20cm-height specimen) were cast for 28-day compressive strength test. Three patterns of concrete specimen the longitudinal distribution of chloride content were cast as shown in Figure 5.2.

5.3.2 Conditions of specimen

Table 5.3 concludes the conditions and number of specimen used in this experiment. As written in the section 5.1, the considered factors were longitudinal distributions of chloride content in concrete, concrete cover and conductive strengthening layer. Therefore, three patterns of longitudinal distribution of Cl^- content and seven conditions of surface were considered to measure HCP.

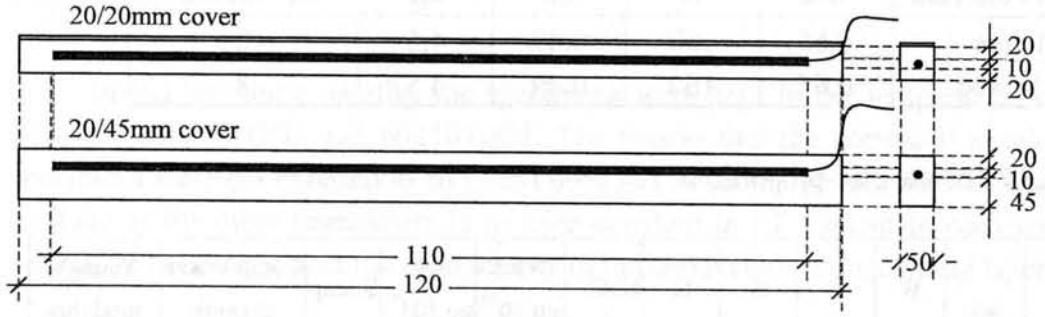

Figure 5.1 Details of specimen with longitudinal distribution of Cl^- content in concrete

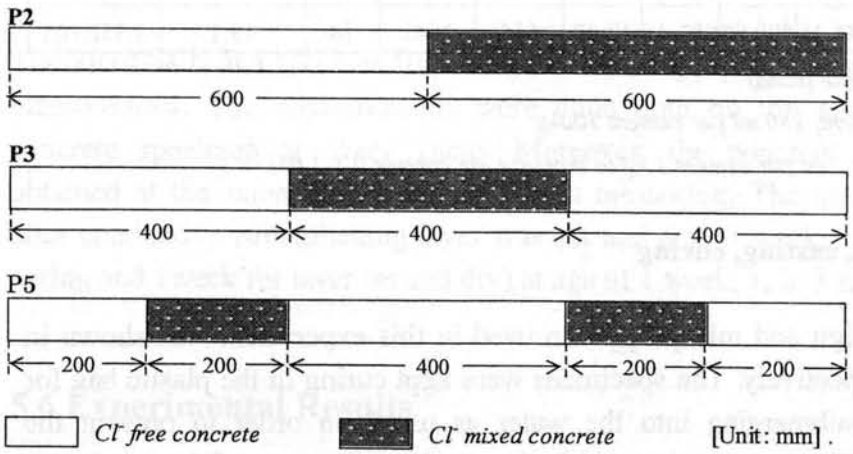

Figure 5.2 Patterns of concrete specimen with longitudinal distribution of Cl^- content in concrete

Table 5.3 Type of layer, abbreviation and number of testing specimens

	Specimen details	Code	Number of specimens in each series and pattern		
			P2	P3	P5
1	20/20mm concrete cover	Con20/20	2	2	2
2	20/45mm concrete cover	Con20/45	2	2	-
3	20/20mm concrete cover with 5%CB CER	5%CB	2	2	-
4	20/20mm concrete cover with 8%CB CER	8%CB	2	2	-
5	20/20mm concrete cover with 5%CB CER and 1ply of CF sheet	5%CB1CF	2	2	2
6	20/20mm concrete cover with 8%CB CER and 1ply of CF sheet	8%CB1CF	2	2	2
7	20/20mm concrete cover with 5%CB CER and 2plies of CF sheet	5%CB2CF	2	2	-

Table 5.4 Concrete mix design

Type of concrete	**w/c**	**W**	**s/a**	**air**	**Cl- content**
Cl^- free	0.65	160	0.49	4.5	0
Cl^- Mixed	0.65	160	0.49	4.5	8

Table 5.5 Concrete mix-proportions

Mix	w/c	W	C	S	G	NaCl[*1]	WRA no.70[*2]	AE no.303[*3]	Slump	Compressive strength	Young's modulus
		kg/m^3					ml/m^3		cm	N/mm^2	N/mm^2
Cl^- free	0.65	160	246.15	913.27	983.45	0	615	1642	12	21.2	3.20E+05
Cl^- mixed	0.65	160	246.15	899.60	983.45	13.67	615	1642	18	19.1	3.35E+05

[*1] *Substitute in fine aggregate (sand)*

[*2] *WRE, water reducing agent, 250 ml per cement 100kg*

[*3] *AE, air entraining agent, 2ml per cement 1 kg to increase air content 0.5-1.0%*

5.3.3 Mix proportion, casting, curing

The concrete mix-design and mix-proportion used in this experiment was shown in Table 5.4 and 5.5, respectively. The specimens were kept curing in the plastic bag for 28 days, instead of submerging into the water as usual, in order to prevent the diffusion of different Cl^- concentration within the specimen because of the specimens were cast with longitudinal distribution of Cl^- free- and Cl^- mixed-concrete.

5.3.4 Application of Conductive Strengthening Layers

The conductive strengthening layer was applied on concrete specimen's surface on day 29, and left it for a week for set and dry. The applications of conductive strengthening layers in this section are as same as done in chapter 3. Figure 3.6 demonstrates the application procedure of the conductive strengthening layers.

5.4 Exposure Conditions

A week after applied the conductive strengthen layer on concrete surface, the specimens were kept at the basement of the Civil Engineering building, Kyoto University for the first three months (June to September 2006), and were place in the 30'C temperature control chamber for the next 3 months (September to December 2006).

In the first three-month, the water was sprayed from left and right surfaces of the specimen once a day in order to accelerate the corrosion of embedded steel. The ambient temperature and relative humidity were about 26 °C to 31°C and 60% to 90%, respectively.

In the last three months, the specimens were kept in the temperature control chamber with 30±2°C and 60±10%RH. The reason that the corrosion acceleration specimens were not exposed to 50°C and 60% RH or submerge into the NaCl solution as done as the other researchers is to keep constant in Cl^- content in each concrete region, and also to protect the conductivity of the conductive strengthening layers.

5.5 Measurements

The SRI CM II and SRI CM III machines were employed to measure the HCP in this measurement. The measurements were done both on top and bottom surface of concrete specimen at every 10cm. Moreover, the concrete resistance was also obtained at the same time when HCP was measuring. The measurement was done after conductive strengthening layer was set and dry (5 weeks, 28days for specimen curing and 1week for layer set and dry) at age of 1 week, 1, 2, 3 and 6 months.

5.6 Experimental Results

The experimental results of HCP reading on concrete specimen with longitudinal distribution of chloride content in concrete at 3months and 6 months are demonstrated in Figure 5.3 to 5.5 and Figure 5.6 to 5.8, respectively.

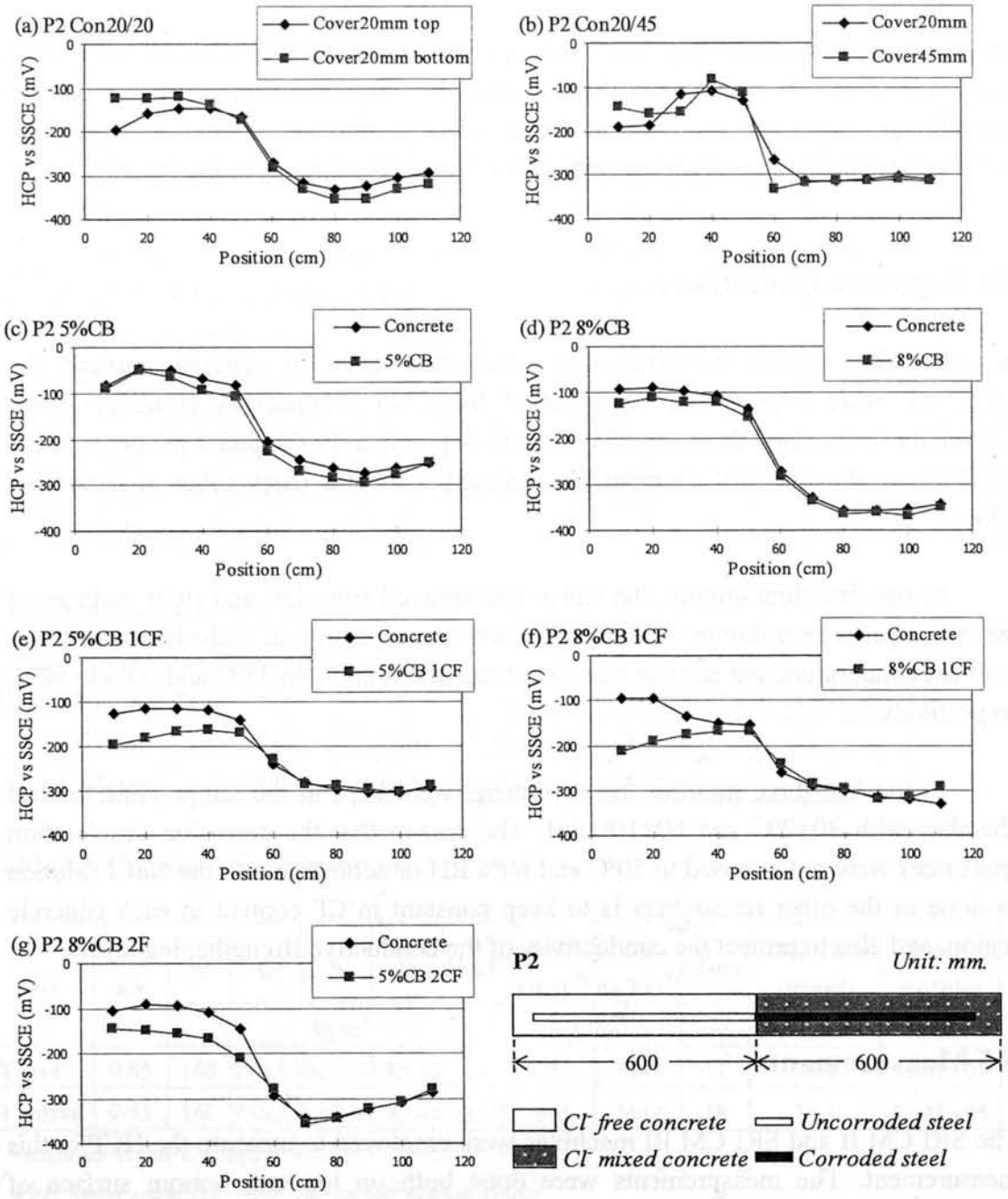

Figure 5.3 Half-cell potential reading of specimen P2 at 3months

The criteria of HCP evolution for silver chloride saturated electrode, (Ag/AgCl)KCl sat., is –80 and –230mV. The HCP readings on concrete surface in Cl^- free region are nobler than –150mV that indicates the uncertain of corrosion. The readings in Cl^- mixed region are poorer than –230mV that indicates 90% probability of corrosion, except in P5 5%CB1CF at 6 months that is acceptable due to the fluctuation of HCP reading. Then, the longitudinal distribution of chloride content in concrete successfully induced the different potential between Cl^- free and Cl^- mixed regions.

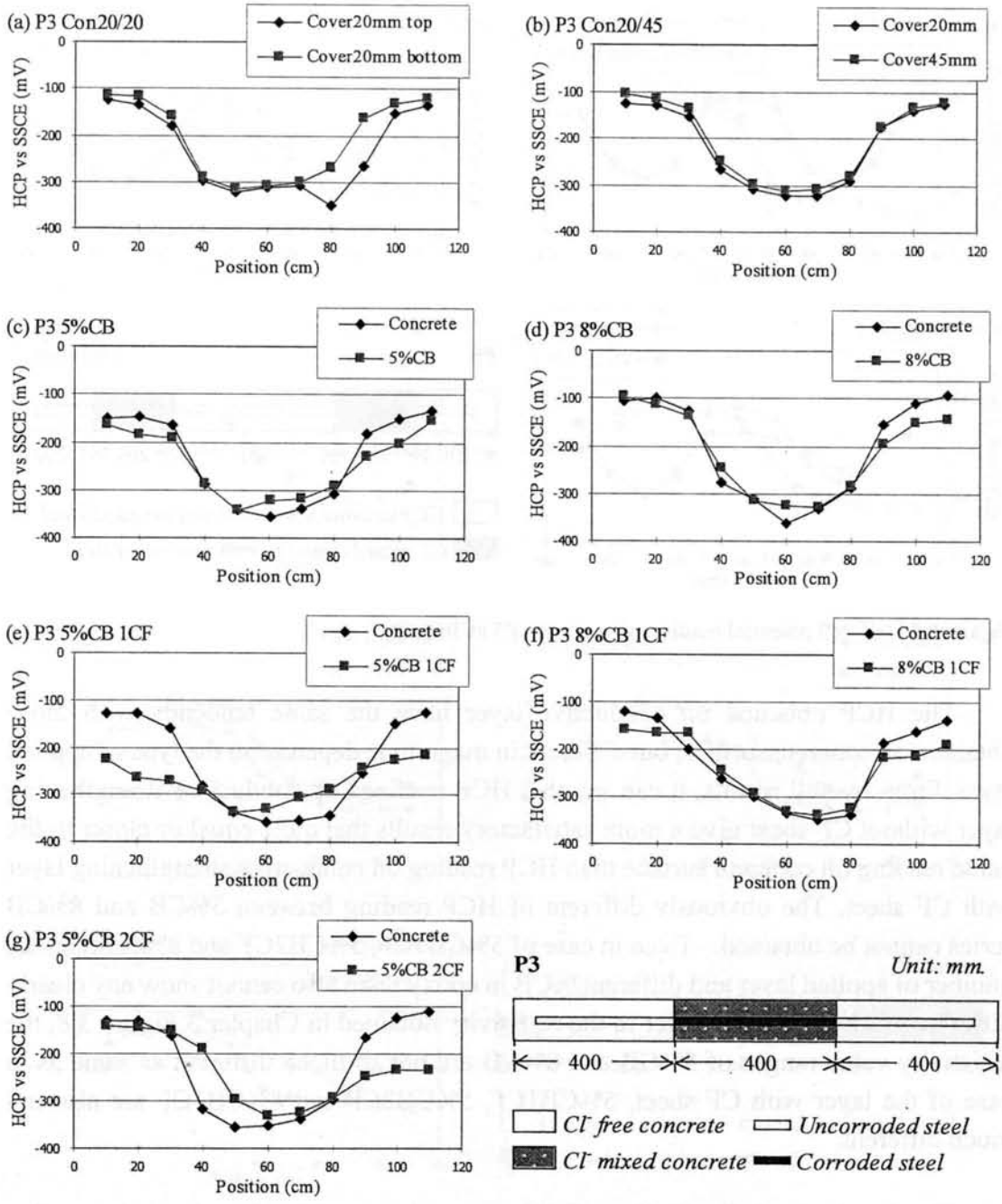

Figure 5.4 Half-cell potential reading of specimen P3 at 3months

In specimen series Con20/20 in P2, P3 and P5 (figure (a)), HCP readings on top and bottom surface have the same tendency and magnitude, even some scatter occurs when measure at 3 months. Then again, the readings from concrete surface in case of layer bonded specimen are used to directly compare to the reading on conductive strengthening layer. The reading on concrete surface with different cover thickness both Con20/20 and Con20/45 both in case of P2 and P3 (figure (a) and (b)), the same tendency is obtained only a little different in magnitude is found that may occur in HCP reading.

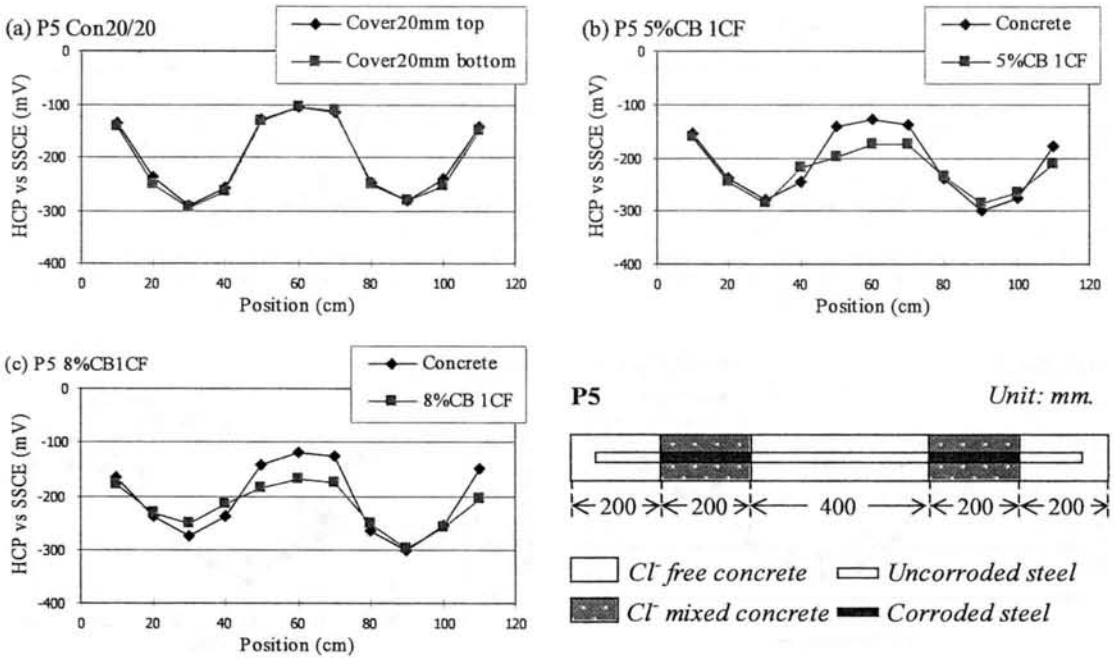

Figure 5.5 Half-cell potential reading of specimen P5 at 3months

The HCP obtained on conductive layer have the same tendency with those obtained on concrete surface, but different in magnitude depends on the type of applied layer. From overall results, it can say that HCP readings on conductive strengthening layer without CF sheet give a more satisfactory results that quite equal or closer to the value reading on concrete surface than HCP reading on conductive strengthening layer with CF sheet. The obviously different of HCP reading between 5%CB and 8%CB series cannot be obtained. Even in case of 5%CB1CF, 5%CB2CF and 8%CB1CF, the number of applied layer and different %CB in epoxy resin also cannot show any clearly difference between them. Refer to the resistivity obtained in Chapter 3 Figure 3.8, the resistivity value ranges of 5%CB and 8%CB are not so much different as same as in case of the layer with CF sheet, 5%CB1CF, 5%CB2CF and 8%CB1CF are also not much different.

The longitudinal distribution of Cl^- content in concrete also shows interesting effect to the HCP measurement. By comparison HCP reading in three patterns of Cl^- content distribution in concrete, specimen pattern P2 and P3 have a range of HCP (maximum to minimum) wider than those obtained in specimen pattern P5. The ranges are about 250 mV in case of P2 and P3, and not more than 200mV in case of P5. Therefore the distance from the boundary between 2 concrete mixes with different Cl^- have the effect for HCP reading.

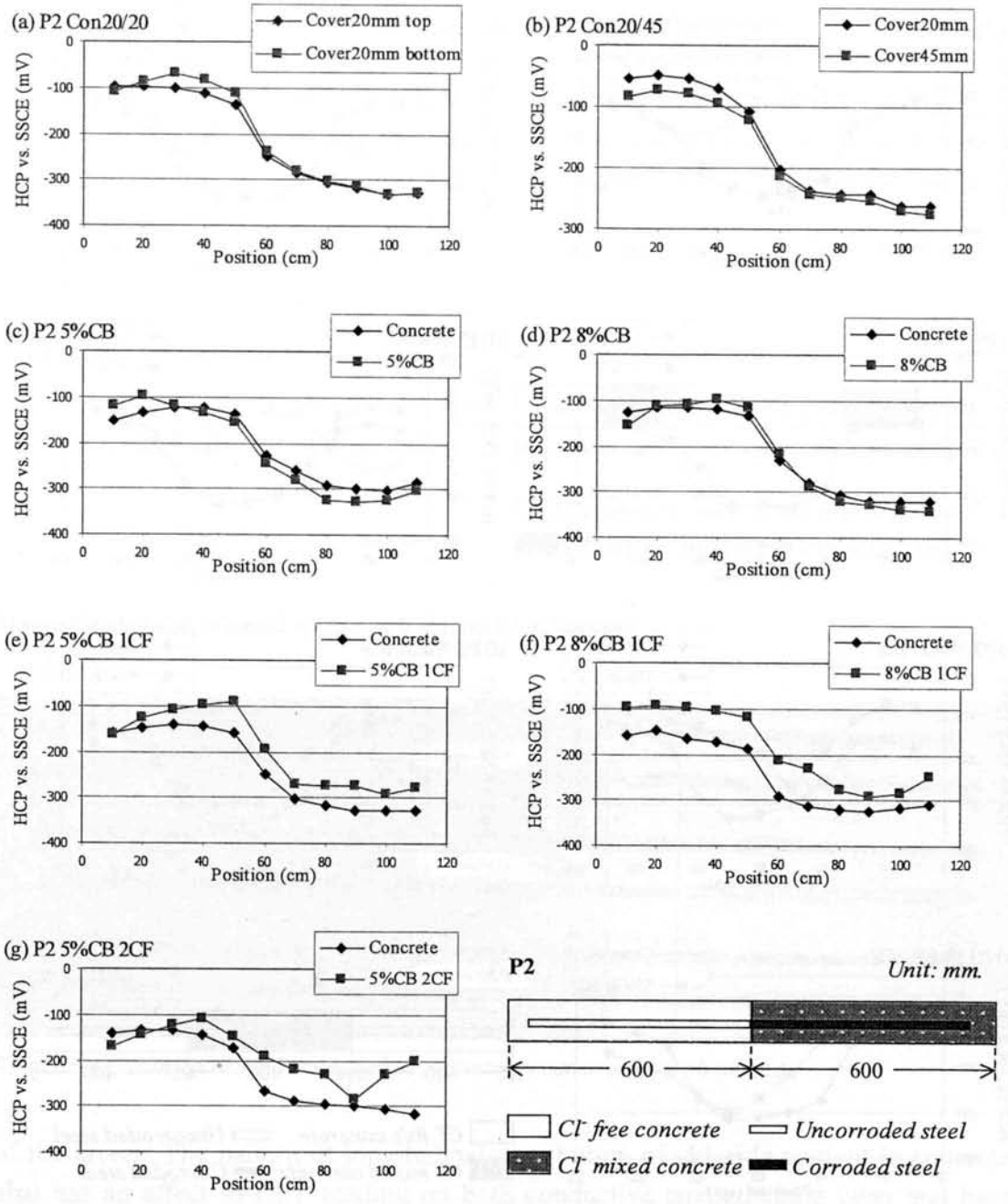

Figure 5.6 Half-cell potential reading of specimen P2 at 6months

Figure 5.9 shows the corroded steel after breaking the concrete specimen at age of 6 months. From the figure, it can see that the corrosion occurs on the steel that locates in the chloride mixed concrete for all patterns (P2, P3 and P5). Therefore, it shows that the variation of potential obtained in Figure 5.3 to Figure 5.8 can accurately indicate the corrosion activity of the embedded steel inside concrete.

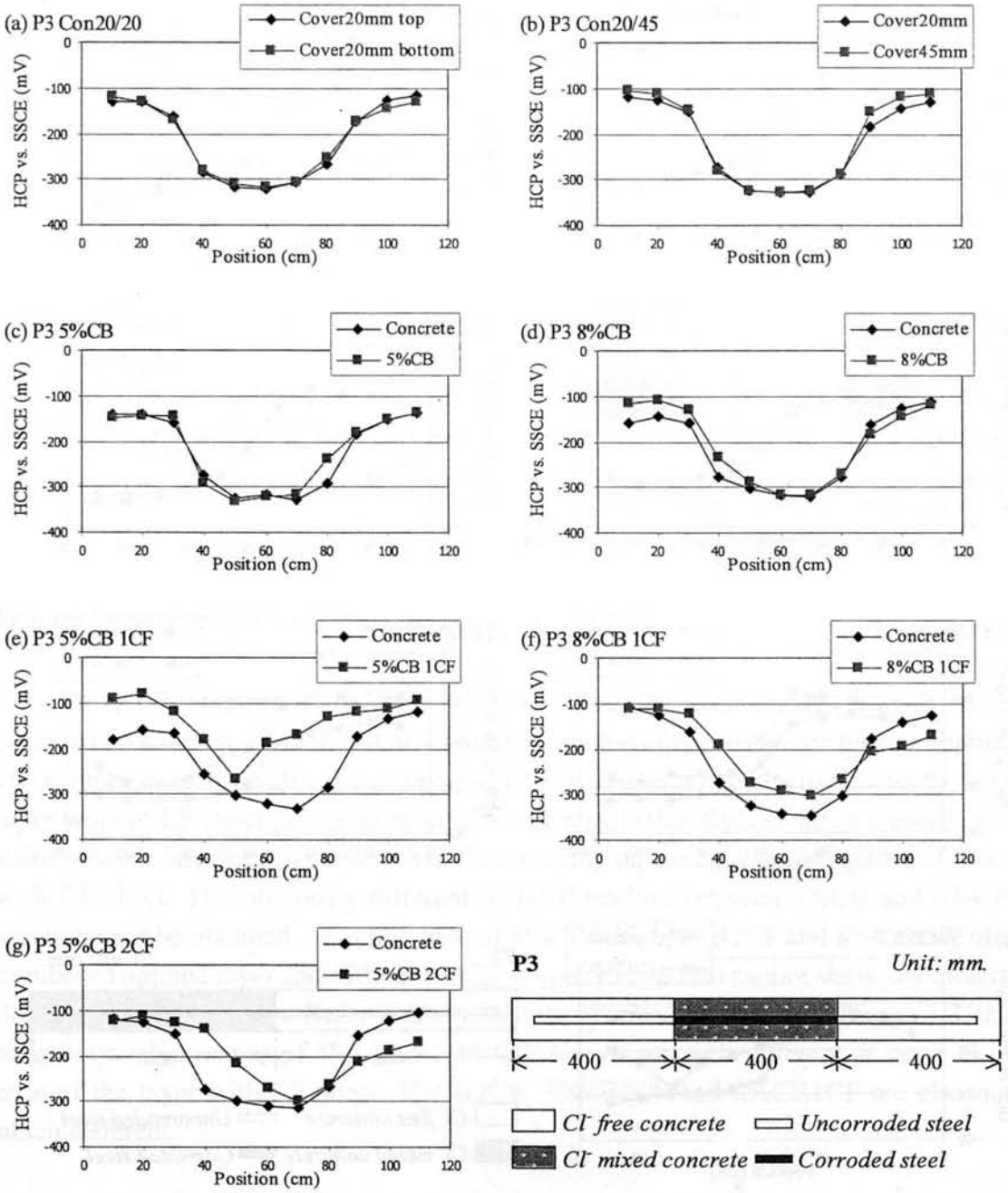

Figure 5.7 Half-cell potential reading of specimen P3 at 6months

5.7 Summary

It can be concluded from the experimental results obtained in this chapter that HCP reading in concrete specimen with longitudinal distribution of chloride content in concrete on conductive strengthening layer is successfully giving the same tendency with HCP reading on concrete surface. Moreover, the value reading on layer without CF sheet gives more satisfactory to the value reading on the concrete surface than the value reading on the layer with CF sheet. It may be explained by the effect of resistivity

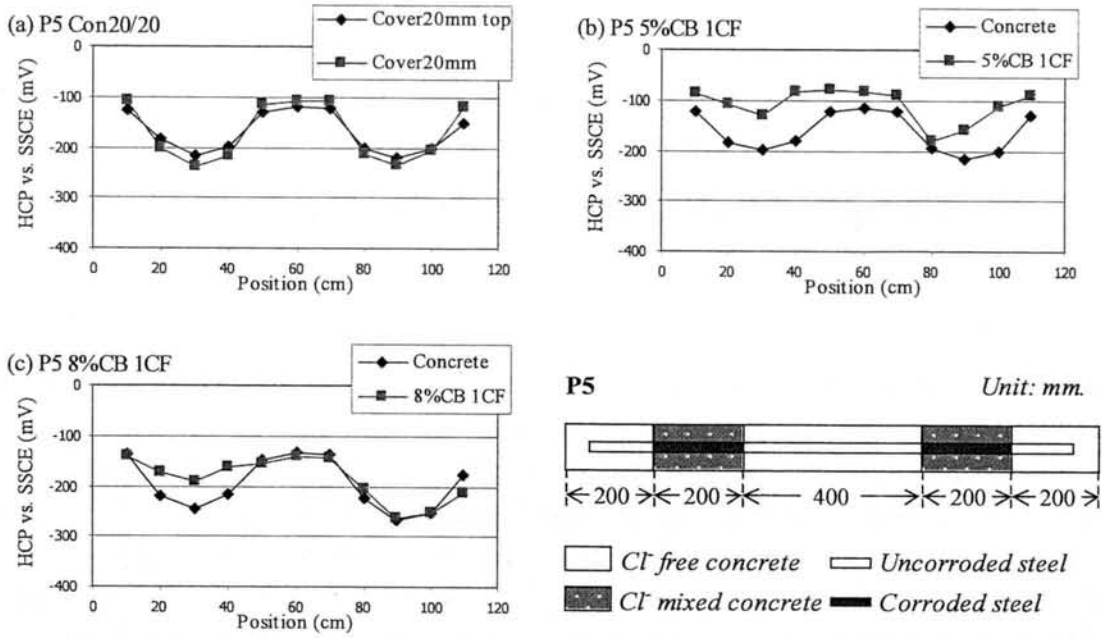

Figure 5.8 Half-cell potential reading of specimen P5 at 6months

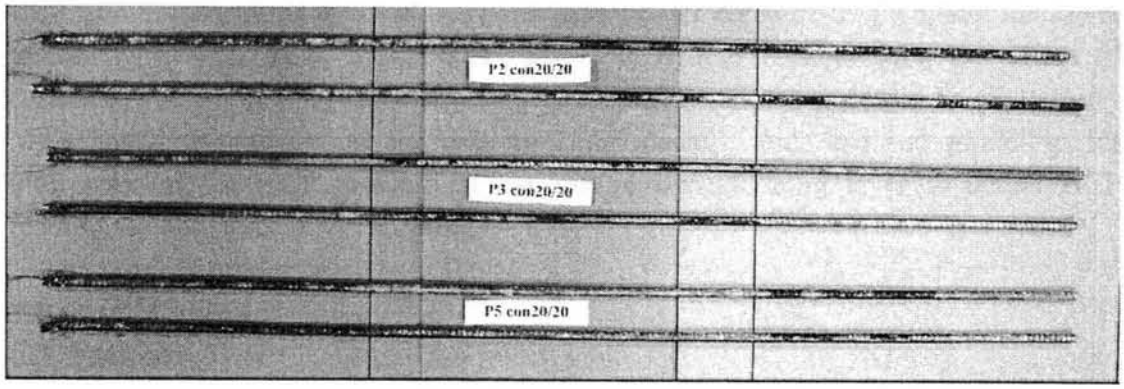

Figure 5.9 Corrosion of steel embedded in concrete specimen at age of 6 months

of the layers. The pattern of longitudinal distribution of chloride content in concrete also has an effect to HCP reading on both conductive strengthening layer and bare concrete surface.

Chapter 6

Analysis of Half-Cell Potential Distribution

In the previous chapters, the results show that HCP reading on conductive strengthening layer give a good consistency with HCP reading on surface of concrete. In Chapter 4, the specimens with uniform chloride content in concrete, HCP readings both on the conductive strengthening layer (in all conditions; no-hole, hole and artificial gap) and concrete surface are quite satisfactory both in magnitude and tendency even in long-term period of 2 years and 9 months (about 1000days). In Chapter 5, the specimens with longitudinal distribution of chloride content, HCP readings on the conductive strengthening layer give the consistent tendency to HCP reading on concrete surface, but different in magnitude. The higher resistivity (5%CB CER and 8%CB CER) gives closer reading to one of concrete surface than the lower resistivity (5%CB 1CF, 5%CF 2CF, and 8%CB 1CF). Therefore, the effect of conductive strengthening layer's resistivity to HCP distribution should be analytically investigated to understand its behavior, relationship, and also the guideline for interpretation the HCP reading on conductive strengthening layer to actual HCP reading (as one on concrete surface).

6.1 Factors

The factors that were considered in this analysis were listed below.

The resistivity of conductive strengthening layer – the resistivity of conductive strengthening layer is the main parameter of this study. The effect of this parameter was investigated by using the value obtained in Chapter 3 that divided the resistivity into 2 classes. High resistivity groups are 8%CB, 8%CB1AF and 5%CB. Low resistivity group are 8%CB1CF, 5%CB1CF and 5%CB2CF. Moreover, the different of resistivity in longitudinal and vertical direction as obtained from the experimental results in Chapter 3 are also taken into account.

The resistivity of concrete cover – the resistivity of concrete is one parameter that sensitive to the surrounding environment. In the experiment, the resistivity of concrete cover in different two concrete mix-proportions was different, and even on the opposite side of specimen (top and bottom surface) it was also different. Therefore, four values of concrete resistivity, which Cl^- free concrete both top and bottom, Cl^-

mixed concrete both top and bottom, were used in the analysis. And in the real situation, the concrete resistivity under the strengthening layer may not be known. Then, the variation of this parameter affects the potential distribution in concrete specimen was also investigated.

6.2 Finite Element Analysis

The commercial program for first order triangle element in 2D FEA for steady DC conduction analysis, which bases on Laplace's equation as shown in equation (6.1), was employed in the analysis.

$$\frac{\partial}{\partial x}\left(\frac{1}{\rho_x}\frac{\partial U}{\partial x}\right)+\frac{\partial}{\partial y}\left(\frac{1}{\rho_y}\frac{\partial U}{\partial y}\right)=0 \qquad (6.1)$$

where U *Potential (V)*
ρ_x *Electric resistivity in x-direction (Ω.m)*
ρ_y *Electric resistivity in y-direction (Ω.m)*

Corresponding to the half-cell potential measurement, the boundary conditions used in the analysis are prescribed in Figure 6.1. Due to the different of reinforcement's potential (corrosion activity) in each concrete region leads to the potential distribution on both the conductive strengthening layer and concrete surface, therefore, the boundary conditions of potentials are defined on the surface of reinforcement in Cl^- free and Cl^- mixed regions, $S_{pr,\ Cl\text{- free}}$ and $S_{pr,\ Cl^- \text{mixed}}$, respectively (Figure 6.1). Another S_0 is electrically free where electrical current outward flow is equal to zero. The boundary conditions are given,

$$U_1 = E_1 \quad ; \text{on } S_{pr,\ Cl\text{- free}} \qquad (6.2a)$$
$$U_2 = E_2 \quad ; \text{on } S_{pr,\ Cl^- \text{mixed}} \qquad (6.2b)$$
$$\frac{\partial}{\partial n}(u/\rho) = 0 \quad ; \text{on } S_0 \qquad (6.2c)$$

Here, E_1 is the potential on the reinforcement in Cl^- free region, E_2 is the potential on the reinforcement in Cl^- mixed region, and n is the outward normal vector on the surface.

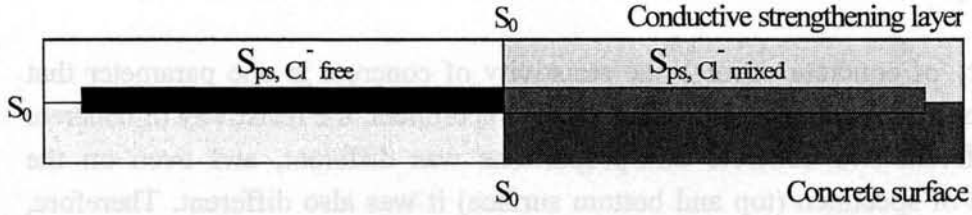

Figure 6.1 Boundary condition of concrete specimen (example specimen type P2)

6.3 Simple Analysis

The individual effect of each parameter is investigated in this section. Therefore, some parameters out of the interesting one need to be simplified and controlled. Some assumptions are given as list below;

1. Uniform material properties and uniform boundary conditions in each section (each concrete mix region) are assumed.
2. The resistivity of top concrete cover (both in Cl^- free and Cl^- mixed region) is equal to 1.225 times of the resistivity of bottom concrete cover. The value of 1.225 comes from the data analysis from non-attached concrete specimen.
3. The potential on the top and bottom surface of the reinforcement is equal to the potential on bottom surface in each concrete region.

6.3.1 Analytical Model

The 2-D analytical models used in the analysis are demonstrated in Figure 6.2. Three patterns of analytical models that have the dimension of 1200x50mm by placing D10 rebar at the center and 1200x0.5mm of layer on the top are employed. From the figure, the model is vertically divided into 2, 3 and 5 section for specimen P2, P3 and P5, respectively.

From assumption 2, four values of resistivity used in the analysis were 300, 370, 180and 220 Ω.m for bottom and top Cl^- free concrete, and bottom and top of Cl^- mixed concrete, respectively. And from the assumption 3, two values of potential on steel surface were assumed to be –100 and –300 mV for Cl-free and Cl- mixed concrete regions, respectively.

The application program automatically performed mesh generation, as show in the Figure 6.3. The spacing between the meshes was automatically specified at the defined vertices by smaller spacing at the conductive strengthening layer and gradually increased bigger and bigger downward to the steel and bottom concrete surface. For example, the spacing of mesh generation from top (layer) to bottom (concrete surface) specified at each vertex in each section (Figure 6.3(b) and (c)) are written below:

Section (1)-(1), 4 vertices: 0.025, 0.025, 0.4025 and 0.7225mm from top to bottom
Section (2)-(2), 3vertices: 0.25, 0.25, and 0.25mm from top to bottom
Section (3)-(3), 4 vertices: 0.025, 0.3263, 0.4290 and 0.668 mm from top to bottom

The term "resistivity ratio (r)" was introduced in the analysis to indicate the different between the resistivity of material x and material y, as written in equation (6.3).

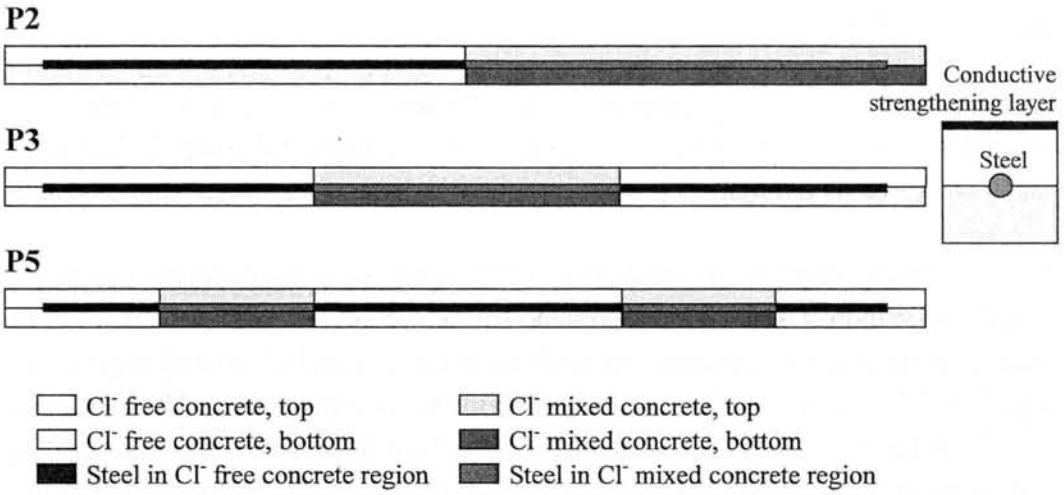

Figure 6.2 Analytical models for simple analysis

(a) Example: left tip of specimen P5

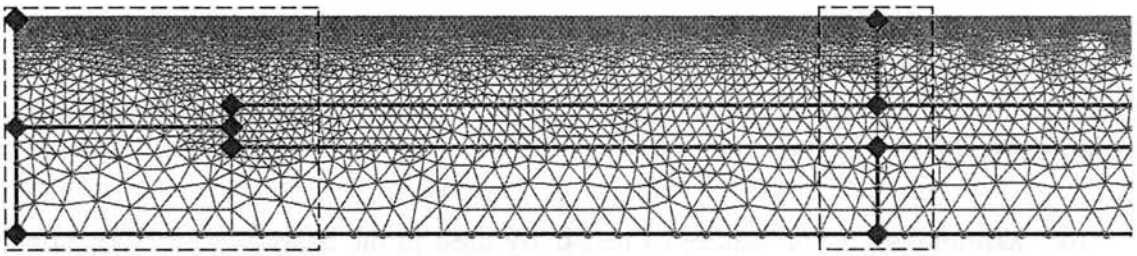

(b) Enlarge picture, left rectangular in (a)

(c) Enlarge picture, right rectangular in (a)

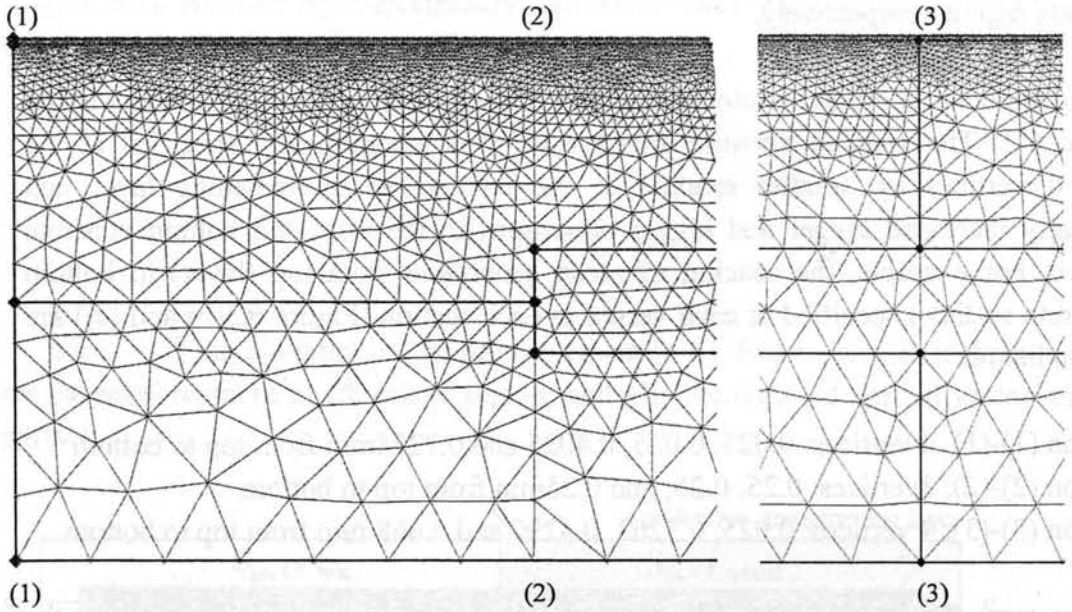

Figure 6.3 Mesh generation

$$r = \frac{\rho_x}{\rho_y} \tag{6.3}$$

where r *The resistivity ratio*
ρ_x *The resistivity of material x*
ρ_y *The resistivity of material y*

6.3.2 Analytical Methods

From those two factors were written in the section 6.1, three parameters could be considered in the simple investigation the potential distribution in the concrete specimen with conductive strengthening layer.

6.3.2.1 Variation of Resistivity of Conductive strengthening Layer (Isotropic)

The resistivity of conductive strengthening layer was varied to investigate its effect to potential distribution in the concrete specimen. Two conditions, which were constant concrete resistivity and isotropic properties of the layer's resistivity (the layer's resistivity is equal in all axes), were kept control in the analysis. Then, the layer-concrete resistivity ratio ($r_{l/c}$), was introduced to indicate the relative different of the layer's resistivity to the concrete resistivity as written in equation (6.4).

$$r_{l/c} = \frac{\rho_{layer}}{\rho_{ConCl^- free,top}} \tag{6.4}$$

where $r_{l/c}$ *The layer-concrete resistivity ratio*
ρ_{layer} *The resistivity of conductive strengthening layer*
$\rho_{ConCl\text{-}free,\ top}$ *The resistivity of concrete cover at top surface (under conductive strengthening layer) of Cl^- free concrete*

The resistivity of top concrete cover with Cl^- free was selected to use in the equation (6.4) because it is the most common one that locates under the layer and free with chloride as in the real situation. Therefore, the layer-concrete resistivity ratio is one parameter that was varied in this analysis in order to investigate the effect of the layer's resistivity to the potential distribution. The boundary condition and material properties are shown in Table 6.1.

Table 6.1 Boundary conditions and material properties for variation of the resistivity of conductive strengthening layer (isotropic)

Location	Potential on surface of steel (mV)
E_1 on $S_{pr,\ Cl\text{-}\ free}$	-100
E_2 on $S_{pr,\ Cl\text{-}\ mixed}$	-300
Location	**Resistivity of Concrete, ρ_{Con} (Ω.m)**
$\rho_{Con,\ Cl^-\ free,\ bottom}$	300
$\rho_{Con,Cl^-\ mixed,\ bottom}$	180
$\rho_{Con,Cl^-\ free,\ top}$*	370
$\rho_{Con,Cl^-\ mixed,\ top}$*	220
Resistivity ratio ($r_{l/c}$)	**Resistivity of Conductive Strengthening Layer, ρ_{layer}** (Ω.m)**
$r_{l/c} = 10^{-6}$	0.00037
$r_{l/c} = 10^{-3}$	0.37
$r_{l/c} = 10^{-2}$	3.7
$r_{l/c} = 10^{-1}$	37
$r_{l/c} = 1$	370
$r_{l/c} = 10$	3700

* $\rho_{i,\ top} = 1.225\,\rho_{i,\ bottom}$

** $\rho_{layer} = r \times \rho_{Cl^-\ free,\ top}$

6.3.2.2 Variation of Resistivity of Conductive Strengthening Layer (Anisotropic)

From the experimental results in section 3.1, the obtained resistivity of the conductive strengthening layer in longitudinal direction ($\rho_{layer,x}$) and vertical direction ($\rho_{layer,y}$) were not equal and the later were much bigger than the former. Therefore, in this section the vertical resistivity was varied while the longitudinal resistivity and concrete resistivity were fixed in the analysis, and see the effect of the variation of the vertical resistivity of the layer to potential distribution. The resistivity ratio between the conductive strengthening layer's resistivity in vertical and longitudinal direction (r_l, hereafter the layer resistivity ratio) is introduced, as written in equation (6.5) The layer resistivity ratio of layer, r_l, was varied from 1, 10, 10^2, 10^3.

$$r_l = \frac{\rho_{layer,y}}{\rho_{layer,x}} \tag{6.5}$$

The value of the resistivity of conductive strengthening layer in longitudinal direction was selected. Then, the resistivity of conductive strengthening layer in vertical direction was calculated, and used in the analysis. The values used in the analysis are written in Table 6.2

Table 6.2 Boundary conditions and material properties for variation of resistivity of conductive strengthening layer (anisotropic)

Location	**Potential on surface of steel (mV)**	
E_1 on $S_{pr,\ Cl\text{-}\ free}$	-100	
E_2 on $S_{pr,\ Cl\text{-}\ mixed}$	-300	
Location	**Resistivity of Concrete, ρ_{Con} (Ω.m)**	
$\rho_{Cl^-\ free,\ bottom}$	300	
$\rho_{Cl^-\ mixed,\ bottom}$	180	
$\rho_{Cl^-\ free,\ top}$ *	370	
$\rho_{Cl^-\ mixed,\ top}$ *	220	
Resistivity ratio (r_l)	**Resistivity of Conductive Strengthening Layer, ρ_{layer} (Ω.m)**	
	$\rho_{layer,x}$	$\rho_{layer,y}$ **
$r_l = 1$	0.37	0.37
$r_l = 10$	0.37	3.7
$r_l = 100$	0.37	37
$r_l = 1000$	0.37	370

* $\rho_{i,\ top} = 1.225\ \rho_{i,\ bottom}$

** $\rho_{layer,y} = r_l \times \rho_{layer,x}$; $\rho_{layer,x}$ *was fixed to the value of 0.37 Ω.m.*

6.3.2.3 Variation of Concrete Resistivity under Conductive strengthening Layer

The resistivity of concrete cover under the conductive strengthening layer seems to be a factor that should be considered in the analysis. In the real situation, the concrete resistivity is unable to obtain when the surface of the structure is bonded with strengthening layer. Hence, the effect of the variation of the resistivity of concrete cover to the potential distribution was analyzed in this section. The resistivity ratio of the top concrete cover, r_c, is introduced, as written in equation (6.6). The resistivity ratio of layer, r_c, was varied from 2, 5, 10, 20, 100.

$$r_c = \frac{\rho_{Con,new}}{\rho_{Con,control}} \tag{6.6}$$

where $\rho_{Con,\ new}$ *New value of concrete resistivity using in analysis*

$\rho_{Con,\ control}$ *Control value of concrete resistivity*

Table 6.3 Boundary conditions and material properties for variation of concrete resistivity under conductive strengthening layer

Location	**Potential on surface of steel (mV)**	
E_1 on $S_{pr,\ Cl\text{-}\ free}$	-100	
E_2 on $S_{pr,\ Cl\text{-}\ mixed}$	-300	
Location	**Resistivity of Concrete, ρ_{Con} (Ω.m)**	
$\rho_{Con,Cl^- free,\ bottom}$	300	
$\rho_{Con,Cl^- mixed,\ bottom}$	180	
$\rho_{Con,Cl^- free,\ top}$ *	370	
$\rho_{Con,Cl^- mixed,\ top}$ *	220	
Resistivity ratio ($r_{y/x}$)	**Resistivity of Conductive Strengthening Layer, ρ_{layer} (Ω.m)**	
	$\rho_{layer,x}$ **	$\rho_{layer,y}$
$r_{y/x} = 1$	0.37	0.37
Resistivity ratio (r_c)	**Resistivity of Concrete, ρ_{Con} (Ω.m)**	
	$\rho_{Con,Cl^- free,\ top}$	$\rho_{Con,Cl^- mixed,\ top}$
$r_c = 1$	370	220
$r_c = 2$	740	440
$r_c = 5$	1850	1100
$r_c = 10$	3700	2200
$r_c = 20$	7400	4400
$r_c = 100$	37000	2200

* $\rho_{i,\ top} = 1.225\ \rho_{i,\ bottom}$

** $\rho_{layer,y} = r_t \times \rho_{layer,x}$; $\rho_{layer,x}$ *was fixed to the value of 0.37 Ω.m.*

6.3.3 Results and Discussions

6.3.3.1 Variation of Resistivity of Conductive strengthening Layer (Isotropic)

Figure 6.4 shows the analytical results of specimen P2, P3 and P5 (arrange from top to bottom, respectively) by varying the layer-concrete resistivity ratio, $r_{l/c}$. The results showed that the variation of the resistivity of the conductive strengthening layer have much affect to the potential distribution on the strengthening layer, in all specimen type P2, P3 and P5. The smaller resistivity ratio, $r_{l/c}$, gives flatter range of potential compares to bigger one. The potential line is almost horizontal when the value $r_{l/c}$ equals to 10^{-6}. When the value of $r_{l/c}$ increases, the slope of the potential line is also increases, and goes closer to the potential line of concrete surface. Then, the value of

$r_{l/c}$ equals to 10^{-1}, the potential line of the conductive strengthening layer is quite equal to the potential line of concrete surface.

The interesting effect also shows up at the end of the specimen that the potential line on concrete surface at the tip of the specimen comes lower when the value of $r_{l/c}$ decreases. It may be explained by the analytical result that the resistivity of the layer affects the potential line on concrete cover at the opposite side. The lower resistivity of layer, the bigger influence to the potential line on the concrete cover. Moreover, the pattern of the specimen (P2, P3 and P5) also gives an interesting result. Let consider the potential line of $r_{l/c} = 10^{-4}$ or 10^{-5}, the range of analytical potential value (maximum-minimum) of specimen P5 is smallest and of specimen P2 is biggest for the same $r_{l/c}$.

6.3.3.2 Variation of Resistivity of Conductive strengthening Layer (Anisotropic)

The analytical results of specimen P2, P3 and P5 (from top to bottom, respectively) by varying the layer resistivity ratio, $r_{y/x}$, are demonstrated in Figure 6.5. The figure shows that the variation in vertical direction of layer's resistivity (or may say variation of the layer resistivity ratio) does not give even a little effect to the potential distribution on conductive strengthening layer. It made the author doubted why any little effect does not show up in this case.

6.3.3.3 Variation of Concrete Resistivity under Conductive strengthening Layer

Figure 6.6 shows the analytical results of specimen P2, P3 and P5 (arrange from top to bottom, respectively) by varying the concrete resistivity ratio, r_c. The results show that the bigger r_c gives the flatter potential line on conductive strengthening layer than the smaller r_c. That opposes to the result in the section 6.5.1, but consistent. Because the bigger r_c means the smaller $r_{l/c}$ that leads to the flatter potential line on conductive strengthening layer.

At the tip of the specimen, the interesting result also comes out that the potential distribution effect from the conductive strengthening layer reduces when the value of r_c increases. It can be seen in the figure that the potential value on concrete surface increases when the value of r_c increases.

From these three cases of analysis in the individual parameter, it can be concluded that the resistivity of the layer and concrete play an important role to effect the potential distribution on the conductive strengthening while the resistivity of the layer in vertical direction does not.

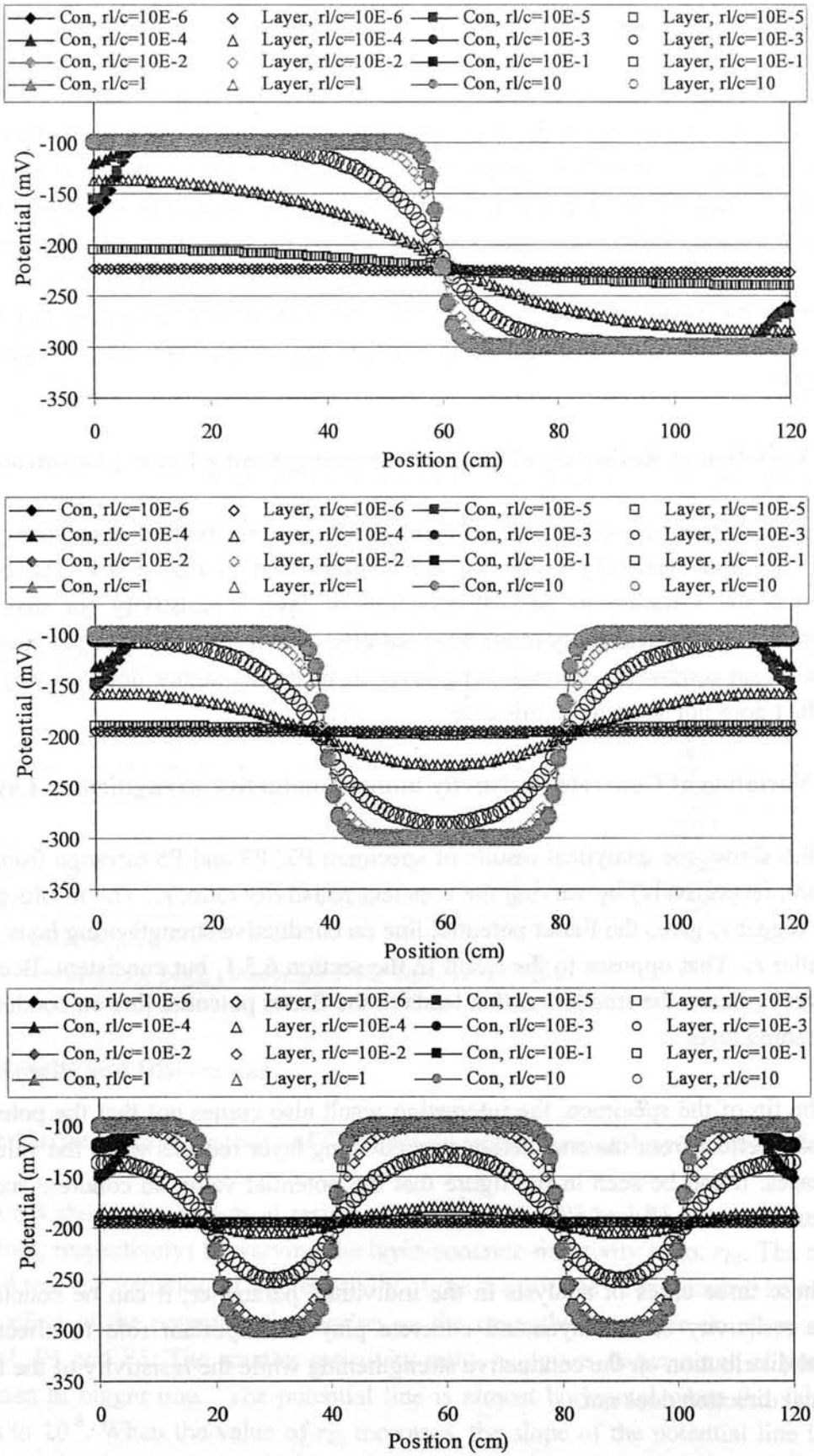

Figure 6.4 Analytical results of variation of the resistivity of conductive strengthening layer (isotropic), specimen P2, P3 and P5, respectively

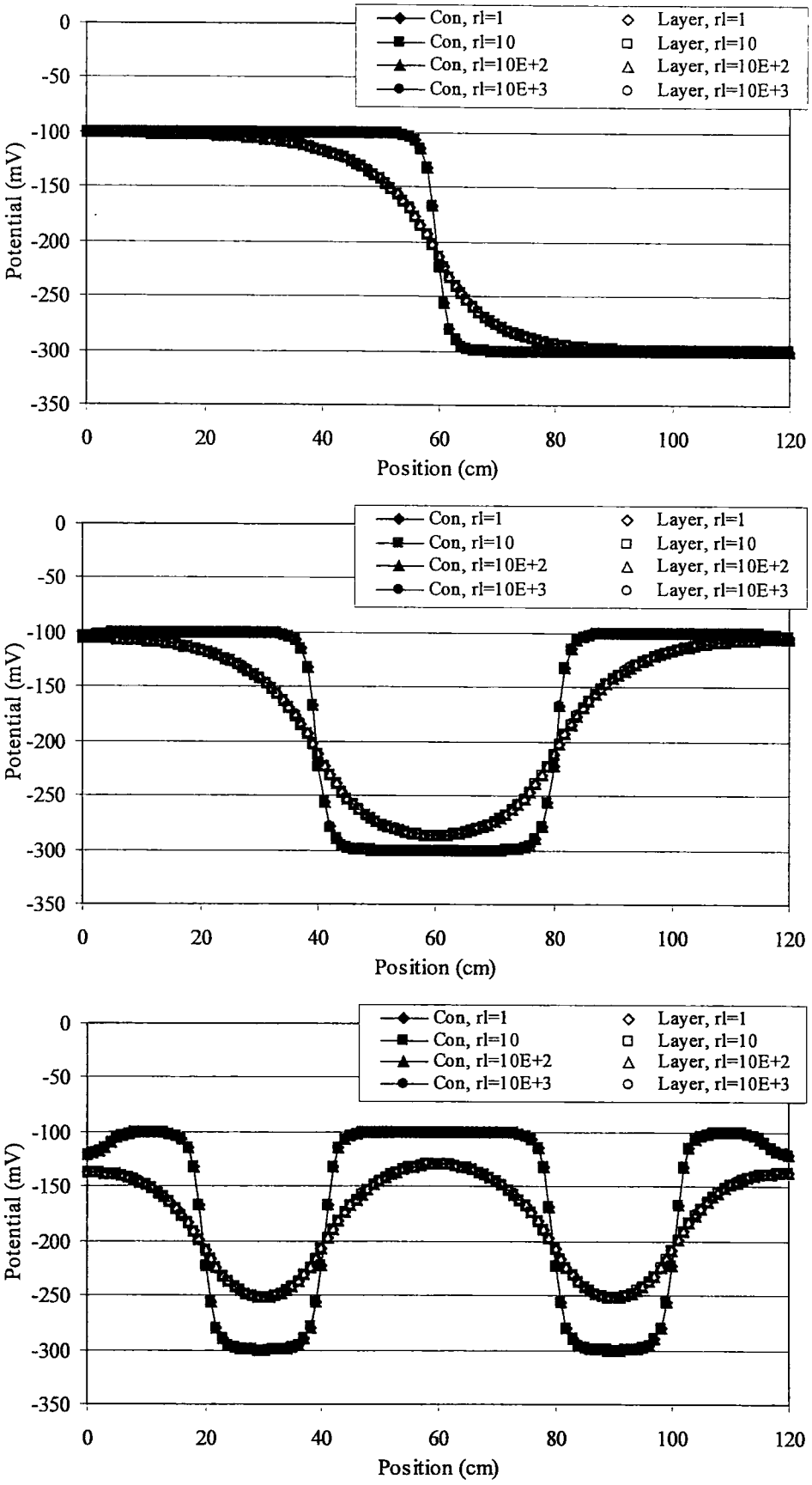

Figure 6.5 Analytical results of variation of the resistivity of conductive strengthening layer (anisotropic), specimen P2, P3 and P5, respectively

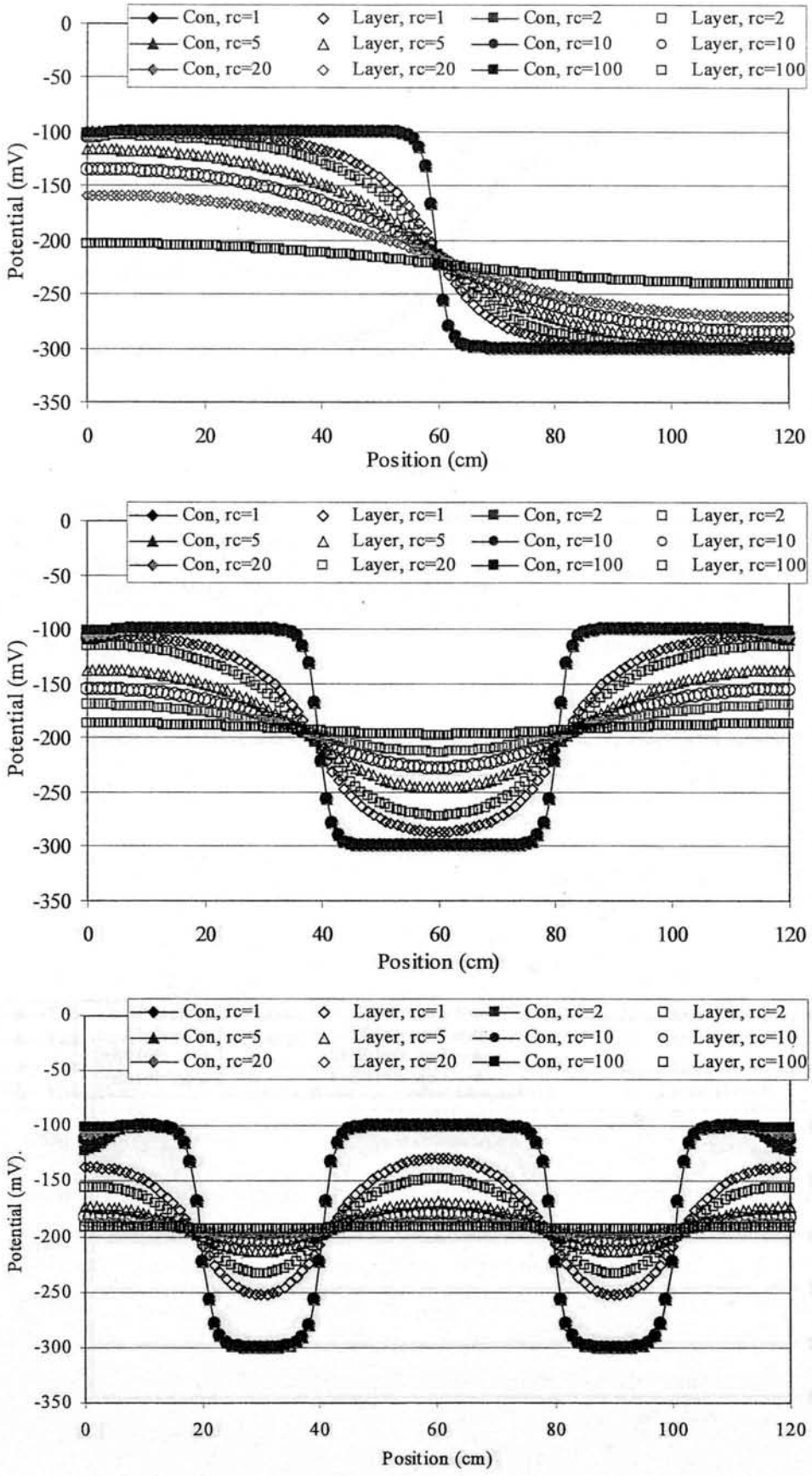

Figure 6.6 Analytical results of variation of the resistivity of concrete cover under conductive strengthening layer, specimen P2, P3 and P5, respectively

Table 6.4 Resistivity of conductive strengthening layer by DC3V

Sample no.	Types of Conductive Strengthening Layer (Ω.cm)					
	8%CB	8%CB1CF	8%CB1AF	5%CB	5%CB1CF	5%CB2CF
Mean	572.78	0.12	711.14	10098.79	0.26	0.13
Max	1160.80	0.57	2761.24	14860.92	0.77	0.25
Min	38.22	0.01	166.32	2142.21	0.04	0.05

6.4 Details Analysis

From the section 6.3, the basic understandings of the effect of each parameter are investigated. In this section, the finer analytical model is used and the experimental data in each case study are employed. The guideline that aimed to find the way to make the analytical potential distribution to meet the experimental potential distribution is proposed. In the analysis, the material properties and boundary conditions were defined from the obtained experimental results. Some definitions and assumption are given below.

1. Due to different applied voltage gave different resistivity of conductive strengthening layer. Then, the resistivity of conductive strengthening layer of DC3V applied voltage was assumed to use in this precise analysis. Table 6.4 shows the experimental data of the resistivity of conductive layer by DC3V.
2. The concrete resistivity of each specimen was calculated from its experimentally measured concrete resistance and used in the analysis individually.

(a) Analytical model in precise analysis

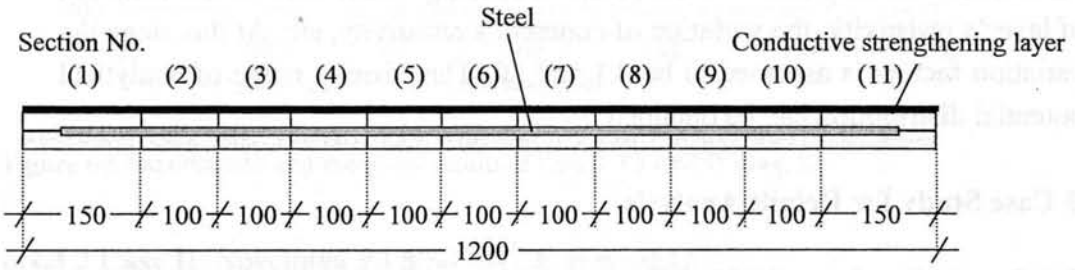

(b) Material properties and boundary conditions used in analytical model: Enlarge picture

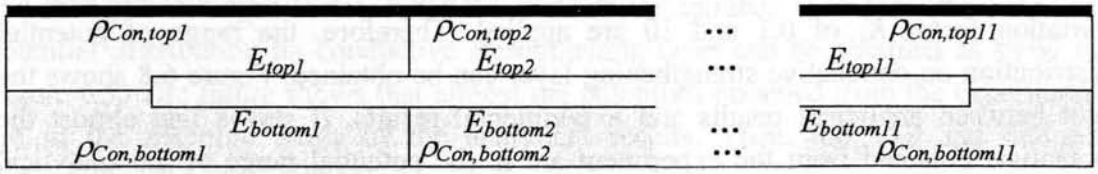

Figure 6.7 Analytical model for details analysis

3. The resistivity of top concrete cover, located under the conductive layer, was assumed to be 1.225 times of the resistivity of bottom concrete cover.
4. The potential on steel surface (the experimental potential obtained from bottom surface) was assumed to be the same for both top and bottom surfaces of steel in analysis.

6.4.1 Analytical Model

The model is finer divided into 11 sections in longitudinal direction as equal to the number of the measured point in the experiment. The material properties of each section from the experimental results, which are the potential reading from bottom (non-attaching concrete) surface and the concrete resistance, are employed in the analysis. Figure 6.7 shows the eleven sections analytical model. The mesh is automatically generated by the program as explained in the previous section.

6.4.2 Analytical Method

From the previous section, the resistivity of conductive strengthening layer is a parameter that effects the potential distribution. Two coefficients are introduced in order to make the analytical potential distribution meet the experimental results.

First, the shifting coefficient, K_s, is used to multiply with the resistivity of the conductive strengthening layer and then the multiplied resistivity will be used in the analysis. It makes a rough shifting of the analytical potential distribution on the conductive strengthening layer.

Secondly, the variation factor, K_v, is the factor that taken the effect of parameters that may affect to the potential reading value, such as the variation of layer's resistivity, the variation of concrete's resistivity, etc. At this stage the variation factors is assumed to be 0.1 and 10. Therefore, a range of analytical potential distribution can be obtained.

6.4.3 Case Study for Details Analysis

6.4.3.1 Case I: Specimen P3 8%CB at week 12

The boundary condition and material properties used in the analysis are concluded in Table 6.5. By trial and error, the best value of shifting coefficient K_s is 1, and then the variation factor K_v of 0.1 and 10 are applied. Therefore, the range of potential distribution on conductive strengthening layer can be obtained. Figure 6.8 shows the plot between analytical results and experimental results. It shows that almost the potentials obtained from the experiment are in the potential range of the analytical results. Then, the idea and defined assumption are applicable.

Table 6.5 Boundary condition and material properties of P3 8%CB week12

Section no., i	Applied potetial[1], E_i (mV)	Concrete resistivity[2], $\rho_{concrete,i}$ (Ω.m)		Conductive strengthening layer resistivity, ρ_{layer} (Ω.m)
		Bottom	Top	
1	-105	1060	1299	Experimental data is 5.73 Ω.m, then rounded value is 6.00 Ω.m
2	-99	888	1088	
3	-127	939	1151	K_s = 1
4	-276	279	342	K_v = 0.1 and 10
5	-312	1278	1566	
6	-364	201	246	K_s. ρ_{layer} = 6.00 Ω.m
7	-333	196	240	K_{v1}.K_s ρ_{layer} = 0.6 Ω.m
8	-286	264	324	K_{v2}.K_s ρ_{layer} = 60 Ω.m
9	-154	885	1084	
10	-109	833	1020	
11	-93	952	1166	

[1] *The experimental data of potential obtained from concrete surface,* $E_{top,i}=E_{bottom,i}$

[2] *The experimental data of concrete resistance and calculate to concrete resistivity,* $\rho_{concrete,i}$ *(top)* = 1.225 $\rho_{concrete,i}$ *(bottom)*

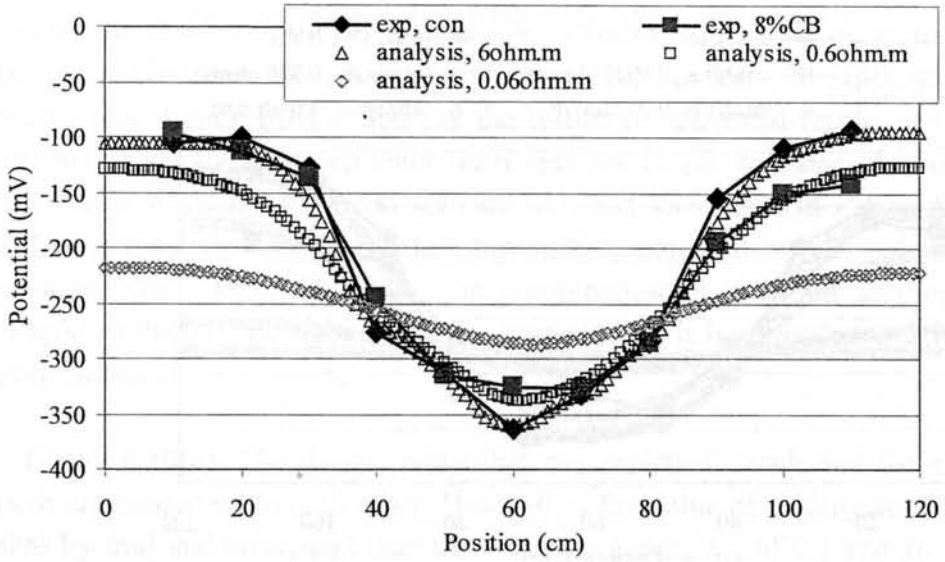

Figure 6.8 Experimental and analytical results of Case I: P3 8%CB week 12

6.4.3.2 Case II: Specimen P3 5%CB1CF at week12

The boundary condition and material properties used in the analysis are concluded in Table 6.6. Here again, the best value of shifting coefficient K_s is 100 by trial and error, and then the variation factor K_v of 0.1 and 10 are applied. Therefore, the range of potential distribution on conductive strengthening layer can be obtained as show in Figure 6.9. The figure shows that almost the potentials obtained from the experiment are in the potential range of the analytical results. Then, the idea and defined assumptions are still applicable.

Table 6.6 Boundary condition and material properties of P3 5%CB1CF week12

Section no., i	Applied potetial[1], E_i (mV)	Concrete resistivity[2], $\rho_{concrete,i}$ (Ω.m)		Conductive strengthening layer resistivity, ρ_{layer} (Ω.m)
		Bottom	Top	
1	-152	635	777	Experimental data is 0.0026 Ω.m.
2	-152	597	731	
3	-186	507	621	K_s = 100 K_v = 0.1 and 10
4	-306	230	282	
5	-347	177	217	K_s. ρ_{layer} = 0.26 Ω.m
6	-357	168	206	K_{v1}.K_s ρ_{layer} = 0.026 Ω.m
7	-359	170	208	K_{v2}.K_s ρ_{layer} = 2.6 Ω.m
8	-321	241	296	
9	-178	593	727	
10	-125	511	626	
11	-116	686	840	

[1] *The experimental data of potential obtained from concrete sureface, $E_{top,i}$=$E_{bottom,i}$*

[2] *The experimental data of concrete resistance and calculate to concrete resistivity, $\rho_{concrete,i}$ (top) = 1.225 $\rho_{concrete,i}$ (bottom)*

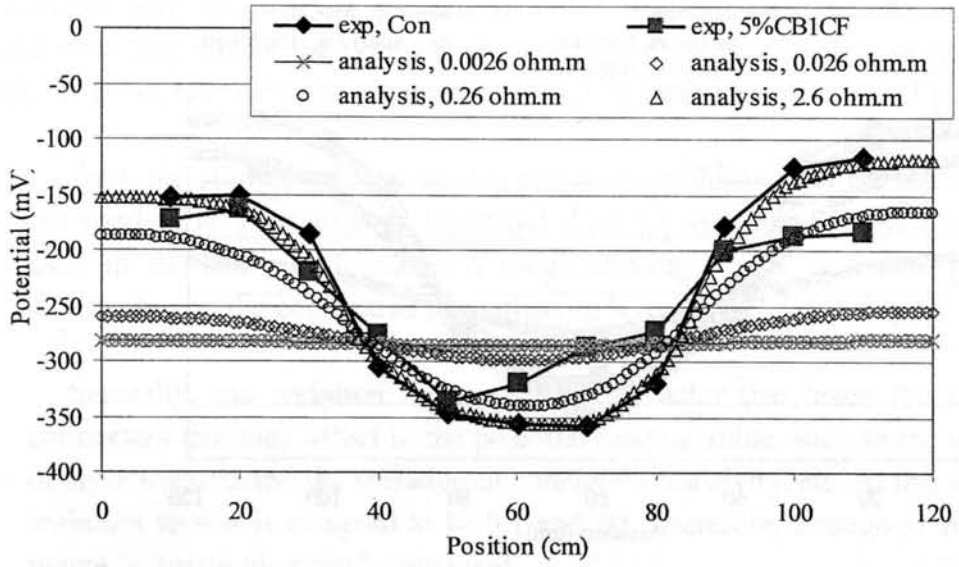

Figure 6.9 Experimental and analytical results of Case II: P3 4%CB1CF week 12

6.4.3.3 Case III: Specimen P2 8%CB1CF at week24

The boundary condition and material properties used in the analysis are concluded in Table 6.7. In this case, the experimental results show that the potential reading on conductive strengthening layer is nobler than and parallel moving with the potential reading on concrete surface. Even through a number value of K_s are used, the range of potential distribution on conductive strengthening layer obtained from the analytical result cannot represent the experimental potential reading as show in Figure 6.10(a).

Table 6.7 Boundary condition and material properties of P2 8%CB1CF week24

Section no., i	Applied potetial, E_i (mV)				Concrete resistivity[1], $\rho_{concrete,i}$ (Ω.m)		Conductive strengthening layer resistivity, ρ_{layer} (Ω.m)
	Bottom	+20	+40	+70	Bottom	Top	
1	-160	-140	-120	-90	991	1213	Experimental data is 0.0012 Ω.m.
2	-149	-129	-109	-79	738	904	
3	-168	-148	-128	-98	591	724	
4	-174	-154	-134	-104	553	677	K_s = 1000
5	-188	-168	-148	-118	672	823	K_v = 0.1 and 10
6	-291	-271	-251	-221	290	356	
7	-314	-294	-274	-244	246	302	K_s. ρ_{layer} = 1.2 Ω.m
8	-321	-301	-281	-251	232	284	$K_{v1}.K_s$ ρ_{layer} = 0.12 Ω.m
9	-324	-304	-284	-254	198	243	$K_{v2}.K_s$ ρ_{layer} = 12 Ω.m
10	-317	-297	-277	-247	225	276	
11	-309	-289	-269	-239	254	312	

[1] *The experimental data of concrete resistance and calculate to concrete resistivity, $\rho_{concrete,i}$ (top) = 1.225 $\rho_{concrete,i}$ (bottom)*

Therefore, an assumption of having the same potential on steel top and bottom surface that is held for all of the previous analysis need to be changed. Figure 6.10(b), (c) and (d) show the analytical results by assuming the potential on top surface of steel is nobler than the potential of bottom surface for +20, +40, and +70 mV, respectively. Figure 6.10(b) and (c), the results of analytical results of the potential distribution on the layer on right hand side are closer to those obtained from the experiment while the left hand side are not, and vice versa in Figure 6.10 (d), the analytical results of the input steel top surface potential equals to bottom surface potential plus 70mV. Therefore, the combination of potential shifting (+70 and +40mV on the left and right hand side, respectively) is investigated and the analytical result shows in

Figure 6.10(e). The figure shows that the analytical result and the experimental result are consistent to each other. Here again, the value of shifting coefficient, K_s, is 1000 by trial and error, and then the variation factor, K_v, of 0.1 and 10 are applied. Therefore, the range of potential distribution on conductive strengthening layer can be obtained as show in Figure 6.10(e). The figure shows that almost the potentials obtained from the experiment are in the potential range of the analytical results. Then, the idea of combination of potential shifting is applicable in this case.

From the results of these three case studies, some ideas for analysis the potential distribution on the conductive strengthening have been proposed. But more trial and error needs to be done to obtain more value of K_s from any other cases. If it is possible, the function of K_s may be obtained.

(a)

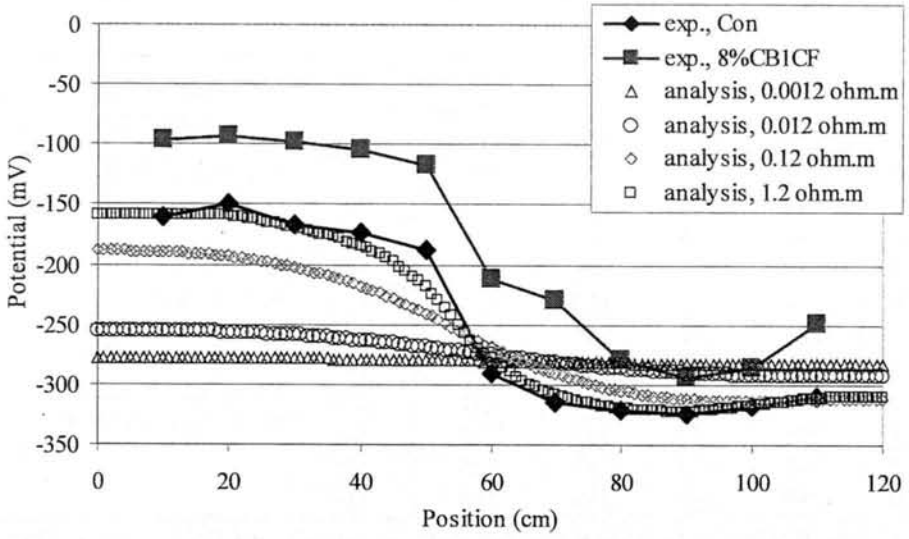

(b)

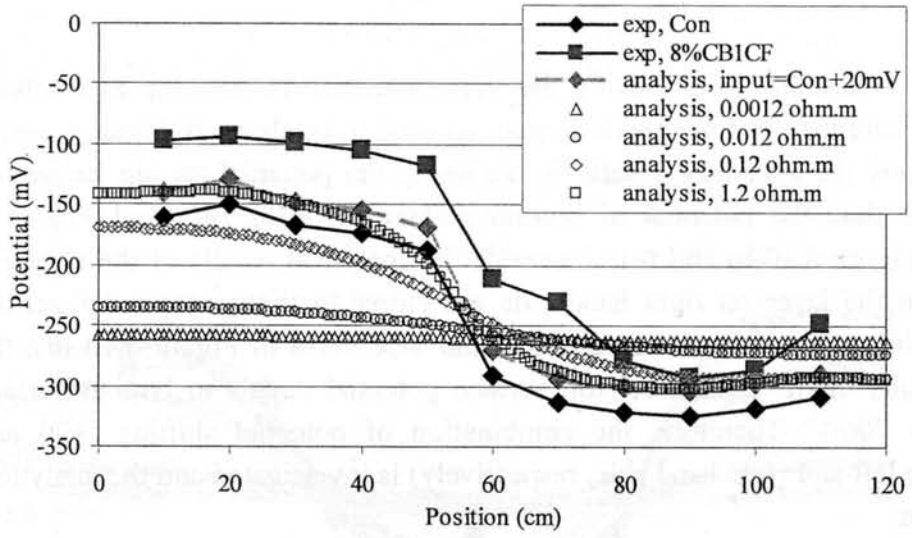

(c)

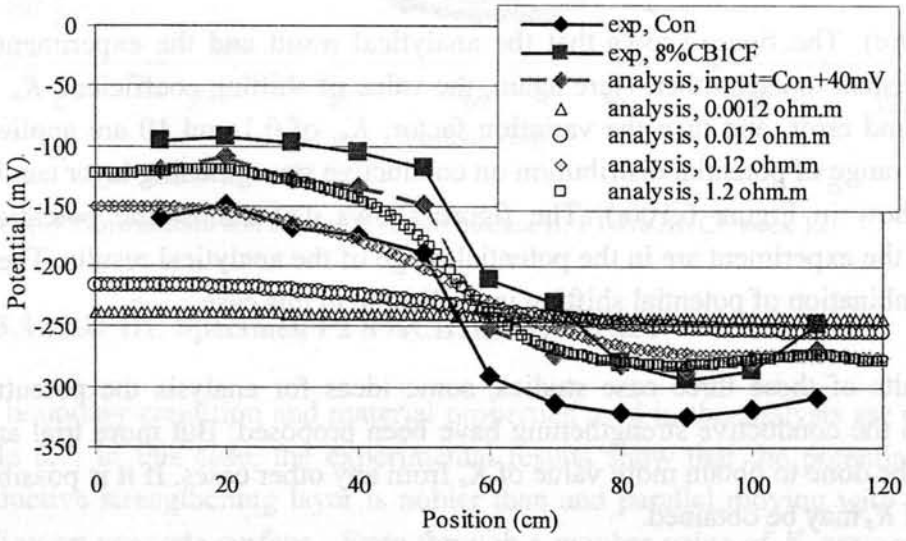

Figure 6.10 Experimental and analytical results of P2 8%CB1CF week 12; (a) Without any shifting input potential on top surface of steel, (b) +20 mV shifting input potential, (c) +40 mV shifting input potential, (d) +70 mV shifting input potential, (e) +70/+40 mV shifting input potential

(d)

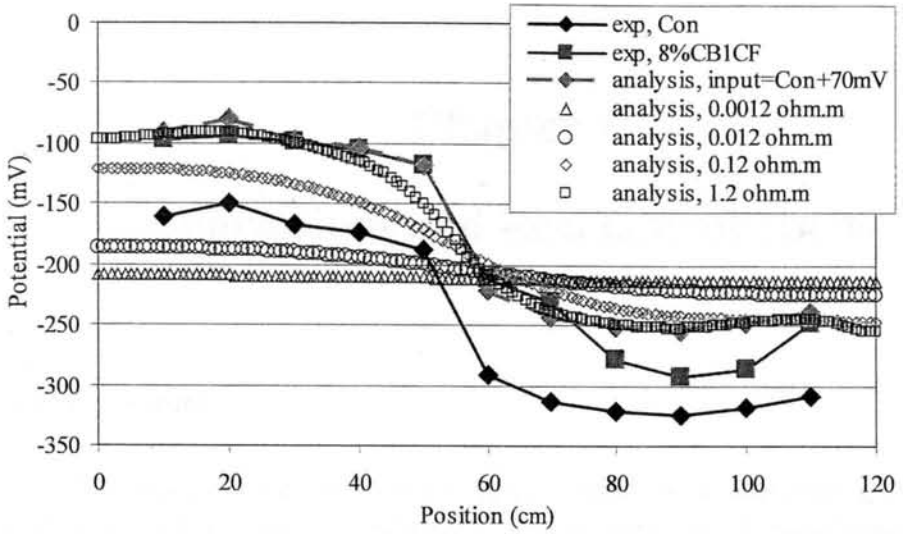

(e)

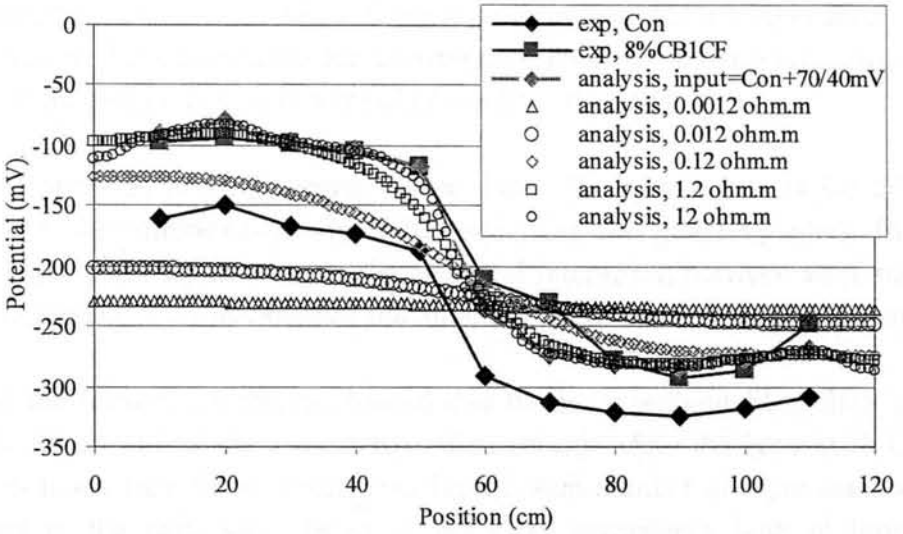

Figure 6.10(cont'1) Experimental and analytical results of P2 8%CB1CF week 12; (a) Without any shifting input potential on top surface of steel, (b) +20 mV shifting input potential, (c) +40 mV shifting input potential, (d) +70 mV shifting input potential, (e) +70/+40 mV shifting input potential

6.5 Summary

In the simple analysis, the effect of individual parameter to the potential distribution on the conductive strengthening is investigated. The results demonstrated that the resistivity of conductive strengthening layer and concrete cover have an important role to influence the potential distribution. In the details analysis, the idea to make the analytical results meet the experimental results is proposed. And two coefficients (shifting coefficient and variation coefficient) are introduced and the assumption of the different potential on top-bottom surface of the embedded steel is employed. However, a number of trial and error needs to be done to understand the other cases and the function of shifting coefficient may be obtainable.

Chapter 7

Conclusions and Recommendations

7.1 Conclusions

In this dissertation, the conductive epoxy resin was introduced to make the strengthening material to be conductive. And its effect to electrochemical corrosion monitoring techniques, half-cell potential and polarization resistance, was studied. Moreover, the experiments for investigation its materials properties were conducted. The following conclusions were obtained from this study.

In **Chapter 3**, two experiments were done. The former one is the experiment for measure the volume resistivity of the conductive strengthening layers. The later one is the experiment for investigate the electrical interaction between steel and conductive strengthening layer by obtained the direction of current flow between them.

In the former, the results showed that the layer without fiber sheet and the layer with AF sheet had the same range of resistivity while the layer with CF sheet was much lower than those former two layers. And number of layer seemed to have no effect to the resistivity. These results were consistency both in longitudinal and vertical direction measurement. The wide range of resistivity, maybe 100 or 1000 times, was obtained in some cases.

In the later, the results confirmed that the steel would be fine, when the conductive layer bonded on concrete surface, in three conditions that are chloride free concrete in dry condition, chloride mixed concrete in dry condition, and chloride free concrete in wet condition.

In **Chapter 4,** the electrochemical corrosion monitoring techniques, half-cell potential and polarization, were employed to investigate the steel corrosion condition under the conductive strengthening layer that bonded on concrete specimen with uniform chloride content. The very good results were found in case of half-cell potential measurement that the obtained value on conductive strengthening layer were quite equal to the value obtained on concrete surface. But in case of polarization resistance, the obtained values were fluctuation and some came out in negative or even enormous value. Then, it can be said that half-cell potential measurement is successful to apply on conductive strengthening layer. And leaded us to do the experiment in **Chapter 5.**

In **Chapter 5**, the half-cell potential measurement was done in the concrete specimen with longitudinal distribution of Cl^- content in concrete. The half-cell potential measured on all conductive strengthening layer had same tendency with that measured on concrete surface. The layer without carbon fiber sheet also showed better results than the layer with carbon fiber sheet.

In **Chapter 6**, the results of the study the effect of individual parameter to the potential distribution on concrete surface show that the resistivity of conductive strengthening layer (isotropic), the resistivity of concrete and their variation have much effect to the potential distribution that reading on conductive layer. Two coefficients (shifting coefficient and variation coefficient) and the assumption of the different potential on top-bottom surface of the embedded steel were employed in the analysis in order to explain the way to make the analytical results meet the experimental results. Finally, a number of trial and error needs to be done for more understanding and find the equation of shifting coefficient that may be the function of conductive strengthening layer and/or material properties.

From the overall results, it may say that it is possible to apply half-cell potential on the conductive strengthening layer to investigate the corrosion activity of the embedded rebar in reinforced concrete structure. Therefore, it may help to scope down the suspected area that has high corrosion activity. And also reduce time of measurement that it has no need to make the window cutting on the strengthening layer for measurement.

7.2 Recommendations for the future work

In the materials properties section, the wide range of resistivity was obtained. Then the application of conductive strengthening layer should be improved in order to get much better uniform or even a narrow range of resistivity.

In the study of the development of repair and strengthening, which is the effect of conductive strengthening layer to the corrosion monitorability, more experimental study should be conducted to confirm the efficiency of half-cell potential measurement on the other pattern of concrete specimen. For example, the concrete slab with longitudinal and transverse reinforcement, the fiber wrapped concrete column or concrete cylinder. But the difficulty is how to accelerate the corrosion under the layer with minimize the aggravation of the resistivity of conductive strengthening layer.

Finally, the analytical part, a number of trial and error needs to be done in order to get more understanding and find the function of shifting coefficient with conductive

strengthening layer and/or material properties. Moreover, the value of variation factor may be revised.

References

[1] Montemor, M.F., Simoes, A.M.P. and Ferreira, M.G.S. 2003, "Chloride-induced corrosion on reinforcing steel: form the fundamental to the monitoring techniques", *Cement&Concrete Composites* Vol.25:491-502

[2] "*Standard Test Method for Half-cell Potentials of Uncoated reinforcing Steel in Concrete*", ASTM Standard C876-91 (Reapproved 1999)

[3] Gu, P., and Beaudoin, J.J. 1998, "Obtaining Effective Half-Cell Potential Measurements in Reinforced Concrete Structures", Construction Technology update No.18, National Research Council of Canada

[4] "*Standard Test Method for Conducting Potentiodynamic Polarization Resistance Measuremene*", ASTM Standard G59-97 (Reapproved 2003)

[5] Feliu, S., Gonzalez, J.A., and Andrede, M.C. 1988, *Corrosion* Vol.44 No.12: 761

[6] Feliu, S., Gonzalez, J.A., and Andrede, M.C. 1988, *Corrosion Science*, Vol.29 No.12: 105

[7] Feliu, S., Gonzalez, J.A., Escudero, M.L., Feliu, S. Jr. and Andrede, M.C. 1990, "Possibilities of Guard Ring for Electrical Signal Confinement in the Polarization Measurement of Reinforcements", *Corrosion* Vol.46 No.12: 1015-1020

[8] Baweja, D., Roper, H., and Sirivivatnanon, V. 2003, "Improved Electrochemical Determinations of Chloride-Induced Steel Corrosion in Concrete", *ACI Material Journal* V.100 No.3: 228-238

[9] Hattori, A., and Miyakawa, T. 2001, "Prediction of Degradation and Performance in RC Beams Subjected to Chloride Attack by Corrosion Monitoring", *7th International Conference on Inspection, Appraisal, Repairs & Maintenance of Building & Structures.*, Nottingham, United Kingdom, 81-88

[10] Yalcyn, H., and Ergun, M. 1996, "The Prediction of Corrosion Rates of Reinforcing Steels in Concrete", *Cement and Concrete Research* Vol.26 No.10: 1593-1599

[11] Law, D.W., Cairns, J.J., Millard, S.G., and Bungey, J.H. 2003, Evaluation of Corrosion Loss of Steel Reinforcement using Linear Polarization Resistance

Measurements. *International Symposium of Non-Destructive Testing in Civil Engineering*

[12] Debaiky, A.S., Green, M.F., and Hope, B.B. 2001, "Corrosion of FRP-Wrapped RC Cylinders-Long Term Study under Severe Environmental Exposure", *FRPRCS-5:*.1073-1082

[13] Fleming, C.J., and King, G.E.M. 1967, "The Development of Structural Adhesives for Three Original Uses in South Africa", RILEM International Symposium on Synthetic Resins in Building Construction, RILEM, Paris, 75-92

[14] Yokota M., Electrochemical Method, Seminar "Diagnosis Technology of Concrete Structure", J.JSMS, pp.26-36, 2001.10

[15] Luca Bertolini, Bernhard Elsener, Pietro Pedeferri, and Rob Polder, "Corrosion of Steel in Concrete", Wiley-VCH

[16] Maaddawy, T. E., Chahrour, A., and Soudki, K. 2006, "Effect of fiber-reinforced polymer wraps on corrosion activity and concrete cracking in chloride-contaminated concrete cylinders.", *J. Comp. Construc.*, 10, 139-147

[17] "*Standard Test Method for Electrical Resistivity of Manufactured Carbon and Graphite Articles at Room Temperature*", ASTM Standard C611-98 (Reapproved 2005)

[18] Hearn, N., and Aiello, J. 1998, "Effect of mechanical restraint on the rate of corrosion in concrete.", *Can. J. Civ. Eng.*, 25(1), 81-86.

[19] Lee, C., Bonacci, J. F., Thomas, M. D.A., Maalej, M., Khajehpour, S., Hearn, N., Pantazopoulou, S. J., and Sheikh, S. 2000. "Accelerated corrosion and repair of reinforced concrete columns using CFRP sheet.", *Can. J. Civ. Eng.*, 27, 941-948

[20] Repair Strategies for Concrete Structures Damaged by Steel Corrosion, RILEM 124-SRC, 1994

[21] Overview of European Concrete Repair Standard EN1504, Building Research Establishment Ltd, 2005

[22] Wootton, I. A., Spainhour, L. K., and Yazdani, N. 2003, "Corrosion of steel reinforcement in carbon fiber-reinforced polymer wrapped concrete cylinders.", *J. Comp. Construc.*, 7, 339-347

[23] "*Standard Test Method for Testing of Embedded Impressed current Anodes for Use in Cathodic Protection of Atmospherically Exposed Steel-Reinforced Concrete*", NACE Standard TM2094-2001

[24] Leelalertkiet, V., Kyung, J.W., Ohtsu, M., 2004, "BEM Analysis on Half-Cell Potential Measurement and Current Flow", *J. Material, Conc. Struct. Pavements, JSCE*, 62, 153-163

[25] "*Standard Test Method for Volume resistivity of Conductive Adhesives*", ASTM Standard D2739-97 (Reapproved 2004)

[26] Bertilini, L., Elsener, B., Pedeferri, P., Ploder, R. 2004. *Corrosion of Steel in Concrete: Prevetion, Diagnosis, Repair.* WILEY-VCH Verlag GmbH & CO. KGaA.

[27] "*Standard Test Method for Electrical Resistivity of Anode and Cathode Carbon Material at Room Temperature*", ASTM Standard D6120-97 (Reapproved 2002)

[28] Kobayashi, K., Miyagawa, T., 2001, "Study on Estimation of Corrosion Rate of Reinforcing Steel in Concrete by Measuring Polarization Resistance", *J. JSCE*, 50, 173-186

[29] Leelalertkiet, V., Kyung, J.W., Ohtsu, M., Yokota, M., 2004, "Analysis of Half-Cell Potential Measurement for corrosion of Reinforced Concrete", *J. Construction and Building Materials*, 18, 155-162

[30] Leelalertkiet, V., Kyung, J.W., Yokota, M., Ohtsu, M., 2003. BEM Analysis on Half-Cell Potential Measurement for Corrosion Estimation. *International Symposium of Non-Destructive Testing in Civil Engineering*

[31] Neville, A.M., 1997. *Properties of Concrete.* Essex: Addison Wesley Longman.

[32] Piboonsak, P., Yamamoto, S., Hattori, A., Miyagawa, T. 2005. Electrochemical Corrosion Monitoring of Steel in RC Member Bonded with Conductive Strengthening Layer. *Proceedings of the Concrete Structure Scenarios, JSMS*, Kyoto, 281-286

[33] Electrochemical Techniques for Measuring Metallic Corrosion, RILEM TC 154-EMC, 2004